

**IMPACT OF PBL ON THE SIMULATION OF HEAVY
RAINFALL EVENTS IN THE MONSOON SEASON
OVER BANGLADESH USING WRF-ARW MODEL**

BY

S. M. RAFIQUL ISLAM

ROLL NO: 0855501

SESSION: JANUARY'2008



***A THESIS SUBMITTED TO THE DEPARTMENT OF PHYSICS,
KHULNA UNIVERSITY OF ENGINEERING & TECHNOLOGY
IN PARTIAL FULFILLMENT OF THE REQUIREMENT FOR THE
DEGREE OF MASTER OF PHILOSOPHY***



DEPARTMENT OF PHYSICS
KHULNA UNIVERSITY OF ENGINEERING & TECHNOLOGY
KHULNA-9203, BANGLADESH
JULY, 2013

***DEDICATED
TO
MY FATHER, LATE MOTHER, WIFE AND KIDS***

DECLARATION

This to certify that the thesis work entitled as “Impact of PBL on the simulation of heavy rainfall events in the monsoon season over Bangladesh using WRF-ARW model” has been carried out in partial fulfillment of the requirement for M. Phil. degree in the Department of Physics, Khulna University of Engineering & Technology, Khulna-9203, Bangladesh. The above research work or any part of this work has not been submitted to anywhere for the award of any degree or diploma. No other person’s work has been used without due acknowledgement.

Supervisor



Dr. Md. Mahbub Alam

Candidate



S. M. Rafiqul Islam

ACKNOWLEDGEMENT

I have had a lot of help with this thesis work from many individuals in various selfless Ways. I take this opportunity here to express my gratitude.

With my great manner it is a pleasure for me to express my deepest sense of gratitude and indebtedness to my reverend supervisor Dr. Md. Mahbub Alam, Professor, Department of Physics, Khulna University of Engineering & Technology, Khulna, for his kind guidance and supervision and for his constant encouragement throughout the research work. His inspiration and friendly cooperation accelerated my works.

It is a matter of great pleasure for me to record the deepest sense of gratitude to Professor Dr. Md. Abdullah Elias Akhter, Head, Department of Physics, Khulna University of Engineering & Technology, Khulna, who has given me a strong support in various ways during the entire period of my study in this department.

I am indebted also for Professor, Dr. Shibendra Shekher Sikder and Professor, Dr. Jolly Sultana, Department of Physics, KUET for their invaluable suggestions and inspiration during my study in this department.

I gratefully acknowledge Mr. Md. Kamrul Hasan Reza and Mr. Md. Asaduzzaman, Assistant Professor, Department of Physics, KUET for their cooperation regarding writing the thesis.

My personal thankful greetings are to my good friends and well wishers for their help and cooperation. I am highly grateful to my parents, brothers, sisters and nearest relatives for their inspiration, encouragement and support to carry out this M.Phil thesis work.

My thanks are for my colleagues Mr. Ashim Kumar Sarkar, Mr. Md. Musfiqur Rahman, Dr. S.M. Shamim Ahsan, Mr. Md. Anowar Hossain and Mr. Md. Ziaur Rahman For their inspiration when I was doing my research works.

My thanks are due to research staff of SMRC and Bangladesh Meteorological Department (BMD) for providing necessary data with other necessary help.

I am very much grateful to my father, father in law and mother in law for their support during the period when I was doing research.

There are numerous people who could not be mentioned individually but their interesting discussions have prompted much thought on various aspects, I would also like to thank them.

I would like to mention the name of my wife Kazi Nasrin Akter Sayeed whose constant and volatile inspiration has inspired me a lot to undergo this thesis work. I possess an everlasting soft corner for my loving daughter and my son who have been deprived of my company during the research period.

I record my sincerest gratitude to Khulna University of Engineering & Technology, Khulna for providing with the financial assistance during the period of the research work.

Finally, I want to express my gratitude to almighty Allah for his mercy.

**KHULNA UNIVERSITY OF ENGINEERING & TECHNOLOGY
DEPARTMENT OF PHYSICS**


Approval


This is to certify that the thesis work submitted by *S. M. Rafiqul Islam* entitled "*Impact of PBL on the Simuaation of Heavy Rainfall Events in the Monsoon Season over Bangladesh Using WRF-ARW Model*" has been accepted by the board of examiners for the partial fulfillment of the requirements for the degree of *Master of Philosophy* in the Department of *Physics*, Khulna University of Engineering & Technology, Khulna, Bangladesh in July 2013.

Board of Examiners


Sl. No. Name, Designation & Address

1. Prof. Dr. Md. Mahbub Alam
Department of Physics
Khulna University of Engineering & Technology
2. Head
Department of Physics
Khulna University of Engineering & Technology
3. Prof. Dr. Shibendra Shekher Sikder
Department of Physics
Khulna University of Engineering & Technology
4. Prof. Dr. Md. Abdullah Elias Akhter
Department of Physics
Khulna University of Engineering & Technology
5. Dr. Samarendra Karmakar, Director (Retd),
Bangladesh Meteorological Department (BMD) and
SAARC Meteorological Research Centre (SMRC)
63, Jafrabad, 2nd floor
Durgamandir Goli
Shankar, Dhaka-1207


..... 27.07.2013
Chairman & Supervisor


.....
Member


.....
Member


.....
Member



.....
Member (External)

Table of content

	Page No
Acknowledgement	i
Table of content	iii
List of figures	v
Table	xi
Abstract	x
Abbreviations	xi
Chapter I Introduction	1
Chapter II Literature Review	7
2.1 WRF Model	8
2.2 Advanced Research WRF (ARW)	8
2.3 Planetary Boundary Layer	8
2.4 Microphysics	11
2.5 Cumulus Parameterization	12
2.6 Relative Humidity	13
2.7 Atmospheric Radiation	15
2.7.1 Outgoing Long wave Radiation	15
2.7.2 Downward long wave radiation	16
Chapter III Data and Methodology	17
3.1 Selection of Model	18
3.2 Experiments on simulation of different heavy rainfall events	18
3.3 Domain and Model Physics	18
3.3.1 Domain set up	18
3.3.2 WRF Model and Domain Configurations	19
3.4 Initial Data Source	21
3.5 Synoptic situation	21
Chapter IV Simulation of heavy rainfall events using WRF-ARW Model	23
4.1 Heavy rainfall event of 27-29 July 2009	24
4.1.1 Accumulated Upward Heat Flux (ACHFX) at the Surface	24
4.1.2 Accumulated Upward Latent Heat Flux (ACLHF) at the Surface	26
4.1.3 Downward Long Wave Flux at Ground Surface (GLW)	28
4.1.4 Outgoing Long Wave Radiation (OLR)	30
4.1.5 Variation of Planetary Boundary Layer (PBL)	32
4.1.6 Reflectivity	34
4.1.7 Wind	36
4.1.8 Relative Humidity (RH)	37

4.1.9	Rainfall	39
4.1.10	Summary	44
4.2	Heavy rainfall event of 15-16 August 2009	45
4.2.1	Accumulated Upward Heat Flux (ACHFX) at the Surface	45
4.2.2	Accumulated Upward Latent Heat Flux (ACLHF) at the Surface	47
4.2.3	Downward Long Wave Flux at Ground Surface (GLW)	49
4.2.4	Outgoing Long Wave Radiation (OLR)	51
4.2.5	Variation of Planetary Boundary Layer (PBL)	53
4.2.6	Reflectivity	55
4.2.7	Wind	57
4.2.8	Relative Humidity (RH)	58
4.2.9	Rainfall	59
4.2.10	Summary	63
4.3	Heavy rainfall event of 26-27 June 2010	64
4.3.1	Accumulated Upward Heat Flux (ACHFX) at the Surface	64
4.3.2	Accumulated Upward Latent Heat Flux (ACLHF) at the Surface	66
4.3.3	Downward Long Wave Flux at Ground Surface (GLW)	68
4.3.4	Outgoing Long Wave Radiation (OLR)	70
4.3.5	Variation of Planetary Boundary Layer (PBL)	72
4.3.6	Reflectivity	74
4.3.7	Wind	75
4.3.8	Relative Humidity (RH)	77
4.3.9	Rainfall	79
4.3.10	Summary	82
4.4	Heavy rainfall event of 7-8 September 2011	84
4.4.1	Accumulated Upward Heat Flux (ACHFX) at the Surface	84
4.4.2	Accumulated Upward Latent Heat Flux (ACLHF) at the Surface	86
4.4.3	Downward Long Wave Flux at Ground Surface (GLW)	88
4.4.4	Outgoing Long Wave Radiation (OLR)	90
4.4.5	Variation of Planetary Boundary Layer (PBL)	92
4.4.6	Reflectivity	94
4.4.7	Wind	95
4.4.8	Relative Humidity (RH)	97
4.4.9	Rainfall	99
4.4.10	Summary	102
	Chapter V Conclusion	103
	References	106

LIST OF FIGURES

Fig. No.	page
Fig.3.1 Domain configuration for grid resolution of 9 km and 3 km.	18
Fig. 1 Spatial distribution of simulated ACHFX using a) YSU, b) MYJ, c) QNSE, d) MYNN3, e) ACM2 and f) BouLac schemes at 1200 UTC of 28 July 2009.	24
Fig. 2 Spatial distribution of simulated ACHFX using a) YSU, b) MYJ, c) QNSE, d) MYNN3, e) ACM2 and f) BouLac schemes at 1200 UTC of 29 July 2009.	25
Fig. 3 Spatial distribution of simulated ACLHF using a) YSU, b) MYJ, c) QNSE, d) MYNN3, e) ACM2 and f) BouLac schemes at 1200 UTC of 28 July 2009.	25
Fig. 4 Spatial distribution of simulated ACLHF using a) YSU, b) MYJ, c) QNSE, d) MYNN3, e) ACM2 and f) BouLac schemes at 1200 UTC of 29 July 2009.	27
Fig. 5 Spatial distribution of simulated GLW using a) YSU, b) MYJ, c) QNSE, d) MYNN3, e) ACM2 and f) BouLac schemes at 1200 UTC of 28 July 2009.	28
Fig. 6 Spatial distribution of simulated GLW using a) YSU, b) MYJ, c) QNSE, d) MYNN3, e) ACM2 and f) BouLac schemes at 1200 UTC of 29 July 2009.	29
Fig. 7 Spatial distribution of simulated OLR using a) YSU, b) MYJ, c) QNSE, d) MYNN3, e) ACM2 and f) BouLac schemes at 1200 UTC of 28 July 2009.	30
Fig. 8 Spatial distribution of simulated OLR using a) YSU, b) MYJ, c) QNSE, d) MYNN3, e) ACM2 and f) BouLac schemes at 1200 UTC of 29 July 2009.	31
Fig. 9 Spatial distribution of simulated PBL height using a) YSU, b) MYJ, c) QNSE, d) MYNN3, e) ACM2 and f) BouLac schemes at 1200 UTC of 28 July 2009.	33
Fig. 10 Spatial distribution of simulated PBL height using a) YSU, b) MYJ, c) QNSE, d) MYNN3, e) ACM2 and f) BouLac schemes at 1200 UTC of 29 July 2009.	34
Fig. 11 Spatial distribution of simulated wind speed (m/s) and reflectivity (dBZ) at 850 hPa level using a) YSU, b) MYJ, c) QNSE, d) MYNN3, e) ACM2 and f) BouLac schemes at 1200 UTC of 28 July 2009.	35
Fig. 12 Spatial distribution of simulated wind speed (m/s) and reflectivity (dBZ) at 850 hPa level using a) YSU, b) MYJ, c) QNSE, d) MYNN3, e) ACM2 and f) BouLac schemes at 1200 UTC of 29 July 2009.	36
Fig. 13 Spatial distribution of simulated RH using a) YSU, b) MYJ, c) QNSE, d) MYNN3, e) ACM2 and f) BouLac schemes at 1200 UTC of 28 July 2009.	37

Fig. 14	Spatial distribution of simulated RH using a) YSU, b) MYJ, c) QNSE, d) MYNN3, e) ACM2 and f) BouLac schemes at 1200 UTC of 29 July 2009.	38
Fig. 15	BMD observed and TRMM daily rainfall in (a-b) 27, (c-d) 28 and (e-f) 29 July 2009 respectively.	40
Fig. 16	Spatial distribution of simulated rainfall (mm) using a) YSU, b) MYJ, c) QNSE, d) MYNN3, e) ACM2 and f) BouLac schemes at 27 July 2009.	41
Fig. 17	Spatial distribution of simulated rainfall (mm) using a) YSU, b) MYJ, c) QNSE, d) MYNN3, e) ACM2 and f) BouLac schemes at 28 July 2009.	42
Fig. 18	Spatial distribution of simulated rainfall (mm) using a) YSU, b) MYJ, c) QNSE, d) MYNN3, e) ACM2 and f) BouLac schemes at 29 July 2009.	43
Fig. 19	Spatial distribution of simulated ACHFX using a) YSU, b) MYJ, c) QNSE, d) MYNN3, e) ACM2 and f) BouLac schemes at 1200 UTC of 15 August 2009.	45
Fig. 20	Spatial distribution of simulated ACHFX using a) YSU, b) MYJ, c) QNSE, d) MYNN3, e) ACM2 and f) BouLac schemes at 1200 UTC of 16 August 2009.	46
Fig. 21	Spatial distribution of simulated ACLHF using a) YSU, b) MYJ, c) QNSE, d) MYNN3, e) ACM2 and f) BouLac schemes at 1200 UTC of 15 August 2009.	47
Fig. 22	Spatial distribution of simulated ACLHF using a) YSU, b) MYJ, c) QNSE, d) MYNN3, e) ACM2 and f) BouLac schemes at 1200 UTC of 16 August 2009.	48
Fig. 23	Spatial distribution of simulated GLW using a) YSU, b) MYJ, c) QNSE, d) MYNN3, e) ACM2 and f) BouLac schemes at 1200 UTC of 15 August 2009.	49
Fig. 24	Spatial distribution of simulated GLW using a) YSU, b) MYJ, c) QNSE, d) MYNN3, e) ACM2 and f) BouLac schemes at 1200 UTC of 16 August 2009.	50
Fig. 25	Spatial distribution of simulated OLR using a) YSU, b) MYJ, c) QNSE, d) MYNN3, e) ACM2 and f) BouLac schemes at 1200 UTC of 15 August 2009.	51
Fig. 26	Spatial distribution of simulated OLR using a) YSU, b) MYJ, c) QNSE, d) MYNN3, e) ACM2 and f) BouLac schemes at 1200 UTC of 16 August 2009.	52
Fig. 27	Spatial distribution of simulated PBL height using a) YSU, b) MYJ, c) QNSE, d) MYNN3, e) ACM2 and f) BouLac schemes at 1200 UTC of 15 August 2009.	53
Fig. 28	Spatial distribution of simulated PBL height using a) YSU, b) MYJ, c) QNSE, d) MYNN3, e) ACM2 and f) BouLac schemes at 1200 UTC of 16 August 2009.	54

Fig. 29	Spatial distribution of simulated wind speed (m/s) and reflectivity (dBZ) at 850 hPa level using a) YSU, b) MYJ, c) QNSE, d) MYNN3, e) ACM2 and f) BouLac schemes at 1200 UTC of 15 August 2009.	55
Fig. 30	Spatial distribution of simulated wind speed (m/s) and reflectivity (dBZ) at 850 hPa level using a) YSU, b) MYJ, c) QNSE, d) MYNN3, e) ACM2 and f) BouLac schemes at 0000 UTC of 16 August 2009.	56
Fig. 31	Spatial distribution of simulated RH using a) YSU, b) MYJ, c) QNSE, d) MYNN3, e) ACM2 and f) BouLac schemes at 1200 UTC of 15 August 2009.	58
Fig. 32	Spatial distribution of simulated RH using a) YSU, b) MYJ, c) QNSE, d) MYNN3, e) ACM2 and f) BouLac schemes at 1200 UTC of 16 August 2009.	59
Fig. 33	BMD observed and TRMM daily rainfall in (a-b) 15 and (c-d) 16 August 2009 respectively.	60
Fig. 34	Spatial distribution of simulated rainfall (mm) using a) YSU, b) MYJ, c) QNSE, d) MYNN3, e) ACM2 and f) BouLac schemes at 15 August 2009.	61
Fig. 35	Spatial distribution of simulated rainfall (mm) using a) YSU, b) MYJ, c) QNSE, d) MYNN3, e) ACM2 and f) BouLac schemes at 16 August 2009.	62
Fig. 36	Spatial distribution of simulated ACHFX using a) YSU, b) MYJ, c) QNSE, d) MYNN3, e) ACM2 and f) BouLac schemes at 1200 UTC of 26 June 2010.	64
Fig. 37	Spatial distribution of simulated ACHFX using a) YSU, b) MYJ, c) QNSE, d) MYNN3, e) ACM2 and f) BouLac schemes at 1200 UTC of 27 June 2010.	65
Fig. 38	Spatial distribution of simulated ACLHF using a) YSU, b) MYJ, c) QNSE, d) MYNN3, e) ACM2 and f) BouLac schemes at 1200 UTC of 26 June 2010.	66
Fig. 39	Spatial distribution of simulated ACLHF using a) YSU, b) MYJ, c) QNSE, d) MYNN3, e) ACM2 and f) BouLac schemes at 1200 UTC of 27 June 2010.	67
Fig. 40	Spatial distribution of simulated GLW using a) YSU, b) MYJ, c) QNSE, d) MYNN3, e) ACM2 and f) BouLac schemes at 1200 UTC of 26 June 2010.	68
Fig. 41	Spatial distribution of simulated GLW using a) YSU, b) MYJ, c) QNSE, d) MYNN3, e) ACM2 and f) BouLac schemes at 1200 UTC of 27 June 2010.	69
Fig. 42	Spatial distribution of simulated OLR using a) YSU, b) MYJ, c) QNSE, d) MYNN3, e) ACM2 and f) BouLac schemes at 1200 UTC of 26 June 2010.	70
Fig. 43	Spatial distribution of simulated OLR using a) YSU, b) MYJ, c) QNSE, d) MYNN3, e) ACM2 and f) BouLac schemes at 1200 UTC of 27 June 2010.	71
Fig. 44	Spatial distribution of simulated PBL height using a) YSU, b) MYJ, c) QNSE, d) MYNN3, e) ACM2 and f) BouLac schemes at 1200 UTC of 26 June 2010.	72
Fig. 45	Spatial distribution of simulated PBL height using a) YSU, b) MYJ, c) QNSE, d) MYNN3, e) ACM2 and f) BouLac schemes at 1200 UTC of 27 June 2010.	73
Fig. 46	Spatial distribution of simulated wind speed (m/s) and reflectivity (dBZ) at 850 hPa level using a) YSU, b) MYJ, c) QNSE, d) MYNN3, e) ACM2 and f) BouLac schemes at 1200 UTC of 26 June 2010.	75

Fig. 47	Spatial distribution of simulated wind speed (m/s) and reflectivity (dBZ) at 850 hPa level using a) YSU, b) MYJ, c) QNSE, d) MYNN3, e) ACM2 and f) BouLac schemes at 1200 UTC of 27 June 2010.	76
Fig. 48	Spatial distribution of simulated RH at 850 hPa level using a) YSU, b) MYJ, c) QNSE, d) MYNN3, e) ACM2 and f) BouLac schemes at 1200 UTC of 26 June 2010.	77
Fig. 49	Spatial distribution of simulated RH at 850 hPa level using a) YSU, b) MYJ, c) QNSE, d) MYNN3, e) ACM2 and f) BouLac schemes at 1200 UTC of 27 June 2010.	78
Fig. 50	BMD observed and TRMM daily rainfall in (a-b) 26 and (c-d) 27 June 2010 respectively.	79
Fig. 51	Spatial distribution of simulated rainfall (mm) using a) YSU, b) MYJ, c) QNSE, d) MYNN3, e) ACM2 and f) BouLac schemes at 26 June 2010.	80
Fig. 52	Spatial distribution of simulated rainfall (mm) using a) YSU, b) MYJ, c) QNSE, d) MYNN3, e) ACM2 and f) BouLac schemes at 27 June 2010.	81
Fig. 53	Spatial distribution of simulated ACHFX using a) YSU, b) MYJ, c) QNSE, d) MYNN3, e) ACM2 and f) BouLac schemes at 1200 UTC of 7 September 2011.	84
Fig. 54	Spatial distribution of simulated ACHFX using a) YSU, b) MYJ, c) QNSE, d) MYNN3, e) ACM2 and f) BouLac schemes at 1200 UTC of 8 September 2011.	85
Fig. 55	Spatial distribution of simulated ACLHF using a) YSU, b) MYJ, c) QNSE, d) MYNN3, e) ACM2 and f) BouLac schemes at 1200 UTC of 7 September 2011.	86
Fig. 56	Spatial distribution of simulated ACLHF using a) YSU, b) MYJ, c) QNSE, d) MYNN3, e) ACM2 and f) BouLac schemes at 1200 UTC of 8 September 2011.	87
Fig. 57	Spatial distribution of simulated GLW using a) YSU, b) MYJ, c) QNSE, d) MYNN3, e) ACM2 and f) BouLac schemes at 1200 UTC of 7 September 2011.	88
Fig. 58	Spatial distribution of simulated GLW using a) YSU, b) MYJ, c) QNSE, d) MYNN3, e) ACM2 and f) BouLac schemes at 1200 UTC of 8 September 2011.	89
Fig. 59	Spatial distribution of simulated OLR using a) YSU, b) MYJ, c) QNSE, d) MYNN3, e) ACM2 and f) BouLac schemes at 1200 UTC of 7 September 2011.	90
Fig. 60	Spatial distribution of simulated OLR using a) YSU, b) MYJ, c) QNSE, d) MYNN3, e) ACM2 and f) BouLac schemes at 1200 UTC of 8 September 2011.	91
Fig. 61	Spatial distribution of simulated PBL height using a) YSU, b) MYJ, c) QNSE, d) MYNN3, e) ACM2 and f) BouLac schemes at 1200 UTC of 7 September 2011.	92

Fig. 62	Spatial distribution of simulated PBL height using a) YSU, b) MYJ, c) QNSE, d) MYNN3, e) ACM2 and f) BouLac schemes at 1200 UTC of 8 September 2011.	93
Fig. 63	Spatial distribution of simulated wind speed (m/s) and reflectivity (dBZ) at 850 hPa level using a) YSU, b) MYJ, c) QNSE, d) MYNN3, e) ACM2 and f) BouLac schemes at 1200 UTC of 7 September 2011.	95
Fig. 64	Spatial distribution of simulated wind speed (m/s) and reflectivity (dBZ) at 850 hPa level using a) YSU, b) MYJ, c) QNSE, d) MYNN3, e) ACM2 and f) BouLac schemes at 1200 UTC of 8 September 2011.	96
Fig. 65	Spatial distribution of simulated RH at 850 hPa level using a) YSU, b) MYJ, c) QNSE, d) MYNN3, e) ACM2 and f) BouLac schemes at 1200 UTC of 7 September 2011.	97
Fig. 66	Spatial distribution of simulated RH at 850 hPa level using a) YSU, b) MYJ, c) QNSE, d) MYNN3, e) ACM2 and f) BouLac schemes at 1200 UTC of 8 September 2011.	98
Fig. 67	BMD observed and TRMM daily rainfall in (a-b) 7 and (c-d) 8 September 2011 respectively.	99
Fig. 68	Spatial distribution of simulated rainfall using a) YSU, b) MYJ, c) QNSE, d) MYNN3, e) ACM2 and f) BouLac schemes on 7 September 2011.	100
Fig. 69	Spatial distribution of simulated rainfall using a) YSU, b) MYJ, c) QNSE, d) MYNN3, e) ACM2 and f) BouLac schemes on 8 September 2011.	101

Table

Table No. 1	WRF Model and Domain Configurations	19
-------------	-------------------------------------	----

ABSTRACT

In the present study the Advanced Research WRF (ARW) model version 3.2.1 has been used to simulate the heavy rainfall events of 27-29 July 2009, 15-16 August 2009, 26-27 June 2010 and 7-8 September 2011 over Bangladesh during monsoon season. To simulate the heavy rainfall events Lin *et al.* microphysics in combination with Kain-Fritsch (KF) cumulus parameterization (CP) scheme in a nested configuration has been used. In this study, six different planetary boundary layer (PBL) parameterizations schemes have been used to study the heavy rainfall events in monsoon season. The different PBL schemes have been considered are YSU, MYJ, QNSE, MYNN3, ACM2 and BouLac. The model domains consist of 9 km outer and 3 km inner domain horizontal resolution with 28 vertical sigma levels. NCEP FNL data have been used for the initial and lateral boundary condition. The WRF model has been run 72 hours for the heavy rainfall event 27–29 July 2009 and 48 hours for all other cases. Sensitivity experiments have been conducted with the WRF model to test the impact of Planetary Boundary Layer (PBL) schemes in capturing the extreme weather event. The rainfall, wind speed, relative humidity, accumulated upward heat flux, accumulated upward latent heat flux, downward long wave flux, outgoing long wave radiation, reflectivity, PBL thickness, kinematics and thermodynamic characteristics have been studied to identify the effect of PBL schemes on different heavy rainfall events.

The simulated rainfall is maximum at the position where the outgoing long wave radiation, accumulated upward heat flux and downward long wave flux are minimum. The simulated rainfall is maximum at the position where the reflectivity and the accumulated upward latent heat flux are also maximum. The simulated relative humidity at 850 hPa level is almost 98-100% at different places over the country where maximum rainfall has been simulated.

The simulated rainfall has been compared with observed rainfall of Bangladesh Meteorological Department (BMD) and TRMM 3B42RT rainfall. For the simulation of four heavy rainfall events with four initial conditions, the BouLac PBL scheme has given the better result. After BouLac PBL scheme, YSU and ACM2 have given the better result for the simulation of heavy rainfall events.

ABBREVIATIONS

ACHFX	:	Accumulated Upward Heat Flux
ACLHF	:	Accumulated Upward Latent Heat Flux
ACM2	:	Asymmetric Convective Model version 2
ARW	:	The Advance Research WRF
BMD	:	Bangladesh Meteorological Department
BouLac	:	Bougeault–Lacarrère
CP	:	Cumulus Parameterization
FNL	:	Final Reanalysis
GEWEX	:	Global Energy and Water Cycle Experiment
GLW	:	Downward Long Wave Flux at Ground Surface
KF	:	Kain-Fritsch
MP	:	Microphysics
MRF	:	Medium Range Forecast
MYJ	:	Mellor–Yamada–Janjic
MYNN3	:	Mellor–Yamada–Nakanishi–Nino Level 3
NCEP	:	National Centre for Environmental Prediction
NWP	:	Numerical Weather Prediction
OLR	:	Outgoing Long Wave Radiation
PBL	:	Planetary Boundary Layer
QNSE	:	Quasi-Normal Scale Elimination
RH	:	Relative Humidity
RRTM	:	Rapid Radiative Transfer Model
TEMF	:	Total Energy - Mass Flux
TRMM	:	Tropical Rainfall Measuring Mission
WRF	:	Weather Research and Forecasting
YSU	:	Yonsei University Scheme

CHAPTER I
INTRODUCTION

1.1 Introduction

The Ganges, the Brahmaputra and the Meghna river system forms in the Bengal Basin delta of 25,000 square miles extent, its topography is characterized by very flat plain which dominate most parts of the country and never rise to more than 10 m above sea level. Although a few in numbers there are mountains higher than 1000 m, Sylhet and Chittagong Hill Tracts located near the northeastern and southeastern borders with India and Myanmar.

The southwest monsoon rains mainly sustain the agriculture of the subcontinent and its population. The onset and withdrawal of the monsoon are phenomena of much interest to the subcontinent. Though changes of wind to southwest, decrease in temperature, increase in rainfall etc. are associated with the onset of the monsoon, they are all not synchronous. Westerlies set in the Arabian Sea in May but the rains only in the following month. On account of the preponderating importance of rains, meteorologists in this part of the world have fixed the dates of onset and withdrawal with reference to the rather sharp increase and decrease respectively, seen in 5 - day means of rainfall and changes in circulation pattern. The monsoon rains are sometimes not easy to distinguish from pre-monsoon thundershowers.

The southwest monsoon makes its arrival of Bangladesh coast through the southeastern part, the mean date of onset is 2 June and it takes 13 days [1] to reach the northwestern part of the country. Meteorologically there are four seasons in Bangladesh namely; winter (December-February), pre-monsoon (March-May), monsoon (June-September) and post monsoon (October-November). About 70% of the total rainfall occurs during monsoon season over Bangladesh. Bangladesh routinely receives very heavy rainfall during the southwest monsoon season. July and August are peak months of monsoon rainfall period over Bangladesh due to synoptic and sub-synoptic systems in different active phases. Later monsoon starts its withdrawal process from extreme northwest Bangladesh by 1st September and slowly retreats in opposite direction of advance of monsoon till October. The periods of advance and withdrawal of southwest monsoon are related with variations of winter Eurasian/Himalayan snow cover extent. The southwest monsoon provides considerable portion of rainfall over Bangladesh in both onset and withdrawal phases through heavy precipitation episodes due to synoptic systems; these generally lead to flash floods of great volume in a short duration due to heavy rainfall. Monsoon rainfall is very essential for agriculture. The agricultural and land-use practices depend on the rainfall pattern and water availability.

The country is prone to disasters like floods, droughts and nor'westers. Variability of rainfall causes floods and droughts. The excess rainfall in Bangladesh and in the upper catchments of the Bangladesh rivers causes floods in Bangladesh. It is noted that 92% of the catchments of Ganges, Brahmaputra and Meghan lies outside Bangladesh and the runoff from these areas pass through Bangladesh which accounts for the 8% of the catchments. The severe floods cause the damages to crops, infrastructure, power supply, economic activities and overall livelihood of the affected areas. Besides, the heavy rainfall events cause flash floods and landslides. The later is very common in hilly area of Bangladesh. The deficit rainfall for a long period causes severe droughts affecting the agricultural crops, lack of water recourses for fisheries and livelihood of the people in various ways.

When classified according to amount of precipitation, rain can be divided into (<http://my.athenet.net>):

- very light rain when the precipitation rate is < 0.25 mm/hour
- light rain when the precipitation rate is between 0.25 mm/hour-1.0 mm/hour
- moderate rain when the precipitation rate is between 1.0 mm/hour - 4.0 mm/hour
- heavy rain when the precipitation rate is between 4.0 mm/hour-16.0 mm/hour
- very heavy rain when the precipitation rate is between 16.0 mm/hour-50 mm/hour
- extreme rain when the precipitation rate is > 50.0 mm/hour

The heavy rainfall over Bangladesh and other locations is a combination of a number of features such as the northwestward movement of low pressure systems from the Bay of Bengal along the monsoon trough, the increasing southwesterly monsoon strength over the Arabian Sea, and the presence of a northward moving mesoscale offshore vortex over the northeast Arabian Sea [2]. The formation, intensification and movement of the monsoon depression and the spatial temporal variability of the monsoon trough itself are very important aspects, which need to be studied.

Prediction of heavy rainfall is one of the many challenging problems in meteorology, but very important for issuing timely warnings for the agencies engaged in disaster preparedness and mitigation. For weather prediction, Hong and Pan (1996) [3] have shown that the prediction skills of a medium-range forecast model in forecasting precipitation are sensitive to the vertical mixing formulation, and to parameters such as the critical Richardson number used for determining the boundary layer height. Braun and Tao (2000) [4] and Li and Pu (2008) [5] have suggested that PBL schemes are important for cloud microphysics schemes

in forecasting hurricane intensity and accompanying precipitation. Steeneveld *et al.* (2008) [6] has evaluated the abilities of three regional models in predicting diurnal cycles, with special attention to the stable boundary layer (SBL) in the CASES-99 experimental campaign. Holtslag and Boville (1993) [7], and Steeneveld *et al.* (2008) [6] have shown that model results are dependent on the choice of PBL parameterization both at daytime and nighttime, while the simulated results of the nocturnal boundary layer are especially sensitive to the radiation scheme.

The PBL parameterizations executed in large-scale atmospheric numerical models are largely divided into first-order or one-and-a-half order (TKE) closure schemes. Holt and Raman (1988) [8] have evaluated eleven PBL schemes with one dimensional barotropic boundary layer model. They have found that the simulated mean boundary layer structure is hardly sensitive to the order of the closure, while the turbulent structure is better represented using the TKE closure. Musson-Genon (1995) [9] has shown that differences among the different closures occur for cloudy conditions, and the differences mainly occur through varying tunable parameters rather than closure types. Sharan and Gopalakrishnan (1997) [10] have found that under strong (weak) wind conditions, the turbulent diffusivities profiles are quite insensitive (sensitive) to PBL parameterizations, but the resultant mean wind and thermodynamic variables are quite variable (invariable) depending on PBL parameterizations.

Cuxart *et al.* (2006) [11] have compared 19 single column models (SCM), used by major operational NWP centers and research groups, for a moderately stratified atmospheric boundary layer using statistics from a corresponding large-eddy simulation under the first GEWEX (Global Energy and Water Cycle Experiment) Atmospheric Boundary Layer Study (GABLS) project. Generally, it has been that the operational models produce stronger mixing, resulting in the omission of the upper inversion development and overestimation of the surface friction velocity. Svensson and Holtslag (2006) [12] have documented the intercomparison of 18 SCMs to examine the validity of boundary-layer schemes in current and climate models under the second GABLS project. These one-dimensional model studies have revealed that the models produce divergent results in all compared variables, and there are noticeable discrepancies between the simulated values and observations.

Hu *et al.* (2010) [13] have compared with surface and boundary layer observations with 92 sets of daily, 36-h high-resolution WRF V.3.0.1 with three PBL schemes (MYJ, YSU, and ACM2) over south-central United States in a series of simulations spanning three months during summer 2005. They have shown that the simulations with the YSU and ACM2

schemes give much less bias than with the MYJ scheme. Simulations with the MYJ scheme, the only local closure scheme of the three, produced the coldest and moistest biases in the PBL. The differences among the schemes are found to be due to differences in vertical mixing strength and entrainment of air from above the PBL.

Shin and Hong (2011) [14] have compared the five planetary boundary-layer (PBL) parameterizations in the Weather Research and Forecasting (WRF) numerical model for a single day from the Cooperative Atmosphere-Surface Exchange Study (CASES-99) field program. Their result have suggested that the discrepancies among thermodynamic surface variables from different schemes are large at daytime, while the variables converge at nighttime with large deviations from those observed. On the other hand, wind components are more divergent at nighttime with significant biases. Regarding PBL structures, a non-local scheme with the entrainment flux proportional to the surface flux is favorable in unstable conditions. In stable conditions, the local TKE closure schemes show better performance. The WRF model has different PBL schemes, and continuous efforts have been made to investigate the sensitivity of the simulated precipitation and large-scale fields to these PBL schemes. However, there are few studies that document typical characteristics of one scheme compared to others in both unstable and stable boundary-layer regimes, focusing on the main roles of the PBL schemes: prediction of near-surface and PBL properties.

1.2 Objectives of the Study

The objective of the present research is to predict the high impact precipitation events over Bangladesh and its surrounding areas by using WRF-ARW models. Four heavy rainfall events of 27-29 July 2009, 15-16 August 2009, 26-27 June 2010 and 7-8 September 2011 have been simulated using Lin *et al.* MP scheme in combination with Kain-Fritsch (KF) cumulus parameterization (CP) scheme. In this respect, six different PBL schemes have been used for the simulation of these heavy rainfall events. The six different PBL schemes are Yonsei University Scheme (YSU), Mellor–Yamada–Janjic (MYJ), Quasi-Normal Scale Elimination (QNSE), Mellor–Yamada–Nakanishi–Nino Level 3 (MYNN3), Asymmetric Convective Model version 2 (ACM2) and Bougeault–Lacarrère (BouLac) scheme.

To understand the dynamical and thermodynamical characteristics of heavy precipitation systems wind, relative humidity, reflectivity, rainfall, accumulated upward heat flux, accumulated upward latent heat flux, downward long wave flux, outgoing long wave radiation and PBL have been analyzed.

In this study, attempt has been made to identify the effect of PBL for better prediction of heavy rainfall events in the monsoon season over Bangladesh.

1.3 Outline of the thesis

The thesis has been divided into five chapters:

Chapter-1 presents an introduction of thesis. This chapter incorporates background information to assist in understanding the aims and objectives of the thesis, and also reviews recent reports by other researchers.

Chapter-2 briefly describes literature review to understand the present work.

Chapter-3 describes WRF model, domain selection and configuration. **Chapter-4** describes of different meteorological parameter of different heavy rainfall event over Bangladesh.

Chapter-5 contains the concluding remarks.



CHAPTER II
LITERATURE REVIEW

2.1 WRF Model

Weather Research and Forecasting (WRF) is a next generation mesoscale numerical weather forecasting community model. Its simulation capacity is very high and can simulate meteorological phenomena ranging from meters to thousand kilometers. This chapter focuses on the few important feature of the Advance Research WRF (ARW) model using NCAR TECHNICAL NOTE NCAR/TN-475+STR Shamarock *et al.* [15].

2.2.1 Advanced Research WRF (ARW)

The ARW is the ARW dynamics solver together with other components of the WRF system compatible with that solver and used in producing a simulation. Thus, it is a subset of the WRF modeling system that, in addition to the ARW solver, encompasses physics schemes, dynamics option, initialization routines, and a data assimilation package (WRF-Var). The ARW solver shares the WSF with the NMM solver and all other WRF components within the framework. Physics packages are largely shared by both the ARW and NMM solvers, although specific compatibility varies with the schemes considered. The association of a component of the WRF system with the ARW subset does not preclude it from being a component of WRF configurations involving the NMM solver. The following section highlights the major features of the ARW, Version 3, and reflects elements of WRF Version 3, which was first released in April 2008. This technical note focuses on the scientific and algorithmic approaches in the ARW, including the solver, physics options, initialization capabilities, boundary conditions, and grid-nesting techniques.

2.3 Planetary Boundary Layer

The planetary boundary layer (PBL) is the layer in the lower part of the troposphere with thickness ranging from a few hundred meters to a few kilometers within which the effects of the Earth's surface are felt by the atmosphere. The PBL processes represent a consequence of interaction between the lowest layer of air and the underlying surface. The interactions can significant impact on the dynamics of the upper air flows. The influences of the small-scale eddies on large scale (model resalable scale) atmospheric circulations may be included in the model equations. Accurate depiction of meteorological conditions, especially within the PBL, is important for air pollution modeling, and PBL parameterization schemes play a critical role in simulating the boundary layer. This study examines the sensitivity of the performance of the WRF model to the use of six different PBL schemes. It is a very important portion of the

atmosphere to correctly model to provide accurate forecasts, e.g., air pollution forecasts (Deardorff 1972; Pleim 2007b) [16, 17]. As important as the PBL is, it has one basic property whose accurate and realistic prediction is paramount to its correct modeling: its height. After all, the height of the top of the PBL defines its upper boundary. This is critical since PBL parameterizations schemes in WRF-ARW models need to know the extent through which to mix properties such as heavy rainfall, relative humidity, outgoing long wave flux, downward long wave flux.

PBL schemes were developed to help resolve the turbulent fluxes of heat, moisture, and momentum in the boundary layer. However, due to the complex nature of turbulence, closure has remained a problem. Two solutions to the problem of closure, local and non-local, will be discussed below. The first type, local closure, estimates unknown fluxes using known values and/or gradients at the same point. The second type, non-local closure, estimates unknown fluxes using known values and/or gradients at many points in space (Stull 1988, Bélair et al. 1999) [18, 19]. Of the PBL schemes tested, the ACM2 and YSU schemes are non-local while the MYJ, QNSE, BouLac and MYNN 3.0 are local closure schemes. A brief description of the six PBL schemes used in this study follows. PBL Schemes options available in ARW model are discuss below:

Yonsei University (YSU) scheme: The Yonsei University (YSU) PBL [3] is the next generation of the MRF, Non local-K scheme with explicit entrainment layer and parabolic K profile in unstable mixed layer. The YSU scheme is a bulk scheme that expresses non-local mixing by convective large eddies. Non-local mixing is achieved by adding a non-local gradient adjustment term (counter gradient term) to the local gradient. At the top of the PBL, the YSU scheme uses explicit treatment of the entrainment layer, which is proportional to the surface layer flux (Hu *et al.* 2010, Shin and Hong 2011, Hong *et al.* 2006) [13, 14, 20].

Mellor- Yamada Janjic (MYJ) scheme: The MYJ PBL scheme is classified as TKE closure (one-and-a-half order closure) scheme, requiring one additional prognostic equation of the TKE. The MYJ PBL scheme is a local turbulent kinetic energy (TKE), 1.5 order (2.5 levels) closure scheme. Being a 1.5 order closure, it requires one additional prognostic equation to solve for the turbulent quantities (Hu *et al.* 2010, Shin and Hong 2011, Janjic 1990, 1994) [13, 14, 21, 22].

Quasi-Normal Scale Elimination (QNSE) PBL scheme: The QNSE scheme is a local TKE, 1.5 order (2.5 levels) closure scheme that is similar to the MYJ scheme during neutral and

unstable conditions. The QNSE scheme differs from the MYJ scheme during stable conditions, when spectral theory is used to develop eddy diffusivity profiles. This results in waves and turbulent eddies being treated as one entity. Like the MYJ and MYNN schemes, the QNSE scheme applies local mixing from the lowest to highest vertical level (Shin and Hong 2011, Sukoriansky *et al.* 2005) [14, 23].

Mellor-Yamada Nakanishi and Nino Level 2.5 PBL scheme: This MYNN 2.5 PBL scheme has the potential to help reduce some of the common biases associated with the Mellor-Yamada-Janjić (MYJ) (Janjić 2002)[24] scheme, such as shallow PBL and low temperature bias (Zhang and Zheng 2004)[25]. It treats consistently condensation physics in the boundary layer by considering liquid water potential temperature and total water content and allows for partial condensation in a model grid to assure proper interaction with microphysics and radiation.

Mellor-Yamada-Nakanishi-Nino Level 3 (MYNN3) PBL scheme: The MYNN 3.0 PBL scheme is a higher level scheme that was based on the MYJ scheme. The Mellor-Yamada-Nakanishi-Niino (MYNN) PBL scheme is a turbulent kinetic energy (TKE)-based local mixing scheme recently implemented into WRF-ARW. Main features this scheme is:

- Option to run at level 2.5 or 3.0 closure.
- Tuned to a database of LES simulations in order to overcome the typical biases associated with other MY-type schemes (insufficient growth of convective boundary layer and underestimated TKE).
- Updated stability functions allow for more mixing in slightly stable conditions.

Asymmetrical Convective Model version 2 (ACM2) PBL scheme: Asymmetric Convective Model with non-local upward mixing and local downward mixes [27]. The ACM2 scheme is a combination of a simple transilient model (original Blackadar scheme) and an eddy diffusion model. The ACM2 scheme is able to switch between stable conditions (eddy diffusion) and unstable conditions (local and nonlocal transport). During stable or neutral conditions, the scheme uses local closure instead of non-local transport (Hu *et al.*, 2010, Shin and Hong 2011, Pleim 2007a, 2007b,) [13, 14, 27, 17].

Bougeault-Lacarrère (BouLac) PBL scheme: The BouLac PBL scheme is classified as TKE closure (one-and-a-half order closure) schemes, requiring one additional prognostic equation of the TKE [28].

NCEP Global Forecast System (GFS) scheme: First-order vertical diffusion scheme of Troen and Mahrt (1986) [29] further described in Hong and Pan (1996, MWR) [3]. The PBL is determined using an iterative bulk-Richardson approach working from the ground upward whereupon the profile of the diffusivity coefficient is specified as a cubic function of the PBL. Coefficient values are obtained by matching the surface-layer fluxes. A counter-gradient flux parameterization is included (3). (This scheme is well tested and used operationally at NCEP for HWRF.)

Bretherton-Park/UW TKE scheme: TKE scheme from CESM climate model.

TEMF PBL scheme: Total Energy - Mass Flux (TEMF) scheme. Sub-grid total energy prognostic variable plus mass-flux type shallow convection. The Total Energy - Mass Flux PBL scheme for WRF uses eddy diffusivity and mass flux concepts to determine vertical mixing. For the eddy diffusivity part, TEMF could be considered a "1.5 order" or "level 2.5" (Mellor-Yamada) scheme.

MRF PBL scheme: Older version of YSU with implicit treatment of entrainment layer as part of non local K mixed layer. This scheme is described by Hong and Pan [3].

2.4 Microphysics Schemes

Microphysics includes explicitly resolved water vapor, cloud, and precipitation processes. The model is general enough to accommodate any number of mixing ratio variables, and other quantities such as number concentrations. Four-dimensional arrays with three spatial indices and one species index are used to carry such scalars. Memory, i.e., the size of the fourth dimension in these arrays, is allocated depending on the needs of the scheme chosen, and advection of the species also applies to all these required by the microphysics options. In the current version of the ARW, microphysics is carried out at the end of the time step as an adjustment process, and so does not provide tendencies. The rationale for this is that condensation adjustment should be at the end of the time step to guarantee that the final saturation balance is accurate for the updated temperature and moisture. However, it is also important to have the latent heating forcing for potential temperature during the dynamical sub-steps, and this is done by saving the microphysical heating as an approximation for the next time step.

Currently, the sedimentation process is accounted for inside the individual microphysics modules, and, to prevent instability in the calculation of the vertical flux of precipitation, a smaller time step is allowed. The saturation adjustment is also included inside microphysics.

In the future, however, it might be separated into an individual subroutine to enable the remaining microphysics to be called less frequently than the model's advection step for efficiency.

Different schemes of microphysics option available in ARW are discuss as follows:

- a. Kessler scheme: A warm-rain (i.e. no ice) scheme used commonly in idealized cloud modeling studies [30].
- b. Purdue Lin scheme: A sophisticated scheme that has ice, snow, and graupel processes, suitable for real-data high resolution simulations. All parameterization production terms are based on Lin et al [26] and Rutledge and Hobbs [31] with some modifications.
- c. WRF Single-Moment 3-class (WSM3) scheme: A simple efficient scheme with ice and snow processes suitable for mesoscale grid sizes which follows Hong *et al* [32].
- d. WRF Single-Moment 5-class (WSM5) scheme: A slightly more sophisticated version of (c) that allows for mixed-phase processes and super-cooled water [32, 33].
- e. Eta microphysics: The operational microphysics in NCEP models; A simple efficient scheme with diagnostic mixed- phase processes [34].
- f. WRF Single-Moment 6-class (WSM6) scheme: A scheme with ice, snow and graupel processes suitable for high resolution simulations [32, 35].
- g. Goddard microphysics scheme: A scheme with ice, snow and graupel processes suitable for high resolution simulations [36].
- h. Thompson *et al.* scheme: A new scheme with ice, snow and graupel processes suitable for high resolution simulations [37].
- i. Morrison double- moment scheme: Double-moment ice, snow, rain and graupel for cloud-resolving simulations [38].
- j. Milbrandt-Yau Double-Moment 7-class scheme: This scheme includes separate categories for hail and graupel with double-moment cloud, rain, ice, snow, graupel and hail.

2.5 Cumulus Parameterization Schemes

These schemes are responsible for the sub-grid-scale effects of convective and/or shallow clouds. The schemes are intended to represent vertical fluxes due to unresolved updrafts and downdrafts and compensating motion outside the clouds. They operate only on individual columns where the scheme is triggered and provide vertical heating and moistening profiles.

Some schemes provide cloud and precipitation field tendencies in the column, and future schemes may provide momentum tendencies due to convective transport of momentum. The schemes all provide the convective component of surface rainfall.

Cumulus parameterizations are theoretically only valid for coarser grid sizes, (e.g., greater than 10 km), where they are necessary to properly release latent heat on a realistic time scale in the convective columns. Where the assumptions about the convective eddies being entirely sub-grid-scale break down for finer grid sizes, sometimes these schemes have been found to be helpful in triggering convection in 5-10 km grid applications. Generally they should not be used when the model can resolve the convective eddies itself (e.g., <5 km grid).

The available cumulus parameterization options in the ARW are as following:

- a. Kain-Fritsch scheme: Deep and shallow convection sub-grid scheme using a mass flux approach with downdrafts and Convectively Available Potential Energy (CAPE) removal time scale. The modified version of the KF scheme [39] is as based on KF [40] and KF [41].
- b. Bets-Miller-Janjic scheme: Operational Eta scheme. Column moist adjustment scheme relaxing towards a well-mixed profile [22, 24].
- c. Grell-Devenyi Ensemble scheme: Multi closure, Multi-parameter, ensemble method with typically 144 sub-grid members [42].
- d. Grell 2d ensemble cumulus scheme: Scheme for higher resolution domains allowing for subsidence in neighboring columns.
- e. Old Kain-Fritsch scheme: Deep convection scheme using a mass flux approach with downdrafts and CAPE removal time scale.

2.6 Relative Humidity

Relative humidity is the ratio of the partial pressure of water vapor in the air-water mixture to the saturated vapor pressure of water at those conditions. The relative humidity of air depends not only on temperature but also on pressure of the system of interest. So it is defined as the ratio of the observed vapor pressure to that required for saturation at the same temperature. Designating it as f , we have

$$f = e/e_s \times 100 = w/w_s \times 100 = q/q_s \times 100$$

The multiplication by 100 being for the purpose of expressing it as a percentage

Vapor pressure $e = e_s / 100$

The relative humidity is a measure of the amount of water vapor in the air (at a specific temperature) compared to the maximum amount of water vapor air could hold at that temperature, and is given as a percentage value. Relative humidity depends on the temperature of the air, as warm air can hold more moisture than cold air. A relative humidity of 100 percent indicates that the air is holding all the water it can at the current temperature and any additional moisture at that point will result in condensation. A relative humidity of 50 percent means the air is holding half the amount of moisture that it could. As the temperature decreases, the amount of moisture in the air doesn't change, but the relative humidity goes up (since the maximum amount of moisture that cooler air can hold is smaller). When referring to pet care, the terms humidity and relative humidity are usually used interchangeably. For an example, if we say the appropriate humidity for hermit crabs is 70-80 percent, we are speaking of the relative humidity.

In order for cloud formation and rain to occur, the air where the clouds are forming (or from which the rain originates) must reach 100% relative humidity. Often, rain will fall from air at 100% relative humidity to air where humidity is less than 100% (most people with instruments to measure air humidity are measuring the humidity of this "lower" air, which will likely range from 60-100% humidity during a rainstorm). As the rain falls, this means that some of the rain will evaporate into the water of lesser humidity. The air at lower elevations will not usually reach 100% humidity as a result of this, however.

When the air reaches this point, it will feel very wet because the air is completely saturated. It will be foggy and perhaps a bit misty and drizzly, but it takes more than air saturation for rain. For rainfall to begin, the raindrops must be heavier than the surrounding air. Sometimes, there may be 100% humidity, but the raindrops are not large enough to fall...that's why not all clouds create rain. As an interesting side note, most rain actually begins with ice crystals in clouds which draw moisture and then fall when they are sufficiently large.

100% can result in rain, but rain normally results when the atmosphere becomes over saturated with water vapor. 100% humidity is when the atmosphere is holding the maximum amount of water it can. At this point, fog and dew start to form. If that air were too cool further, then it could not hold that moisture in vapor, and it would precipitate out as rain. The faster the drop in temperature, the harder it will rain.

Also think about different layers in the atmosphere. A warm moist air mass can rise, cool, and expand which can raise its humidity past the saturation point. That rain could fall into warmer air and be absorbed back into the air before it hits the ground since that air has not been saturated yet.

100% humidity means complete saturation, but rain is usually caused by the air being over saturated by temperature or pressure changes. When it rains, it is common to report the humidity at 100%, but that is just because the rain is the result of the atmosphere shedding the water vapor it can no longer hold so it can remain at 100% humidity.

2.7.1 Atmospheric Radiation

The radiation schemes provide atmospheric heating due to radiative flux divergence and surface downward long wave and shortwave radiation for the ground heat budget. Long wave radiation includes infrared or thermal radiation absorbed and emitted by gases and surfaces. Upward long wave radiative flux from the ground is determined by the surface emissivity that in turn depends upon land-use type, as well as the ground (skin) temperature. Shortwave radiation includes visible and surrounding wavelengths that make up the solar spectrum. Hence, the only source is the sun, but processes include absorption, reflection and scattering in the atmosphere and its surfaces. For shortwave radiation, the upward flux is the reflection due to surface albedo. Within the atmosphere the radiation responds to model predicted cloud and water vapor distributions, as well as specified carbon dioxide, and (optionally) tracer gas concentrations. All the radiation schemes in WRF currently are column (one-dimensional) schemes, so each column is treated independently, and the fluxes correspond to those in infinite horizontally uniform planes, which is an approximation if the vertical thickness of the model layers is much less than the horizontal grid length. This assumption would become less accurate at high horizontal resolution.

2.7.2 Outgoing Long wave Radiation

The Earth Radiation budget is made up of the incoming solar flux and the outgoing Top-of-the-Atmosphere (TOA) radiative fluxes. The outgoing radiative fluxes consist of the reflected part of the incoming solar flux, as well as the thermal flux emitted by the Earth-atmosphere system. The thermal flux is often referred to as Outgoing Long wave radiation (OLR). The OLR is a very important parameter for the Earth's radiation budget study as well as for weather/climate model validation purposes. Variations in the OLR reflect the response of the

Earth-atmosphere system to solar diurnal forcing. Those variations can be found in particular in surface temperature, cloud cover, cloud top height, and related quantities like precipitation. The OLR is therefore well suited for validation of global circulation models (GCMs) simulating the diurnal cycle, as it constitutes the combination of different model aspects. The OLR can be directly estimated from broadband radiance measurements by a satellite instrument such as the GERB. Alternatively, the OLR can be indirectly inferred from narrowband radiance observations. The SEVIRI OLR is obtained from the IR and WV radiance and the satellite viewing angle via a regression scheme. The OLR is currently not operationally derived - the shown results are the outcome of a feasibility study. This product is a candidate product for a future reprocessing facility within EUMETSAT to support the derivation of climate-relevant parameters.

2.7.2 Downward long wave radiation

The downward long wave radiation is mostly from the atmosphere. It depends on the temperature and moisture of the atmosphere. The water vapor and other gases, aerosols absorb some solar energy and emit some long wave radiation energy computation of downward long wave radiation from the atmosphere is difficult, even when the distributions of water vapor, carbon dioxide, cloudiness, and temperature are measured. Some satellite measurements like TOVS estimates downward long wave radiation. Little long wave radiation is reflected by the surface: natural surface emission is dominant. It is also difficult to measure and define the surface temperature especially vegetation surface. To combine the above four components makes the calculation of net radiation at the surface. This is not accurate because the errors in each accumulate. So it is developed the research to use some satellite measurements-NOAA, GOES etc.

CHAPTER III
METHODOLOGY

3.1 Selection of Model

In this study, the Weather Research and Forecast (WRF-ARW Version 3.2.1) model is used to evaluate its performances for the simulation of some heavy rainfall events and other parameters in the monsoon season.

3.2 Experiments on simulation of different heavy rainfall events

To understand the genesis, characteristics and structure of the heavy rainfall systems, different meteorological parameters have been simulated for different heavy rainfall events. In this research, four heavy rainfall events have been considered. The events are 27-29 July 2009, 15-16 August 2009, 26-27 June 2010 and 7-8 September 2011.

3.3 Domain and Model Physics

Domain and model physics set up are the one of the vital thing for the simulation of any event in WRF-ARW model. Domain set up and discussion of model physics is given in the following sub-sections and in Table 1.

3.3.1 Domain set up

For the heavy rainfall events, two domains are taken; Domain 2 covers the whole Bangladesh region. Ratio of the resolution of the two domains is 3:1 respectively. The horizontal grid resolution of the domain 1 is 9 km and that of the domain 2 is 3 km respectively.

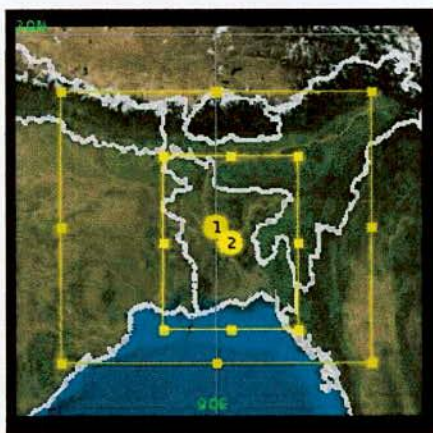


Fig. 3.1: Domain configuration for grid resolution of 9 km and 3 km.

3.3.2 WRF Model and Domain configurations

In this study, the Advanced Research WRF (WRF-ARW Version 3.2.1) model is used. It consists of fully compressible non-hydrostatic equations and different prognostic variables. The model vertical coordinate is terrain following hydrostatic pressure and the horizontal grid is Arakawa C-grid staggering. Third-order Runge-Kutta time integration has been used in the model. The model is configured in nested domain, 9 and 3 km horizontal grid spacing with 28 vertical levels. There are different microphysics and different cumulus parameterization in WRF – ARW model. In this work, Lin *et al.* microphysics scheme is used that contain prognostic equations for cloud water, rainwater, cloud ice, snow, and graupel mixing ratio. The Rapid Radiative Transfer Model (RRTM) scheme is chosen for long-wave (Mlawer *et al.*, 1997) [43] radiation and the Dudhia (1989) [44] scheme for short wave radiation is used for the simulation of heavy rainfall events in the monsoon season over Bangladesh. The 5-layer thermal diffusion option with prognostic soil temperature and land-use-dependent soil-moisture availability represents the land surface. Different PBL schemes e.g. Yonsei University (Hong *et al.*, 2006) [20], Mellor-Yamada-Janjic (Eta) TKE scheme, QNSE, MYNN3 level TKE, ACM2 and BouLac etc. are used for the simulation of heavy rainfall events.

The modified Kain- Fritsch cumulus parameterization scheme is used in this case [39]. The cloud microphysics scheme is Lin *et al.* simple ice scheme, which is a simple efficient scheme with ice and snow processes suitable for mesoscale grid sizes [32]. The long wave radiation parameterization is the Rapid Radiative Transfer Model (RRTM) scheme, which is an accurate scheme using look-up tables for efficiency accounts for multiple bands, trace gases, and microphysics species [43]. The short wave radiation scheme is as per the Dudhia scheme, which allows simple downward integration for efficient cloud and clear- sky absorption and scattering [44]. The Planetary boundary Layer (PBL) parameterizations are the YSU, MYJ, QNSE, MYNN3, ACM2, and BouLac, which are the next generation MRF-PBL. An overview of the model used in this study is provided in Table 1.

Table 1: WRF Model and Domain Configurations

Dynamics	Non-hydrostatic
Number of domain	2
Central points of the domain	D1: Central Lat.: 25.29°N, Central Lon.: 88.77°E D2: Central Lat.: 23.91°N, Central Lon.: 90.52°E
Horizontal grid distance	1) Outer Domain-9 km, 2) Inner Domain-3 km
Integration time step	45 s
Number of grid points	D1: X-direction 198 points, Y-direction 131 points D2: X-direction 157 points, Y-direction 199 points
Map projection	Mercator
Horizontal grid distribution	Arakawa C-grid
Nesting	One way
Vertical co-ordinate	Terrain-following hydrostatic-pressure co-ordinate (28 sigma levels up to 100 hPa)
Time integration	3rd-order Runge-Kutta
Spatial differencing scheme	6th-order centered differencing
Initial conditions	Three-dimensional real-data (FNL: 1° × 1°)
Lateral boundary condition	Specified options for real-data
Top boundary condition	Gravity wave absorbing (diffusion or Rayleigh damping)
Bottom boundary condition	Physical or free-slip
Diffusion and Damping	Simple Diffusion
Microphysics	Lin <i>et al.</i> (1983) scheme
Radiation scheme	Dudhia (1989) for short wave radiation/ RRTM long wave Mlawer <i>et al</i> (1997)
Surface layer	Monin– Obukhov similarity theory scheme (Hong and Pan, 1996)
Land surface parameterization	5 Layer Thermal diffusion scheme (Ek <i>et al.</i> , 2003)
Cumulus parameterization schemes	Kain-Fritsch (KF) scheme, (Kain and Fritsch, 1990, 1993; Kain, 2004)
PBL parameterization	1) Yonsei University Scheme (YSU) (Hong <i>et al.</i> , 2006), (2) Mellor–Yamada–Janjic (MYJ), (3) Quasi-Normal Scale Elimination (QNSE), (4) Mellor–Yamada–Nakanishi–Nino Level 3 (MYNN3), (5) Asymmetric Convective Model version 2 (ACM2) and (6) Bougeault–Lacarrère (BouLac) scheme.

3.4 Initial Data Source

For the simulation of heavy rainfall events, the WRF model has been run for 72 hours and in some cases 48 hours. Final Reanalysis (FNL) data ($1^0 \times 1^0$) from National Centre for Environmental Prediction (NCEP) was used as initial and lateral boundary conditions (LBCs) which is updated at six hourly interval i.e. the model was initialized with 0000, 0600, 1200 and 1800 UTC initial field of corresponding dates of different events. Tropical Rainfall Measuring Mission (TRMM)-3B42RT-daily rainfall data sets were downloaded, while daily rain gauge data set collected by Bangladesh Meteorological Department (BMD) at 31 stations over Bangladesh were used for the same analysis period.

3.5. Synoptic situation

3.5.1 Synoptic situation of Heavy Rainfall event 27-29 July 2009

On 27 July 2009, a low pressure system developed over North Bay and adjoining Bangladesh coast. Again on 28 July 2009, the low over North Bay and adjoining Bangladesh coast moved northwestwards and merged with the axis of the monsoon trough. Under its influence deep convection was taking place over North Bay and adjoining coastal areas of Bangladesh. Steep pressure gradient persisted over North Bay. During 27-29 July 2009, monsoon axis ran through Rajasthan, Uttar Pradesh, Bihar, West Bengal and Northeastwards to Assam across central part of Bangladesh. One of its associated troughs extended to North Bay. Monsoon was active over Bangladesh and strong over North Bay during 27-29 July.

3.5.2 Synoptic situation of Heavy Rainfall event 15-16 August 2009

On 15 August, monsoon axis ran through Punjab, Hariyana, Uttar Pradesh, Madhya Pradesh, Bihar, West Bengal and northeastwards to Assam across northern part of Bangladesh. One of its associated troughs extended to North Bay. Monsoon was active over Bangladesh and moderate over North Bay on the same day. Again on 16 August, monsoon axis ran through Punjab, Hariyana, Uttar Pradesh, Bihar, West Bengal and northeastwards to Assam across central part of Bangladesh. One of its associated troughs extended to North Bay. On this day, monsoon was fairly active over Bangladesh and moderate over North Bay.

3.5.3 Synoptic situation of Heavy Rainfall event 26-27 June 2010

On 26 June, the low was persisting over Northwest Bay and its adjoining area. On the same day, monsoon was fairly active over Bangladesh and strong elsewhere over North Bay. On 27

June, trough of low was found over North Bay and monsoon was fairly active over Bangladesh and moderate over North Bay.

3.5.4 Synoptic situation of Heavy Rainfall event 7-8 September 2011

On 7 September, monsoon axis was found to run through Rajasthan, Uttar Pradesh, Bihar, West Bengal and northeastwards to Assam across central part of Bangladesh. One of its associated troughs extended to Northwest Bay. Monsoon was fairly active over Bangladesh and moderate elsewhere over North Bay on the same day. Again on 8 September, monsoon axis ran through Rajasthan, Hariyana, Uttar Pradesh, Bihar, West Bengal and northeastwards to Assam across central part of Bangladesh. One of its associated troughs extended to Northwest Bay. On this day, monsoon was fairly active over Bangladesh and strong elsewhere over North Bay. Steep pressure gradient was found to lie over North Bay.

CHAPTER IV
SIMULATION OF HEAVY RAINFALL EVENTS
USING WRF-ARW MODEL

4.1 Heavy rainfall event of 27-29 July 2009 using WRF model

4.1.1 Accumulated Upward Heat Flux (ACHFX) at the surface

WRF model simulated accumulated upward heat flux at 1200 UTC of 28 July 2009 at the surface is shown in Fig.1 (a-f). The ACHFX is maximum in the southern part along the land-ocean boundary of Bangladesh for all schemes. Maximum areas of minimum ACHFX have been simulated by QNSE scheme at 1200 UTC of 28 July 2009 in the southern to eastern region. The MYNN3 scheme has also simulated more ACHFX all over the domain than that of all other schemes. From the figure it is also observed that the ACHFX is minimum in the southeastern part but the flux is maximum along the land-ocean boundary.

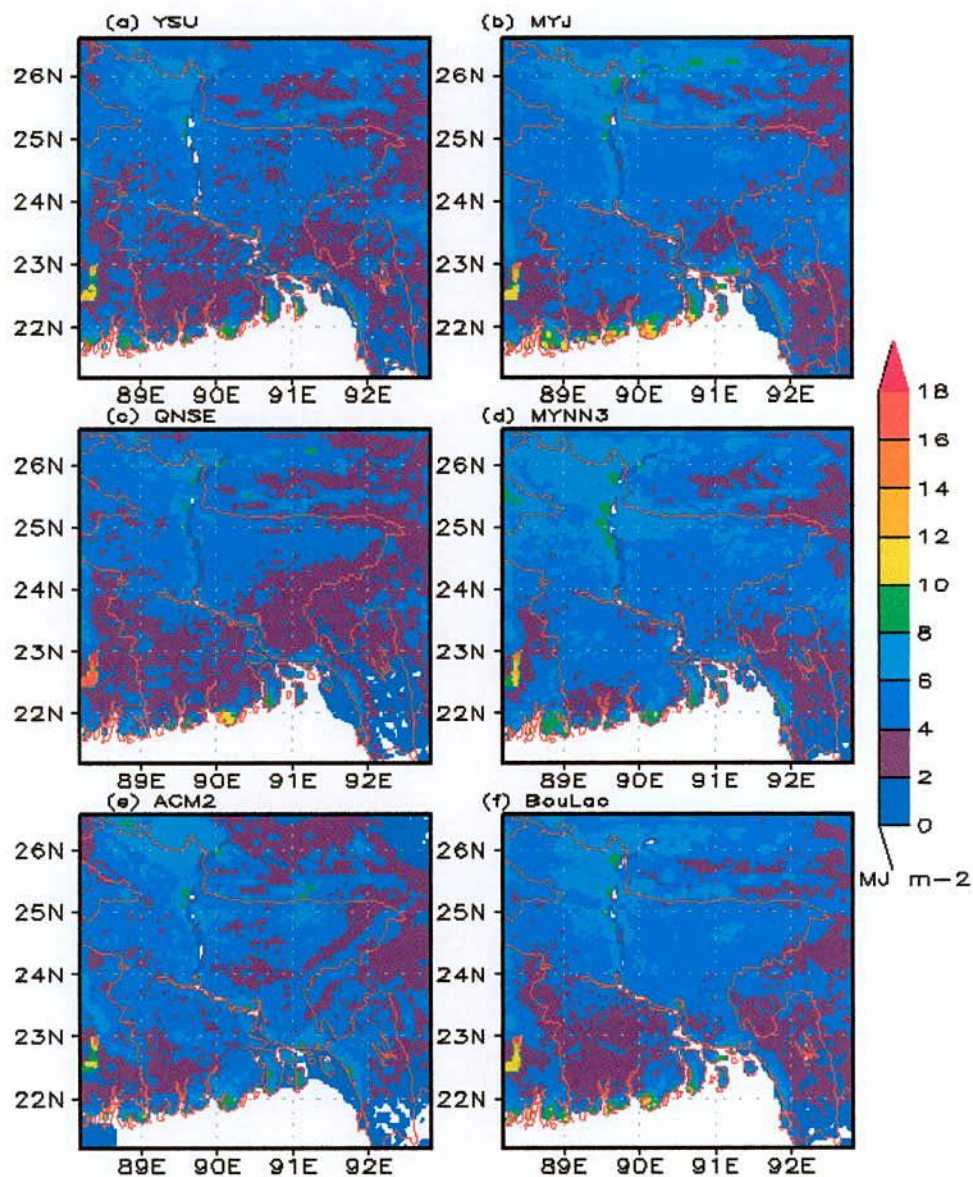


Fig. 1: Spatial distribution of simulated ACHFX using a) YSU, b) MYJ, c) QNSE, d) MYNN3, e) ACM2 and f) BouLac schemes at 1200 UTC of 28 July 2009.

Figure 2(a-f) shows the spatial distribution of ACHFX using different schemes at 1200 UTC of 29 July 2009. On this day the simulated ACHFX has also found maximum in the southern part along the land-ocean boundary of Bangladesh for all schemes. The minimum and maximum ACHFX is simulated all over Bangladesh by ACM2 and MYNN3 schemes respectively on 29 July. Significant amount of ACHFX is simulated in the southern boundary by MYJ scheme. From figure it is also observed that the accumulated upward heat flux simulated minimum in the southeastern part but the flux simulated maximum along the land-ocean boundary.

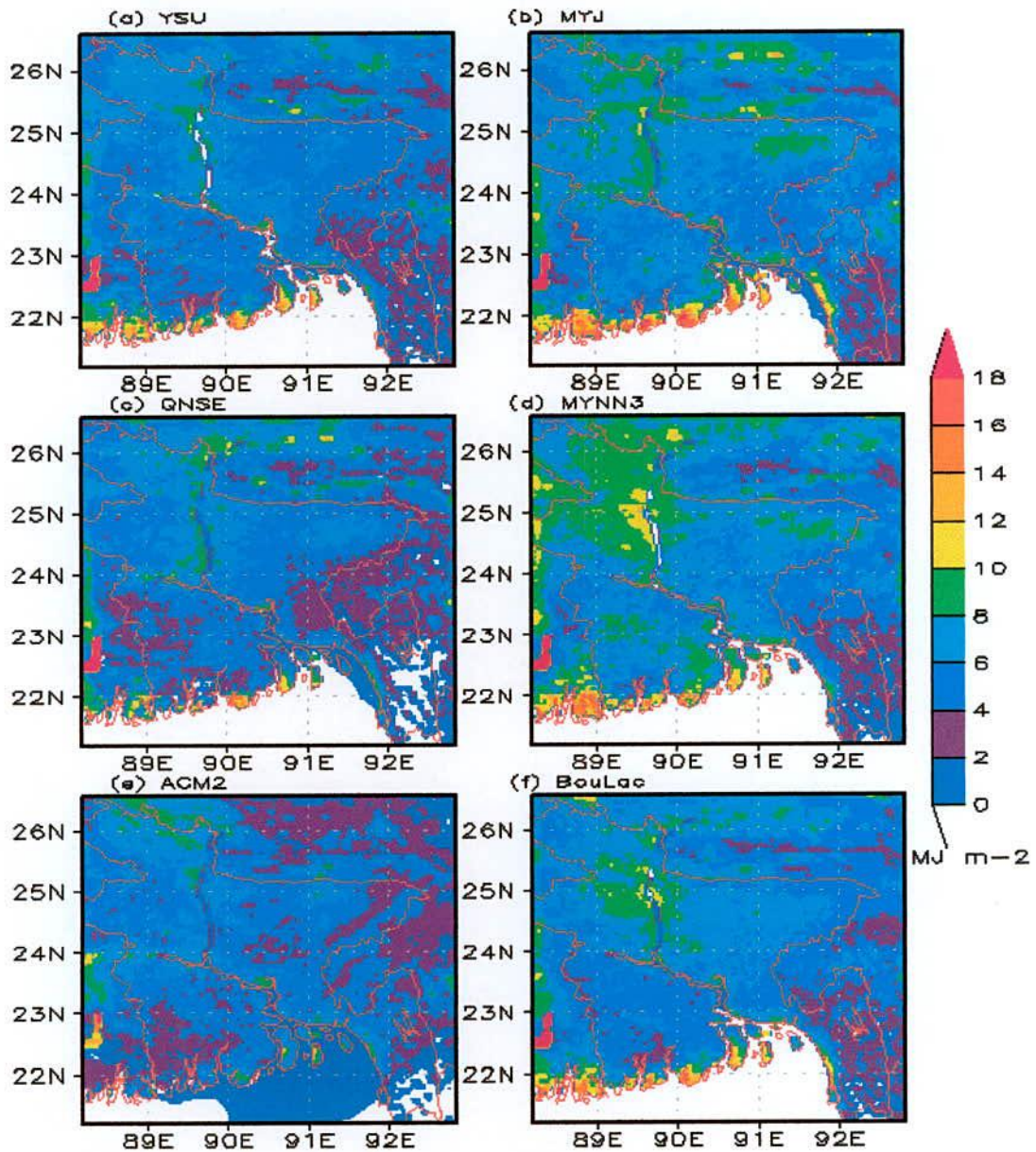


Fig. 2: Spatial distribution of simulated ACHFX using a) YSU, b) MYJ, c) QNSE, d)MYNN3, e) ACM2 and f) BouLac schemes at 1200 UTC of 29 July 2009.

The simulated ACHFX has also been maximum (Fig. not shown) at 0000 UTC of 28 July 2009 in the southern part along the land-ocean boundary of Bangladesh for all schemes and the minimum ACHFX simulated in the southeastern and southwestern region of Bangladesh.

Minimum ACHFX has been simulated at D2, where the location is relatively covered by a cloud sky during the 24-h period of interest and the maximum ACHFX is found over the less rainfall area in that location. From figure it has been found that the ACHFX is minimum in the northwestern, southern region and the model has also simulated maximum rainfall in that region by all schemes.

4.1.2 Accumulated Upward Latent Heat Flux (ACLHF) at the surface

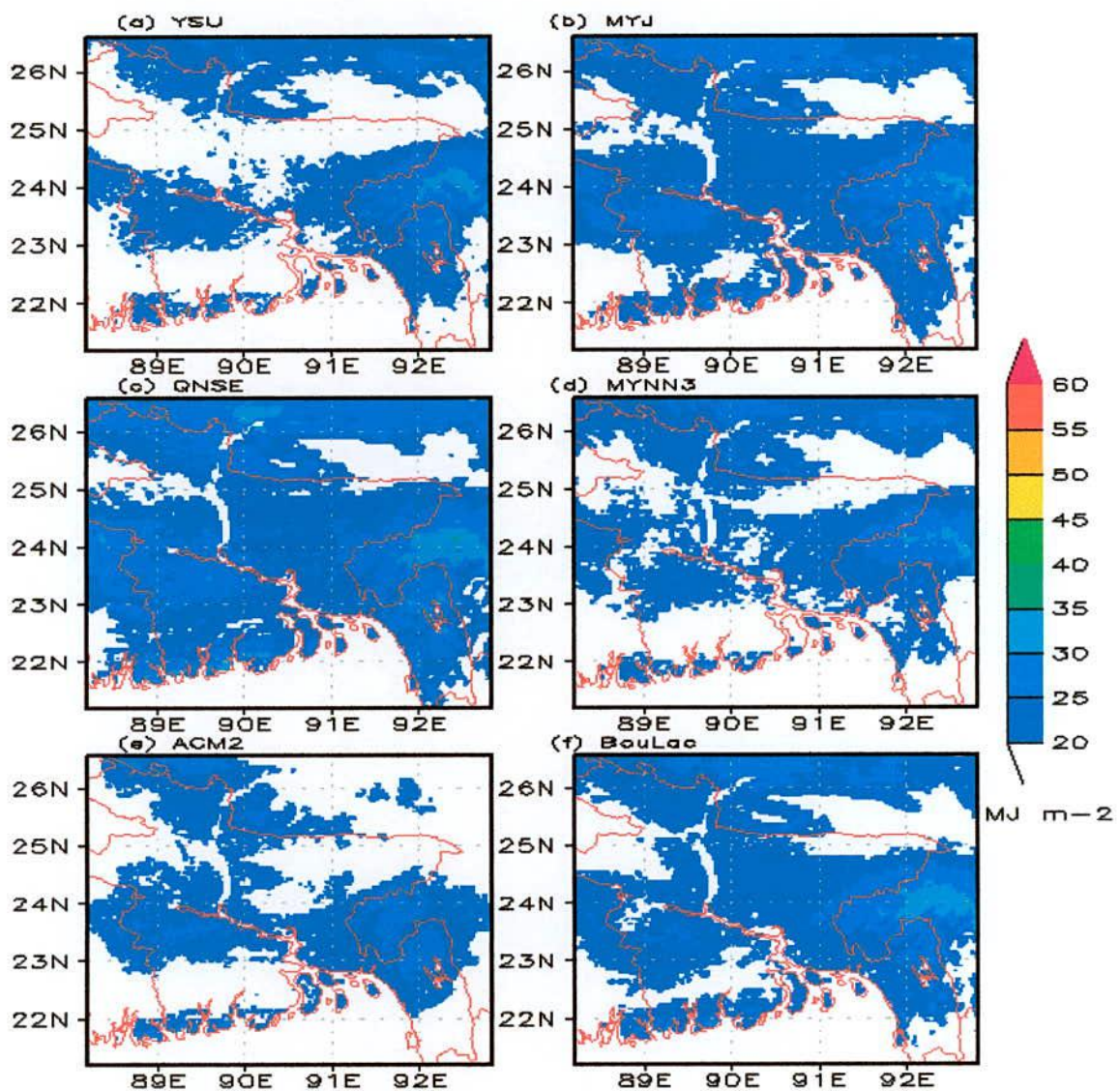


Fig. 3: Spatial distribution of simulated ACLHF using a) YSU, b) MYJ, c) QNSE, d) MYNN3, e) ACM2 and f) BouLac schemes at 1200 UTC of 28 July 2009.

WRF model has simulated accumulated upward latent heat flux (ACLHF) at 1200 UTC of 28 July at the surface by using YSU, MYJ, QNSE, MYNN3, ACM2 and BouLac schemes are shown in Fig. 3(a-f). The YSU, MYNN3 and ACM2 schemes have simulated almost 0-25 MJ m⁻² ACLHF all over the country, which is the lowest value. The simulated ACLHF is 25-30 MJ m⁻² in the western region of Bangladesh by using MYJ (Fig. 3b) and QNSE (Fig. 3c) schemes. From the figure it is also observed that the ACLHF is minimum in the southeastern part of Bangladesh for all PBL schemes. On this day the simulated ACLHF is maximum for QNSE scheme.

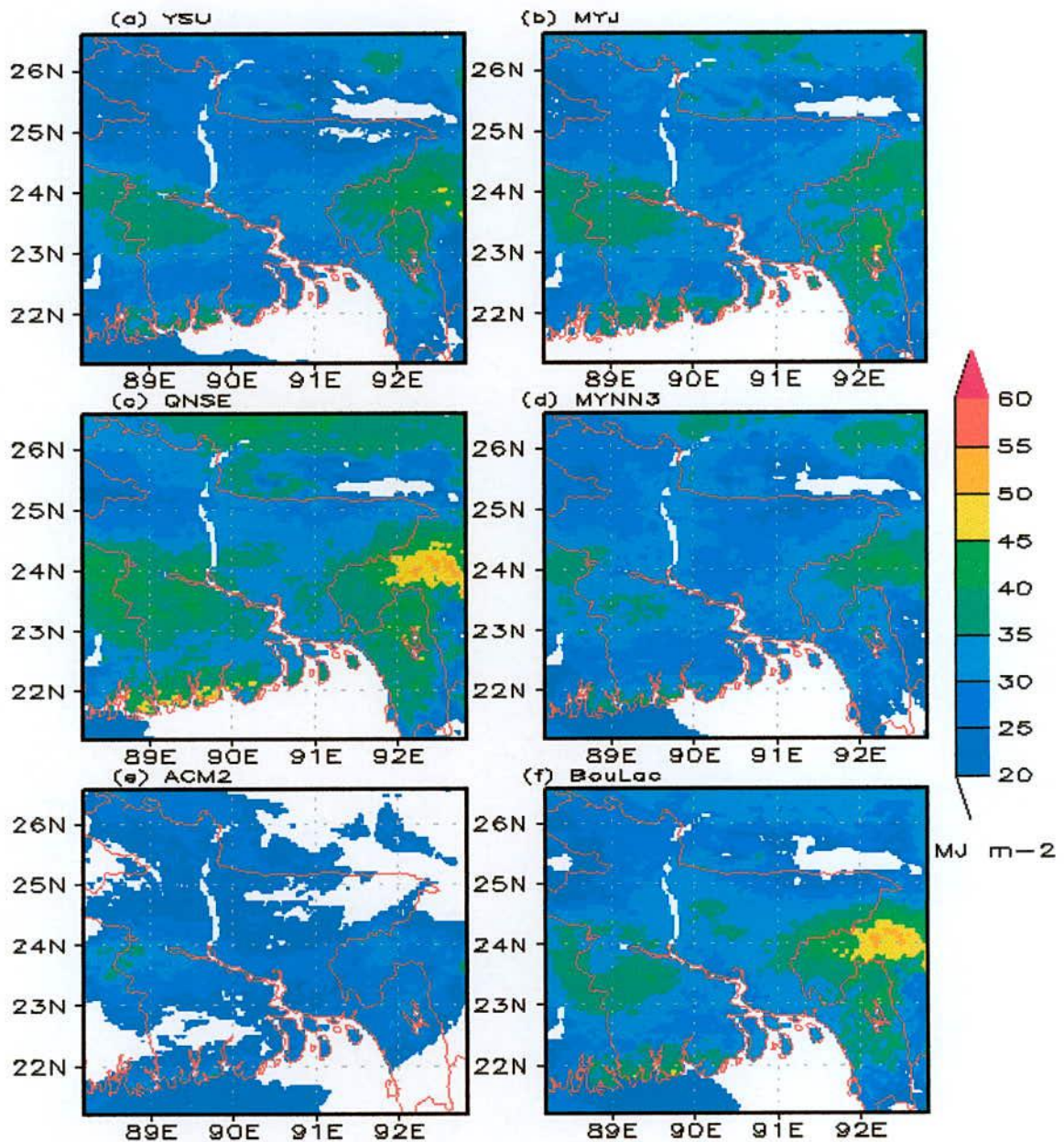


Fig.4: Spatial distribution of simulated ACLHF using a) YSU, b) MYJ, c) QNSE, d) MYNN3, e) ACM2 and f) BouLac schemes at 1200 UTC of 29 July 2009.

Figure 4(a-f) represents the simulated ACLHF at 1200 UTC of 29 July 2009 at the surface for six different schemes. At 1200 UTC of 29 July 2009 the significant amount of ACLHF has been simulated by YSU, MYJ, QNSE, MYNN3 and BouLac schemes. Out of all PBL scheme QNSE has simulated maximum and ACM2 has simulated minimum ACLHF all over Bangladesh. For all schemes, the minimum ACLHF has simulated in the northern region of Bangladesh and the maximum ACLHF has simulated in the eastern and western region. The simulated ACLHF has also significant in the land-ocean boundary of Bangladesh.

4.1.3 Downward Long Wave Flux at Ground Surface (GLW)

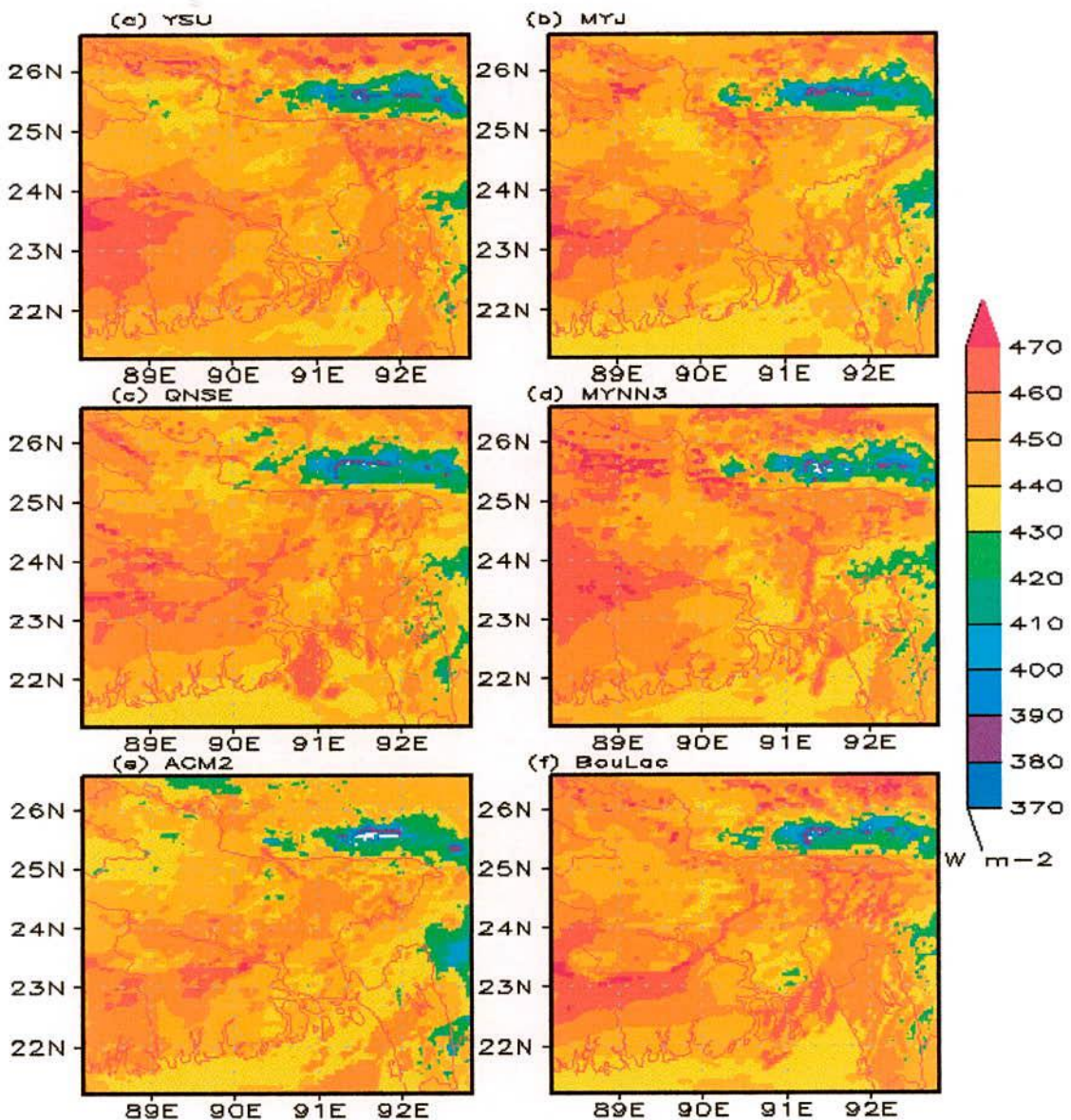


Fig. 5: Spatial distribution of simulated GLW using a) YSU, b) MYJ, c) QNSE, d) MYNN3, e) ACM2 and f) BouLac schemes at 1200 UTC of 28 July 2009.

Figs. 5(a-f) show the spatial distribution of model simulated downward long wave flux ($W m^{-2}$) at the surface using six different schemes at 1200 UTC of 28 July 2009. The simulated GLW is minimum in the northeastern and eastern region of domain D2 (outside Bangladesh) for all schemes. The simulated GLW is maximum in the western region of Bangladesh for all schemes. From figure, it has also been observed that significant amount of GLW have been simulated all over Bangladesh by all schemes.

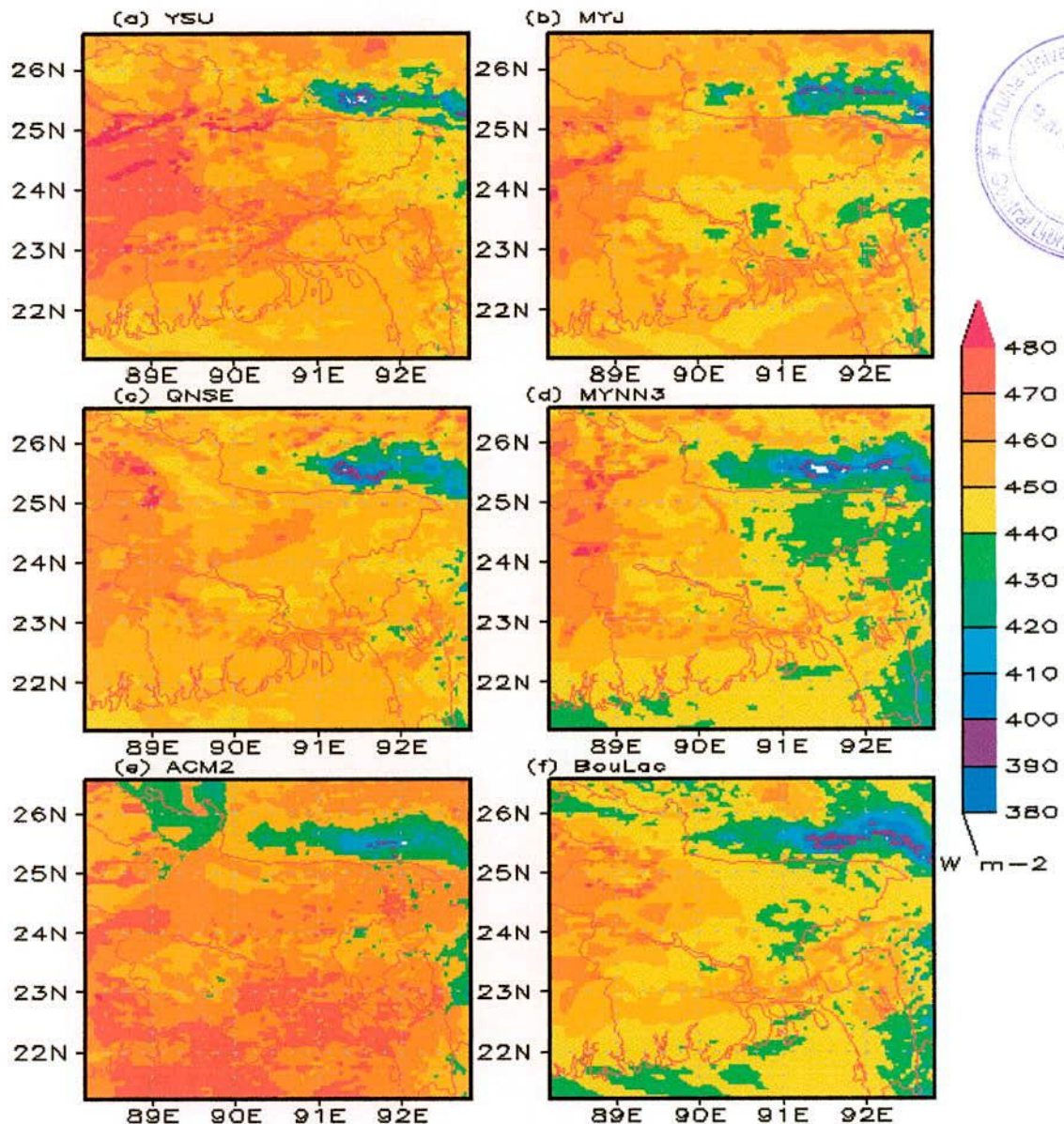


Fig. 6: Spatial distribution of simulated GLW using a) YSU, b) MYJ, c) QNSE, d) MYNN3, e) ACM2 and f) BouLac schemes at 1200 UTC of 29 July 2009.

At 1200 UTC of 29 July 2009, the GLW has been simulated minimum in the northeastern and eastern region of domain D2 (outside Bangladesh) for all schemes. The minimum GLW

has also been simulated in the eastern, southern and southeastern region of Bangladesh by MYNN3 (Fig. 6d) and BouLac (Fig. 6f) schemes. The simulated GLW has been maximum in the western region of Bangladesh for all schemes and significant for YSU (Fig. 6a) and ACM2 (Fig. 6e) schemes. The simulated GLW has also maximum in the southern region for ACM2 scheme.

4.1.4 Outgoing Long Wave Radiation (OLR)

WRF Model simulated outgoing long wave radiation of domain D2 at 1200 UTC of 28 and 29 July 2009 using different PBL schemes are presented in Figs. 7 & 8.

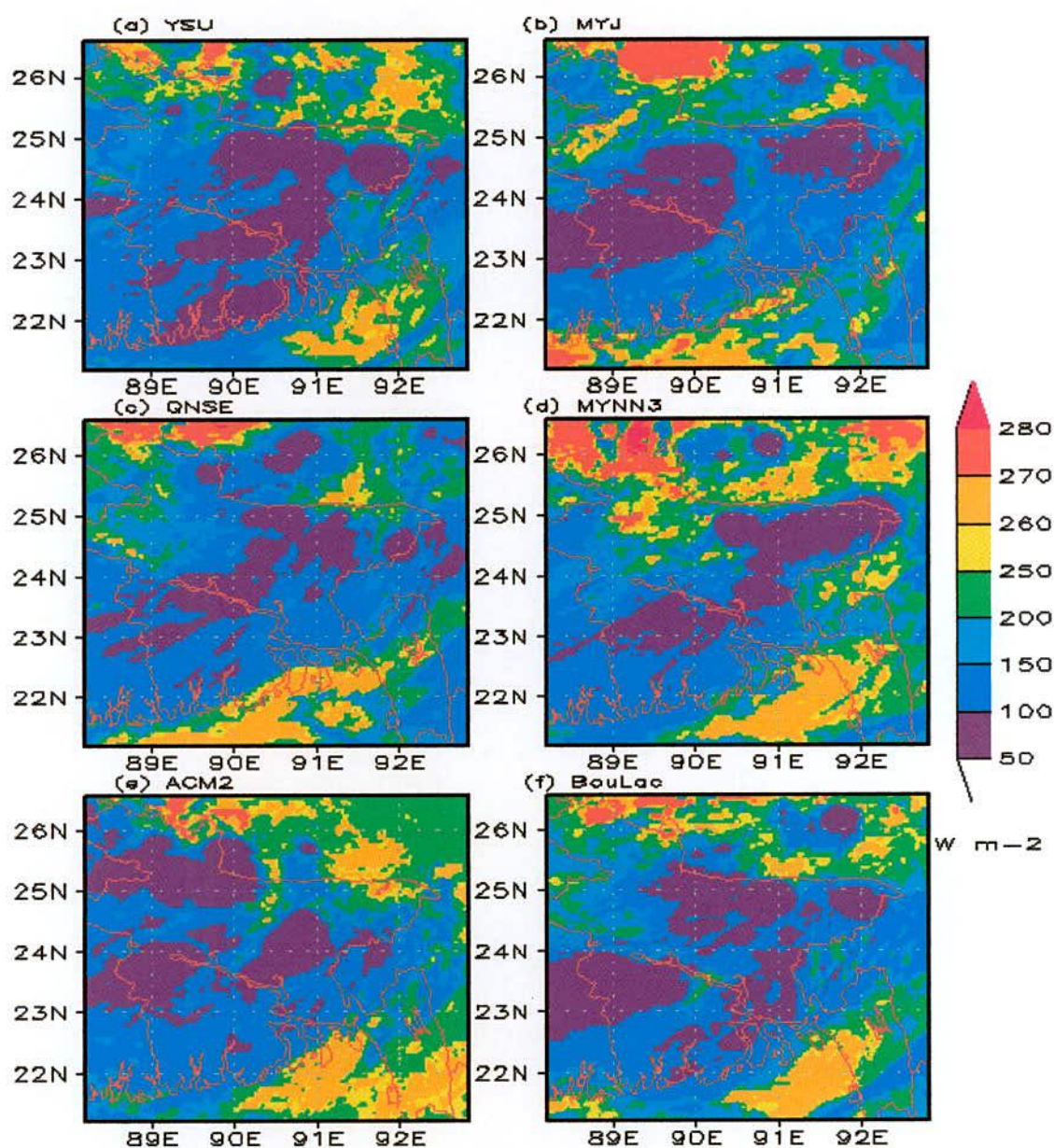


Fig. 7: Spatial distribution of simulated OLR using a) YSU, b) MYJ, c) QNSE, d) MYNN3, e) ACM2 and f) BouLac schemes at 1200 UTC of 28 July 2009.

Figure 7 shows that the simulated the OLR is minimum ($50 - 100 \text{ W/m}^2$) in the central to western region for all schemes. The OLR has also minimum in the northwestern region for ACM2 (Fig. 7e) and southwestern region of Bangladesh for YSU (Fig. 7a) schemes. The maximum OLR is simulated in the northwestern region of Bangladesh by MYNN3 (Fig. 7d) scheme and northwestern region but outside Bangladesh by MYJ (Fig. 7b) scheme.

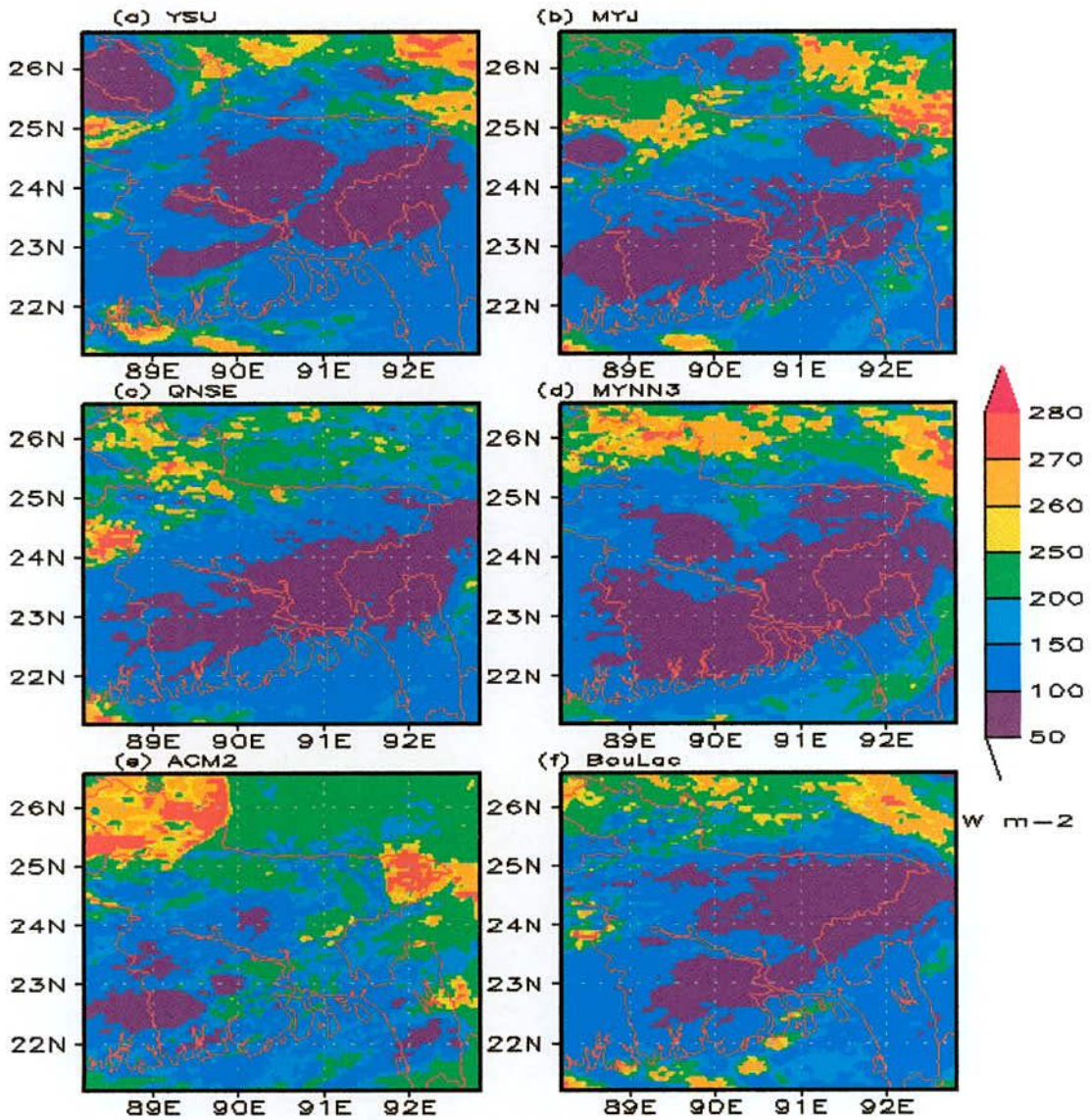


Fig. 8: Spatial distribution of simulated OLR using a) YSU, b) MYJ, c) QNSE, d) MYNN3, e) ACM2 and f) BouLac schemes at 1200 UTC of 29 July 2009.

The minimum OLR has also been simulated in the central to eastern and northeastern region by YSU, MYJ, QNSE, MYNN3 and BouLac schemes. The simulated minimum OLR position has been shifted in the most southern region of Bangladesh for MYNN3 scheme. The ACM2 scheme has simulated maximum OLR in the northwestern region and minimum

OLR in the southwestern region of Bangladesh at 1200 UTC of 29 July 2009. The minimum OLR has also been simulated in the northwestern region by YSU (Fig. 8a) scheme.

The outgoing radiative fluxes consist of the reflected part of the incoming solar flux, as well as the thermal flux emitted by the Earth-atmosphere system. The thermal flux is often referred to as Outgoing Long wave Radiation (OLR). The OLR reflected minimum from the earth to the atmosphere in the rainy and cloudy sky conditions. Overall, model can capture the maximum rainfall over Chittagong region consistent with low values of the OLR data (The daily OLR values $<200 \text{ Wm}^{-2}$ indicate deep convection). The MYJ and ACM2 schemes simulated minimum OLR but at the same time maximum rainfall simulated by MYJ and ACM2 schemes on 28 and 29 July 2009.

4.1.5 Variation of Planetary Boundary Layer (PBL)

WRF Model simulated PBL (meter) extended of domain D2 at 1200 UTC of 28 and 29 July 2009 using different PBL schemes are presented in Figs. 9 & 10 respectively. The YSU (Fig. 9a) scheme has simulated maximum PBL at southeastern, eastern and southwestern region and minimum PBL simulated in the central to northern region. From Fig. 9(b & e) it has been found that the MYJ and ACM2 schemes have simulated maximum PBL in the southeastern region and the minimum PBL has also been simulated in the northwestern region. The maximum and significant PBL has been simulated by using QNSE (Fig. 9c) scheme in the southern, southeastern and northeastern region. Fig. 9d shows that the maximum PBL has been simulated in the northwestern region.

On 29 July, the YSU (Fig. 10a) and QNSE (Fig. 10c) schemes have simulated maximum PBL in the southern and western region and minimum PBL has been simulated in the central to northern and northeastern region. In the cases of MYJ (Fig. 10b) and MYNN3 (Fig. 10d) schemes the simulated PBL has been minimum all over Bangladesh except southern and southeastern region. The maximum PBL has been simulated by using ACM2 scheme (Fig. 10e) in the southern and northwestern region and the minimum PBL has been simulated in the central to northern and northeastern region of Bangladesh. In case of BouLac scheme the constant PBL has been simulated all over the country on 28 and 29 July 2009.

From the figure, if the simulated rainfalls (mm) are compared with the PBL (meter) it has been found that the maximum PBL indicates minimum rainfall occurring and the minimum PBL (meter) indicates the heavy rainfall occurring in that position.

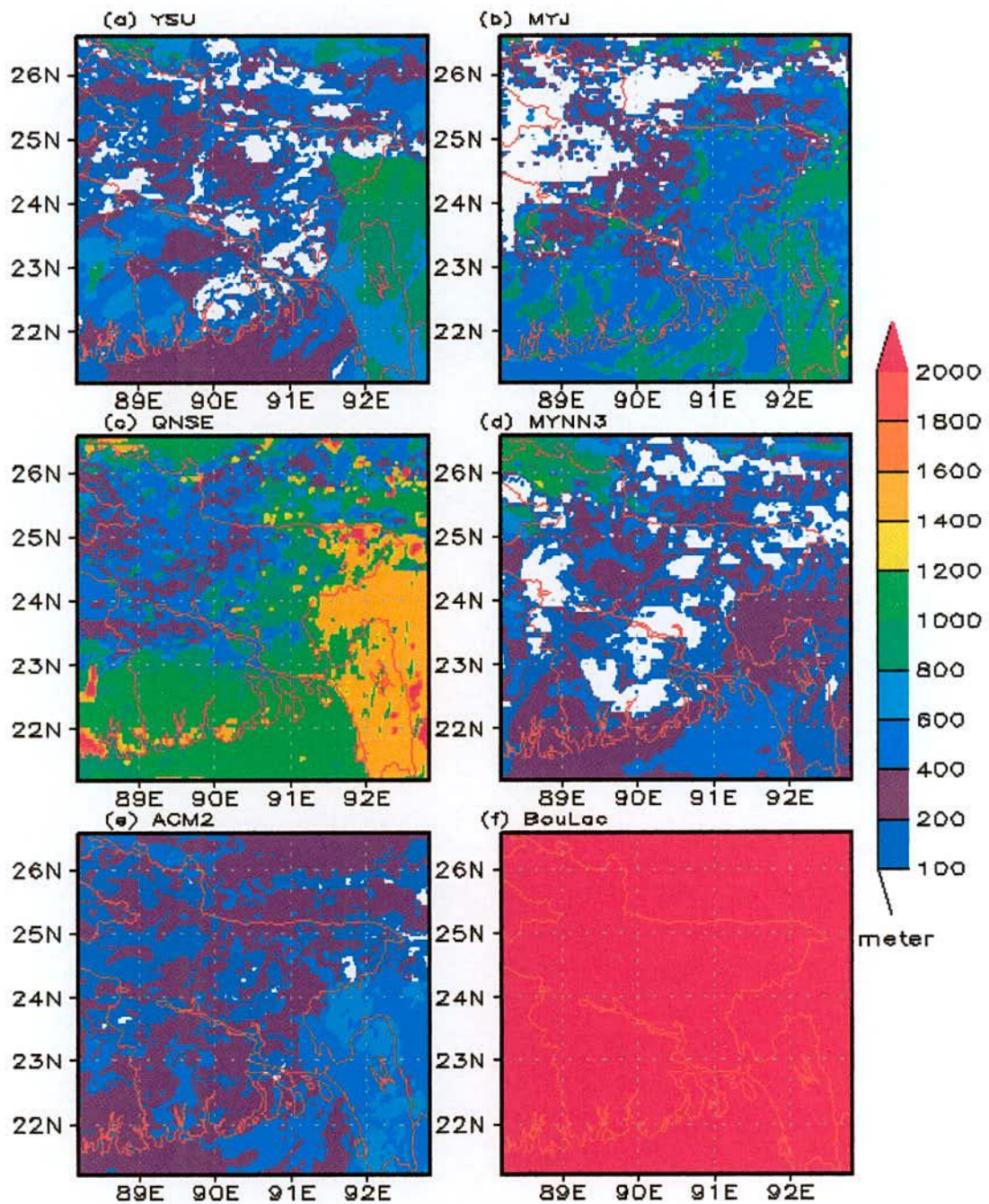


Fig. 9: Spatial distribution of simulated PBL height using a) YSU, b) MYJ, c) QNSE, d) MYNN3, e) ACM2 and f) BouLac schemes at 1200 UTC of 28 July 2009.

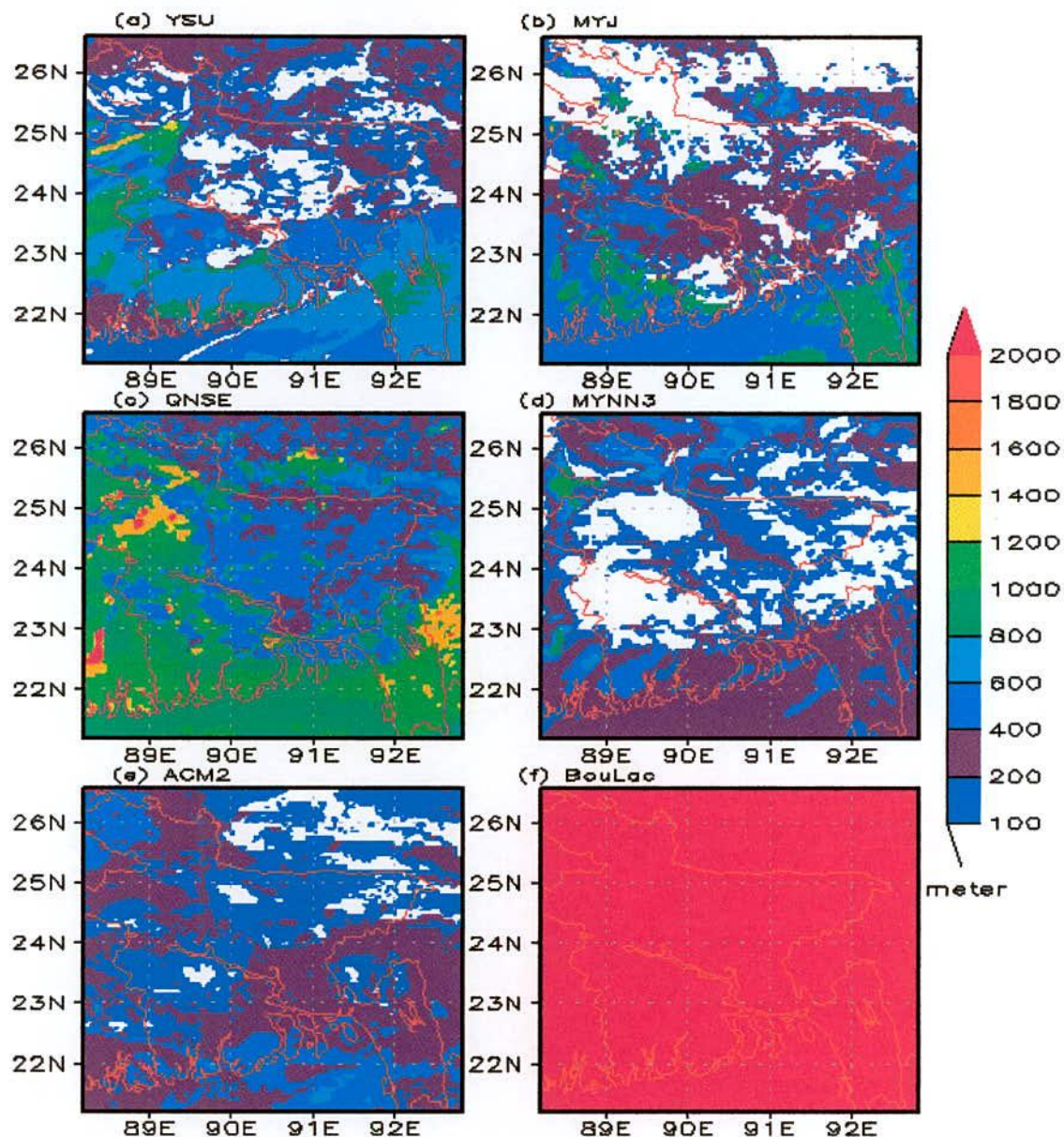


Fig. 10: Spatial distribution of simulated PBL height using a) YSU, b) MYJ, c) QNSE, d) MYNN3, e) ACM2 and f) BouLac schemes at 1200 UTC of 29 July 2009.

4.1.6 Reflectivity

The WRF model simulated spatial distribution of reflectivity (shaded) of 850 hPa levels using different PBL schemes at 1200 UTC of 28 and 29 July 2009 have been presented as in Figs. 11 & 12. The YSU (Fig. 11a) scheme has simulated significant amount of reflectivity in the eastern and northeastern region and maximum reflectivity have been simulated in the western part of Sylhet. The MYJ (Fig. 11b) and BouLac (Fig. 11f) schemes have simulated significant amount of reflectivity in the central and northeastern region and QNSE (Fig. 11c) and MYNN3 (Fig. 11d) schemes have simulated maximum reflectivity in the northeastern region

of Bangladesh at the same time. The ACM2 scheme has simulated maximum reflectivity in the central and northern regions.

The ACM2 (Fig. 12e) scheme has simulated maximum reflectivity in the southern and southeastern region at 850 hPa levels for 1200 UTC of 29 July 2009. The YSU (Fig. 12a), MYJ (Fig. 12b), QNSE (Fig. 12c), MYNN3 (Fig. 12d) and BouLac (Fig. 12f) schemes have simulated significant amount of reflectivity in the eastern region of Bangladesh on 29 July 2009.

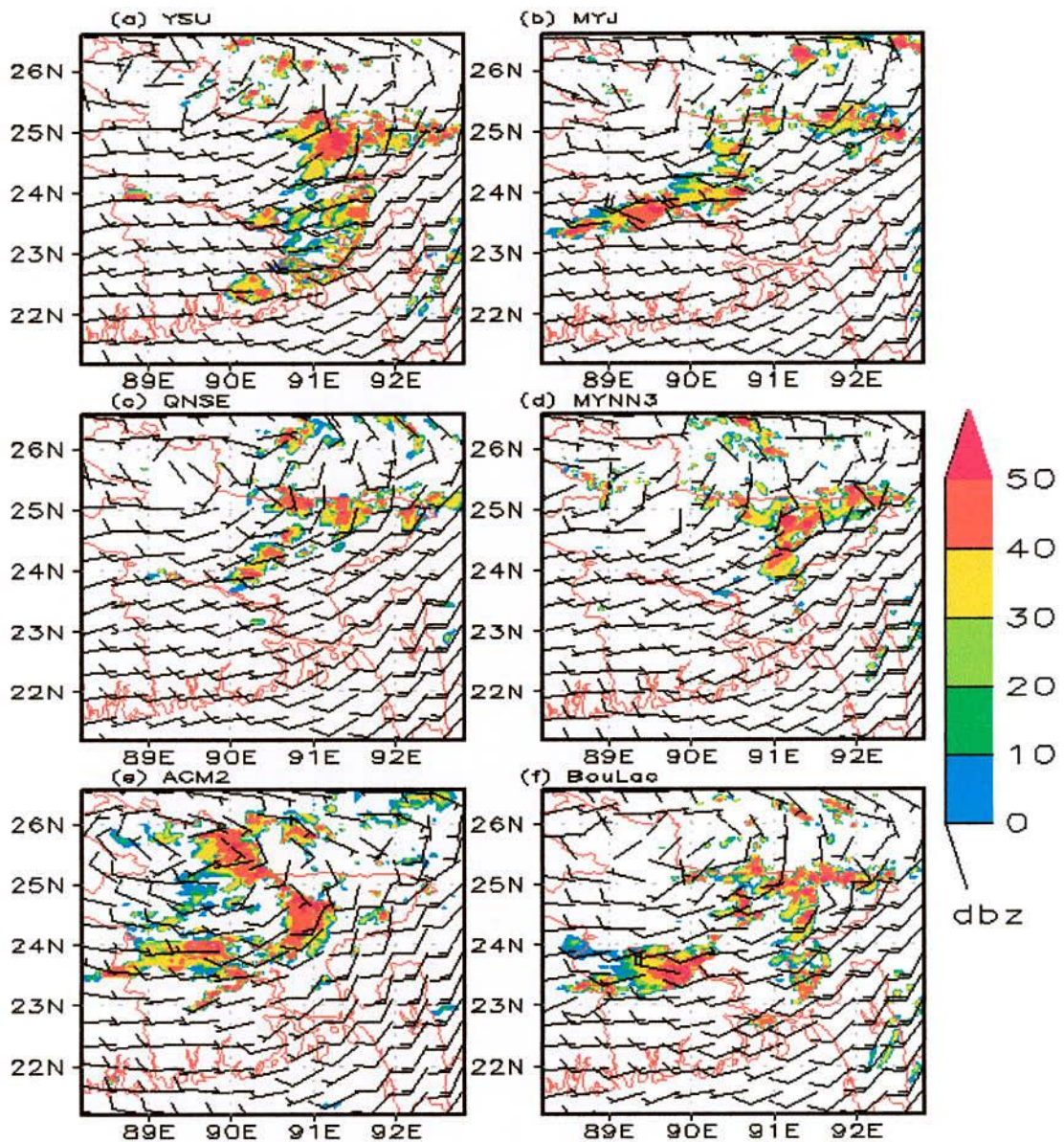


Fig. 11: Spatial distribution of simulated wind speed (m/s) and reflectivity (dBZ) at 850 hPa level using a) YSU, b) MYJ, c) QNSE, d) MYNN3, e) ACM2 and f) BouLac schemes at 1200 UTC of 28 July 2009.

4.1.7 Wind

The maximum wind speed simulated 20 m/s by using YSU, QNSE, MYNN3 and BouLac schemes and 15 m/s by using MYJ and ACM2 schemes in the southeastern side of maximum reflectivity. The maximum wind speed is simulated in the eastern and southeastern region of all PBL schemes at this time. The minimum wind speed is simulated by all schemes in the western and northern side of maximum reflectivity at 850 hPa level of 1200 UTC of 28 July 2009.

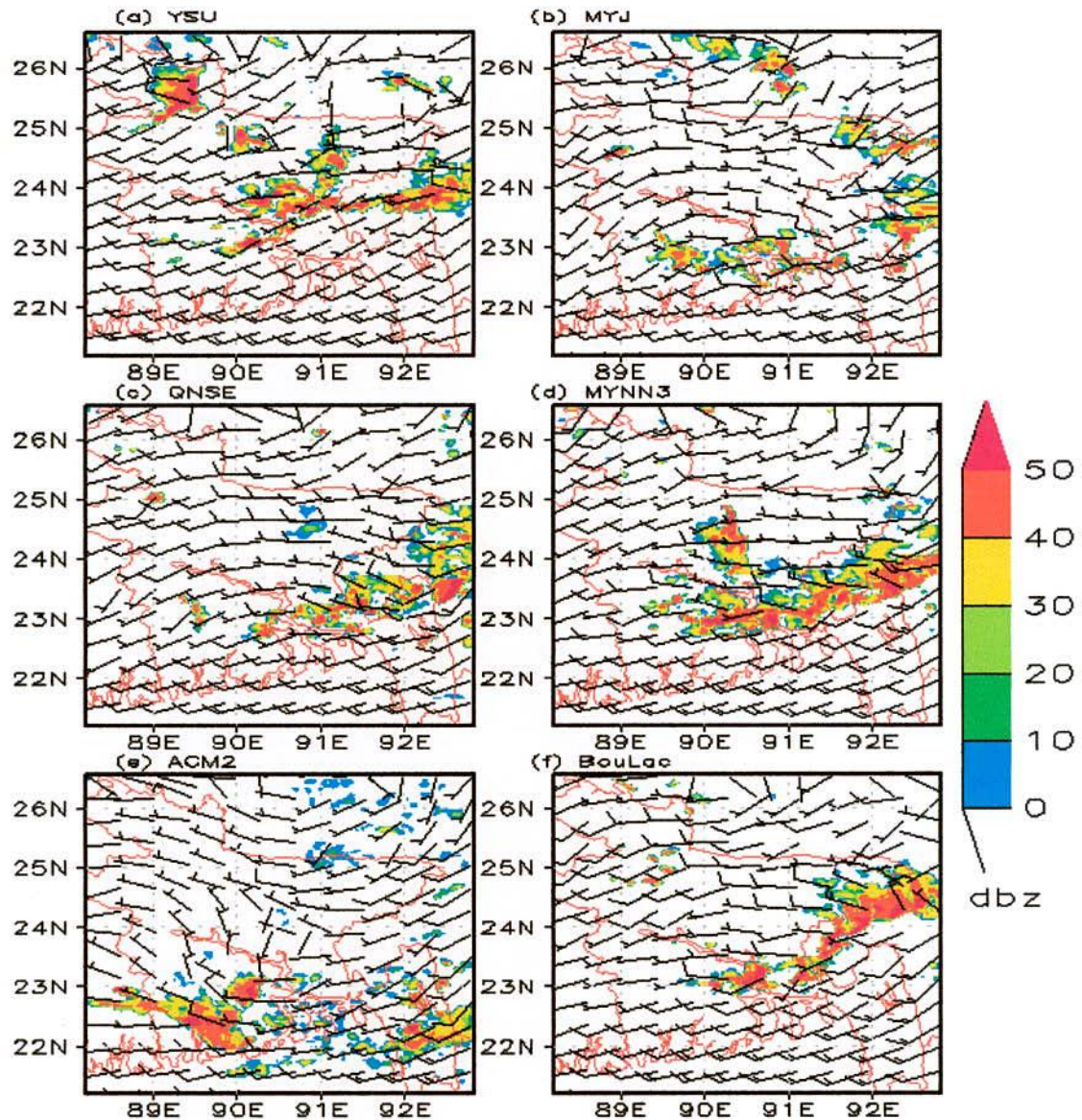


Fig. 12: Spatial distribution of simulated wind speed (m/s) and reflectivity (dBZ) at 850 hPa level using a) YSU, b) MYJ, c) QNSE, d) MYNN3, e) ACM2 and f) BouLac schemes at 1200 UTC of 29 July 2009.

At 0000 UTC of 29 July 2009 (figure not shown), all schemes simulated westerly wind in the southern side and easterly wind in the northern side i.e. cyclonic circulation exist in and

around the maximum reflectivity. The maximum wind speed of 20 m/s has been simulated by using MYJ schemes in the inner portion and 15 m/s by using YSU, QNSE and MYNN3 schemes, 15 m/s by using BouLac scheme and 10 m/s by using ACM2 scheme in the southwestern side of maximum reflectivity. The minimum wind speed has been simulated in the western and northern side of maximum reflectivity by all schemes at 850 hPa level.

The maximum wind speed of 15 m/s has been simulated (Fig. 12) by using all schemes in the southern region of maximum reflectivity at 850 hPa levels on 1200 UTC of 29 July 2009. The minimum wind speed simulated in the northeastern side of maximum reflectivity by using all schemes at the same time and levels.

4.1.8 Relative Humidity (RH)

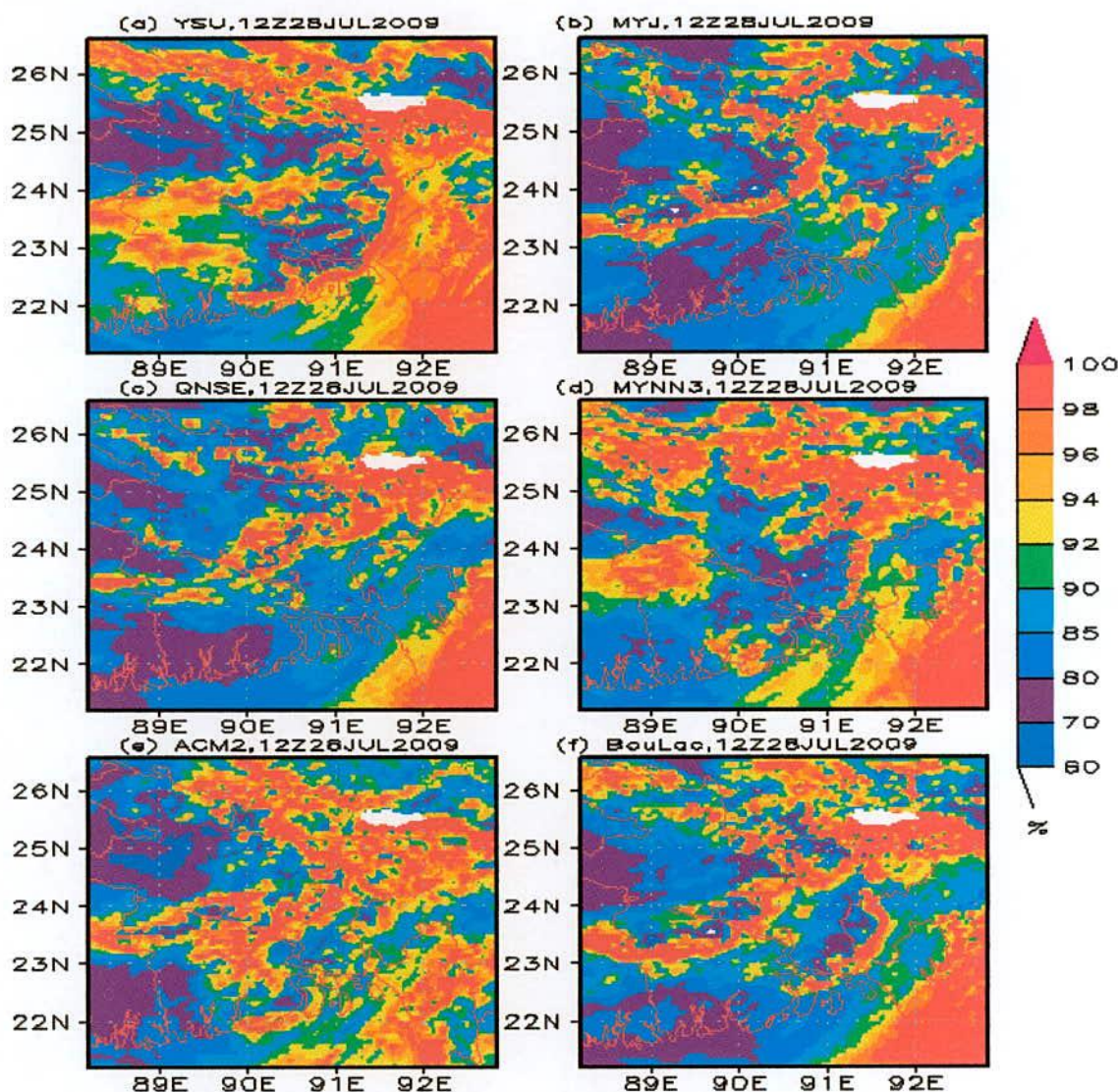


Fig. 13: Spatial distribution of simulated RH using a) YSU, b) MYJ, c) QNSE, d) MYNN3, e) ACM2 and f) BouLac schemes at 1200 UTC of 28 July 2009.

WRF model has simulated relative humidity (RH) of Domain2 at 850 hPa levels for 1200 UTC of 28 July 2009 and are presented in Figure 13(a-f). The YSU, MYJ and BouLac schemes have simulated maximum RH in the southeastern region and minimum RH is in the western and southwestern regions of Bangladesh. The maximum RH is simulated by QNSE scheme in the southeastern and northeastern regions of Bangladesh. In the case of ACM2 schemes, the maximum RH is simulated all over the country except western region. The maximum RH is simulated by using MYNN3 scheme all over Bangladesh except central region.

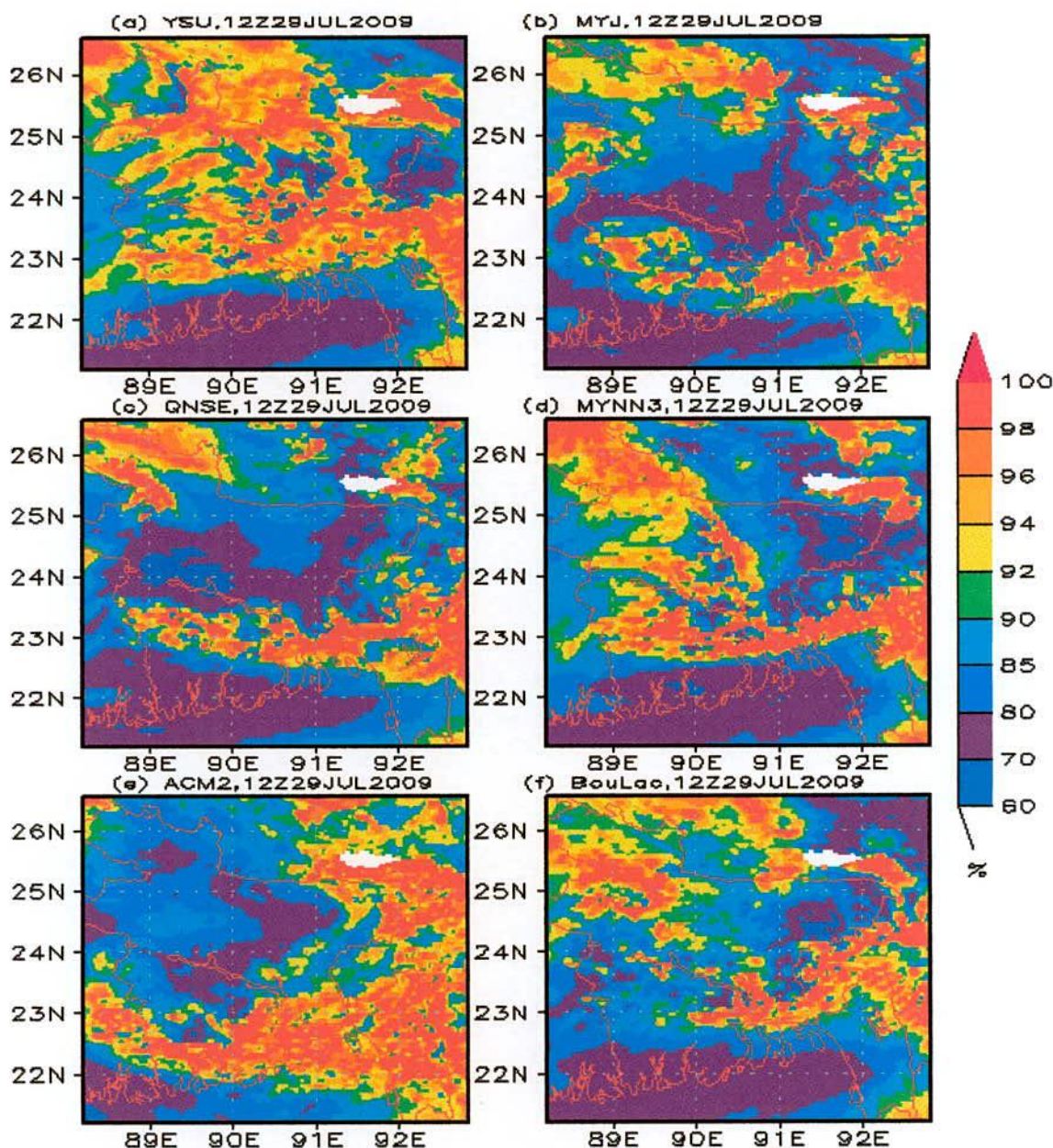


Fig. 14: Spatial distribution of simulated RH using a) YSU, b) MYJ, c) QNSE, d) MYNN3, e) ACM2 and f) BouLac schemes at 1200 UTC of 29 July 2009.

Figures 14 (a-f) show that the maximum RH has been simulated by YSU scheme all over the country except southern region at 1200 UTC of 29 July, 2009. The QNSE, MYNN3 and BouLac schemes have simulated maximum RH in the northwestern and southeastern region. The simulated maximum RH position has been shifted from the southern to southeastern region of Bangladesh in case of ACM2 scheme. The MYJ scheme has simulated maximum RH in the southeastern region of the country.

4.1.9 Rainfall

The BMD observed rain gauge and TRMM daily rainfall during 27 – 29 July 2009 are shown in Figs. 15(a,c & e) and 15 (b,d&f) respectively. From Figs. 15(a&b), it has been observed that the maximum rainfall has occurred at Dhaka station (333 mm and 150-250 mm respectively) and in the south south-western region on 27 July 2009. The maximum rainfall has occurred in the southeastern region (Chittagong) on 28 and 29 July 2009 [Fig. 15(c-d) & 15(e-f)]. The WRF-ARW Model is simulated rainfall using Lin *et al* MP scheme and KF CP scheme in combination with YSU, MYJ, QNSE, MYNN3, ACM2 and BouLac schemes during 27 – 29 July 2009 are presented in Figs. 16-18 respectively.

Figure 16a shows the distribution of WRF model simulated rainfall pattern using YSU schemes. The YSU scheme produces maximum rainfall at southeastern and northeastern (outside Bangladesh) region and almost no rainfall has been simulated in the northern and northwestern region (Rangpur, Dinajpur, Sayedpur, Jamalpur and Mymensing). From Figs. 16(b-d & f) it has also been found that the MYJ, QNSE, MYNN3 and BouLac schemes have simulated maximum rainfall in the northeastern (Sylhet) and southeastern region (Teknaf, Chittagong and Rangamati) and almost no rainfall has been simulated in the northern (Jamalpur and Mymensing) and northwestern region (Rangpur, Dinajpur and Sayedpur).

The BouLac scheme has also simulated maximum rainfall close to Dhaka region on 27 July 2009. The ACM2 scheme (Fig. 16e) has been simulated less but scattered rainfall all over the country except southeastern region. The maximum rainfall has been simulated along the boarder line of land and ocean (Fig. 16e) from Chittagong to Teknaf region. The MYJ, MYNN3 and BouLac schemes have simulated rainfall of 100 to 150, 75 to 100 and 150 to 200 mm respectively over Dhaka region.

Figures 17(a – f) shows the distribution of WRF model simulated rainfall pattern on 28 July 2009 using different PBL schemes. The YSU (Fig. 17a) and MYNN3 (Fig. 17d) schemes have simulated maximum rainfall at the eastern and northeastern region and the minimum

rainfall has simulated in western region. From Fig. 17(b, c & f), it has also been found that the MYJ, QNSE, and BouLac schemes have produced maximum rainfall in the northeastern region (Sylhet and Srimangal) and southeastern region (Teknaf, Chittagong and Rangamati) and the minimum rainfall have been simulated in the west-southwest (Mongla) region. The significant amount of rainfall has also been simulated in the central region on 28 July 2009. The ACM2 scheme (Fig. 17e) has been simulated significant amount of rainfall in the central to eastern region. The maximum rainfall simulated along the boarder line of land and ocean (Fig. 17(d-e)) from Chittagong to Teknaf region. The YSU, MYJ, MYNN3 and BouLac schemes have been simulated 150 to 200 mm rain over Chittagong and Sandwip region.

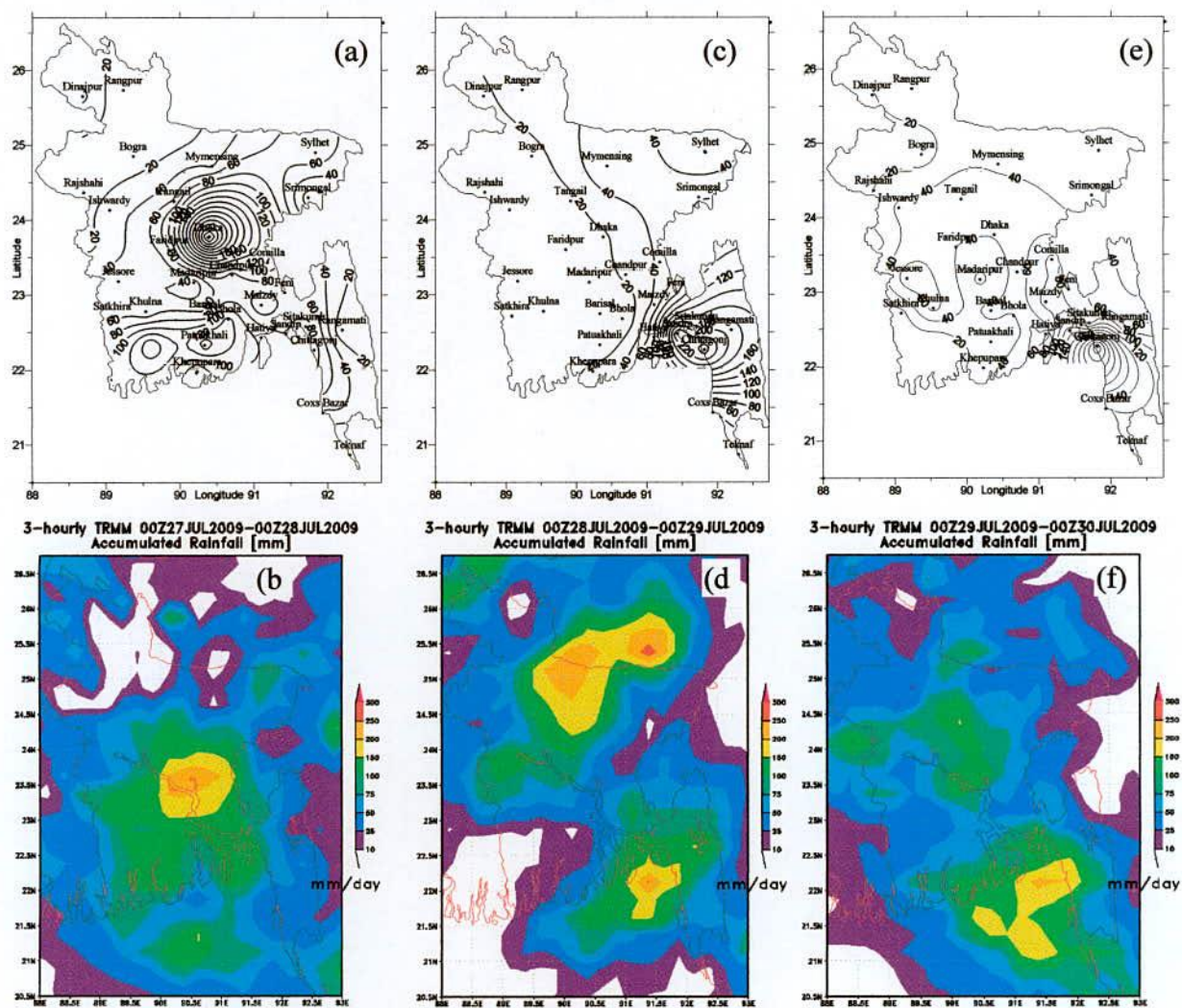


Fig. 15: BMD observed and TRMM daily rainfall in (a-b) 27, (c-d) 28 and (e-f) 29 July 2009 respectively.

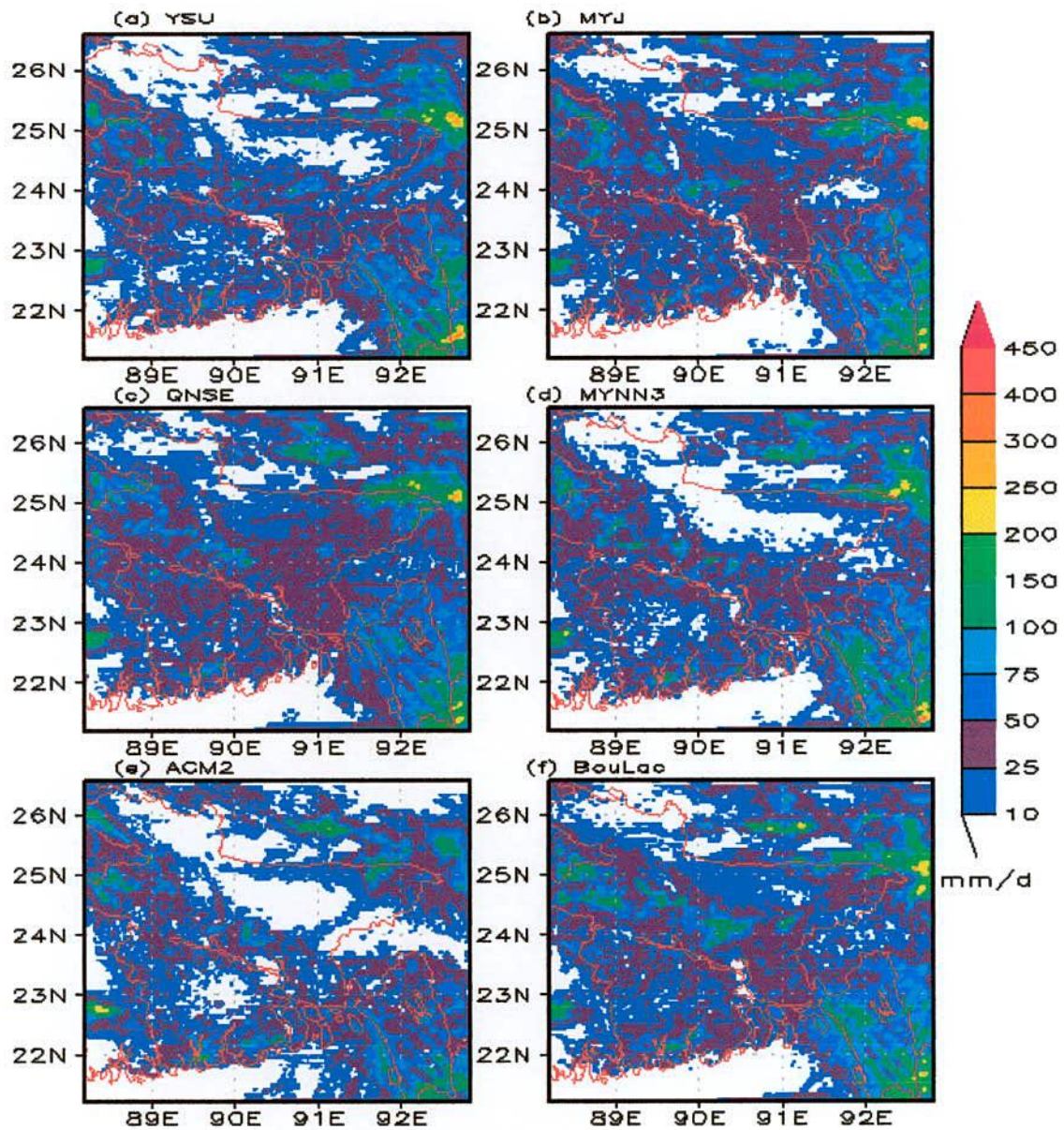


Fig.16: Spatial distribution of simulated rainfall (mm) using a) YSU, b) MYJ, c) QNSE, d) MYNN3, e) ACM2 and f) BouLac schemes at 27 July 2009.

Figure 18(a – f) shows the distribution of WRF model simulated rainfall pattern on 29 July 2009 using six different PBL schemes. The YSU (Fig. 18a) and BouLac (Fig. 18f) scheme have simulated maximum rainfall at the southeastern and northwestern region of Bangladesh. The MYJ (Fig. 18b), MYNN3 (Fig. 18d) and ACM2 (Fig. 18e) schemes have simulated the significant amount of rainfall in the southeastern region. From Fig. 18e, it has also been found that the QNSE scheme has simulated maximum rainfall in the southeastern region and the northwestern region. The YSU, MYJ, MYNN3, QNSE, ACM2 and BouLac schemes have simulated 150 to 200 mm rain over Chittagong and Sandwip region.

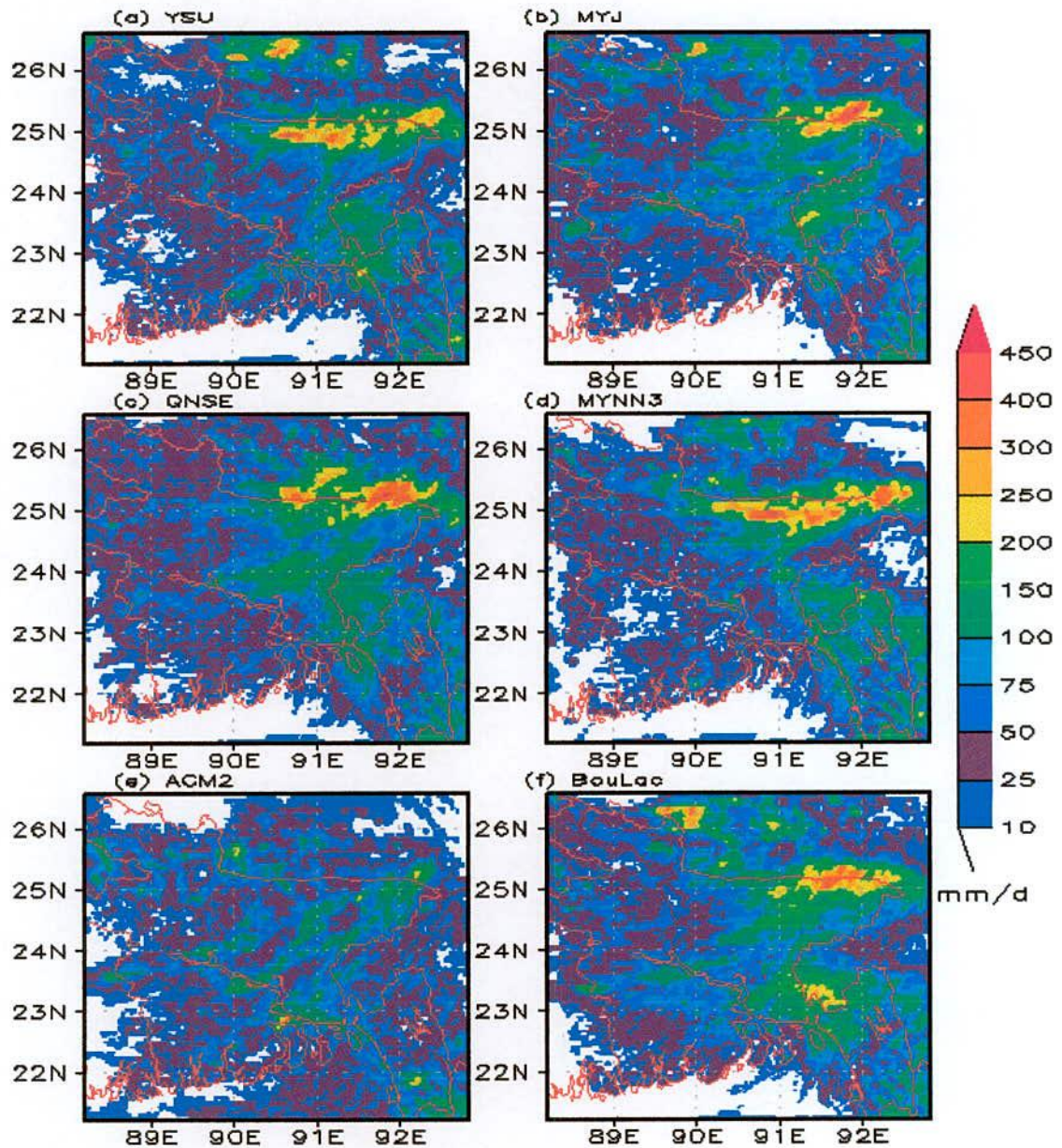


Fig.17: Spatial distribution of simulated rainfall (mm) using a) YSU, b) MYJ, c) QNSE, d) MYNN3, e) ACM2 and f) BouLac schemes at 28 July 2009.

On 27 July 2009, the MYJ, MYNN3 and BouLac schemes have simulated rain over Dhaka region and the amounts are 100 to 150, 75 to 100 and 150 to 200 mm respectively. Out of six PBL schemes, only the rainfall simulated by BouLac scheme is almost closest to the actual rainfall recorded by BMD and TRMM daily rainfall. The YSU, MYJ, MYNN3, QNSE and BouLac schemes have simulated 150 to 200 mm rain over Chittagong and Sandwip region on 28 and 29 July 2009 respectively. The maximum rainfall is observed in the southeastern region on 28 July (252 mm at Chittagong) and 29 July 2009 (281 mm at Chittagong) (Figs. 15b and 15c).

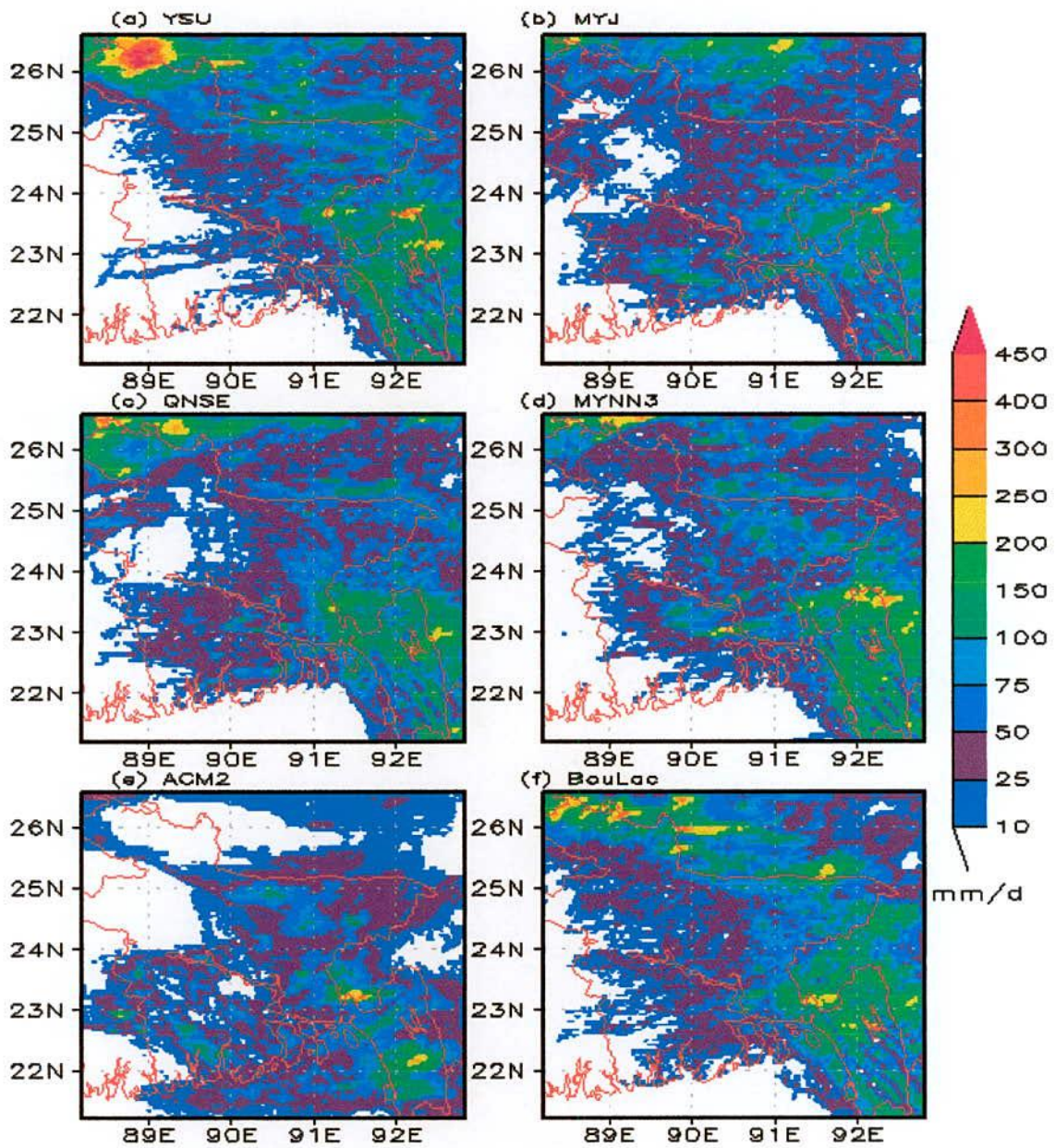


Fig. 18: Spatial distribution of simulated rainfall (mm) using a) YSU, b) MYJ, c) QNSE, d) MYNN3, e) ACM2 and f) BouLac schemes at 29 July 2009.

4.1.10 Summary

The BouLac, MYJ, MYNN3 and ACM2 schemes have simulated 150 to 200 mm, 100 to 150 mm, 75 to 100 mm and 75 to 100 mm rain respectively but the observed rainfall is 333 mm over Dhaka region on 27 July 2009. The YSU, MYJ, MYNN3, QNSE BouLac and ACM2 schemes have simulated 150 to 200 mm and 100 to 150 mm rain over Chittagong and Sandwip region on 28 July 2009 whereas the observed rain is 252 mm over Chittagong and 112 mm over Sayedpur. The MYJ, BouLac and ACM2 schemes have also simulated 150 to 200 mm, 75 to 100 mm and 25 to 50 mm rain over Sayedpur region on 28 July 2009. On 29 July 2009, the BouLac, YSU, MYNN3 and QNSE scheme simulated 150 to 200 mm rain and the observed rainfall also maximum over Chittagong was 281 mm. The QNSE, ACM2 and BouLac schemes have simulated minimum ACHFX in the southeastern region where maximum rainfall is observed. Maximum area of minimum ACHFX have simulated by BouLac scheme in the southeastern region on 28 and 29 July 2009. The QNSE and BouLac schemes have simulated maximum ACLHF in the southeastern region where maximum rainfall is observed on 28 and 29 July 2009. The result shows that where the ACLHF is maximum (minimum) the rainfall is also maximum (minimum) in that region. The simulated PBL is minimum at the position where the rainfall is maximum and the MYNN3 scheme has simulated minimum PBL in the southeastern region on 28 and 29 July 2009. The BouLac and YSU schemes have simulated maximum rainfall in the southeastern region and Sayedpur region where the simulated GLW is minimum on 28 and 29 July 2009. On 28 and 29 July 2009 the YSU, ACM2 and BouLac schemes have simulated minimum OLR and ACM2 has simulated maximum reflectivity in the eastern and southeastern region. The MYJ, ACM2 and BouLac schemes have simulated maximum wind speed at 850 hPa in the southeastern region at 1200 UTC of 28 and 29 July 2009. The relative humidity simulated by ACM2 and BouLac scheme is 98 to 100% in the southeastern region.

4.2 Heavy rainfall event of 15-16 August 2009 using WRF model

4.2.1 Accumulated Upward Heat Flux (ACHFX) at the surface

In this study, the WRF model simulated accumulated upward heat flux at 1200 UTC of 15 August 2009 at the surface is shown in Figs. 19(a-f). The ACHFX is maximum in the southern part along the land-ocean boundary of Bangladesh for all schemes. The ACM2 scheme has also simulated lesser ACHFX all over the domain than that of all other schemes. From the figure, it is also observed that the ACHFX is minimum in the western to northeastern region for all schemes at 1200 UTC of 15 August 2009.

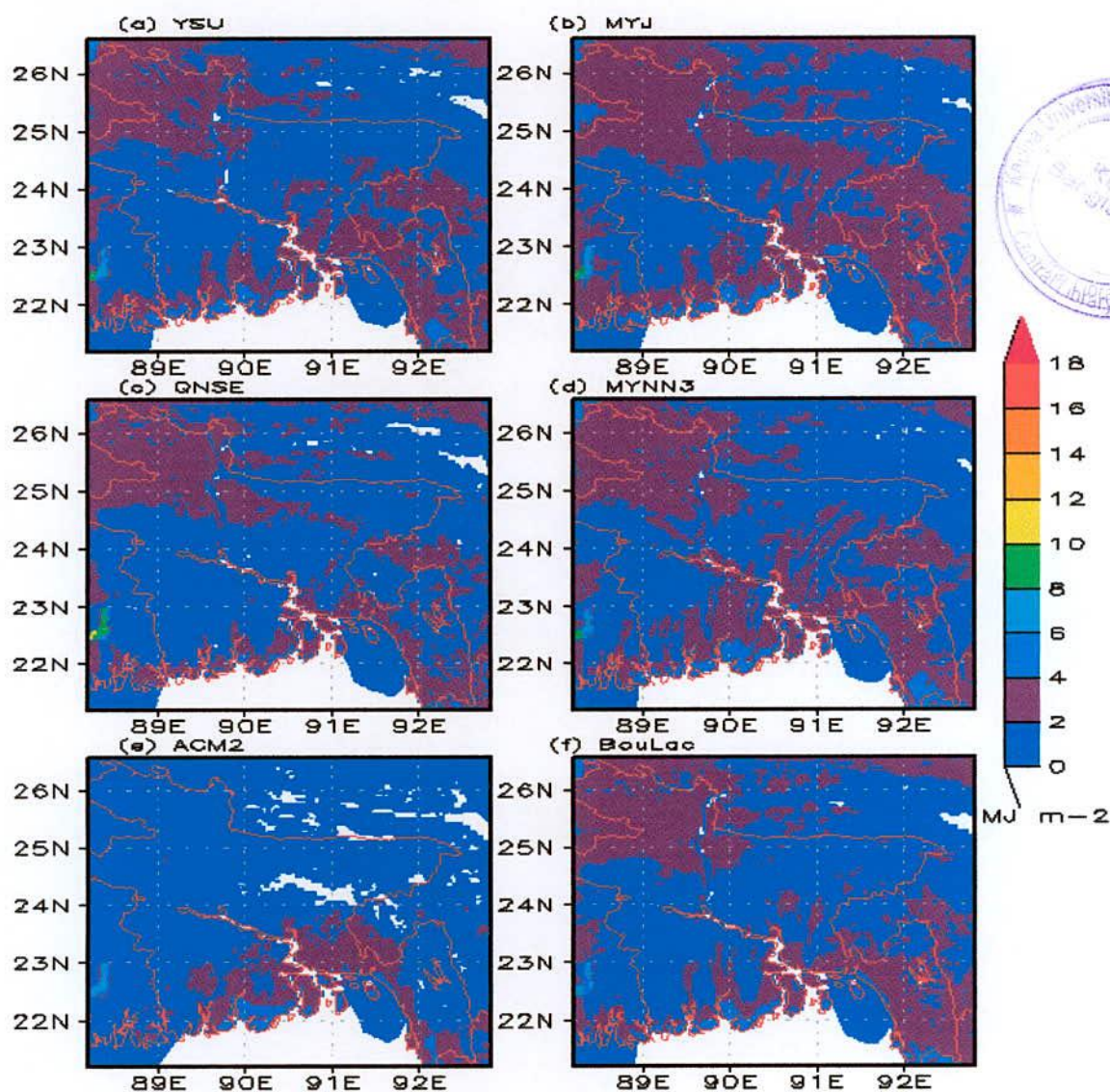


Fig. 19: Spatial distribution of simulated ACHFX using a) YSU, b) MYJ, c) QNSE, d) MYNN3, e) ACM2 and f) BouLac schemes at 1200 UTC of 15 August 2009.

Figure 20 (a-f) shows the spatial distribution of ACHFX using different schemes at 1200 UTC of 16 August 2009. It has been found that the simulated ACHFX is maximum in the southern part along the land-ocean boundary of Bangladesh for all schemes. Maximum areas of minimum ACHFX have been simulated by ACM2 (Fig. 20e) scheme at 1200 UTC of 16 August 2009 in the western to northeastern region. From the figure it is also observed that the simulated ACHFX is minimum in the western region by using all schemes.

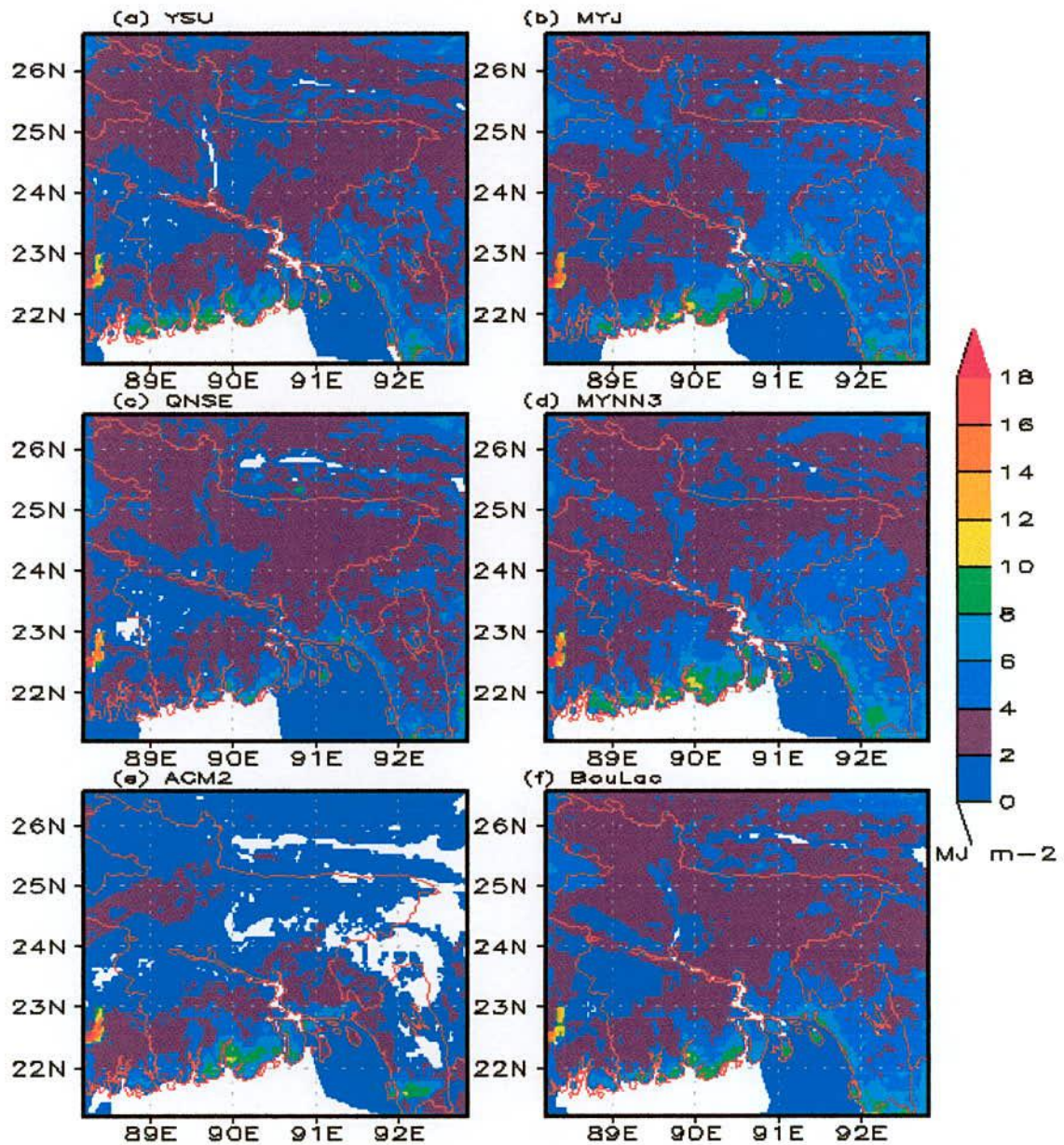


Fig. 20: Spatial distribution of simulated ACHFX using a) YSU, b) MYJ, c) QNSE, d) MYNN3, e) ACM2 and f) BouLac schemes at 1200 UTC of 16 August 2009.

Minimum ACHFX has been simulated at D2, where the location is relatively covered by a cloud sky during the 24-h period of interest and the maximum ACHFX is found over the less rainfall area in that location. From figure it has been found that the ACHFX is minimum in the northwestern, southern region and the model has also simulated maximum rainfall in that region by all schemes.

4.2.2 Accumulated Upward Latent Heat Flux (ACLHF) at the surface

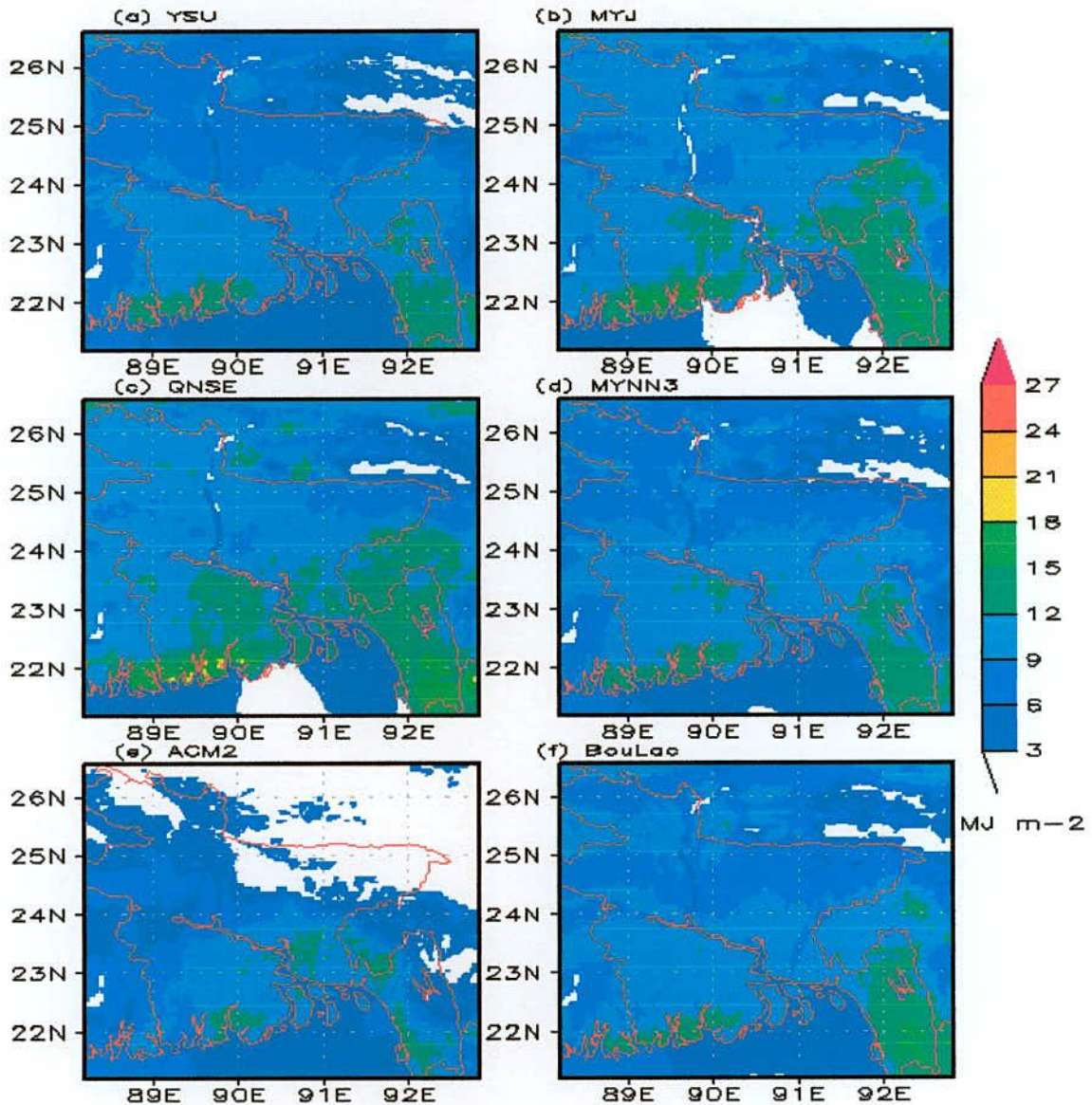


Fig. 21: Spatial distribution of simulated ACLHF using a) YSU, b) MYJ, c) QNSE, d) MYNN3, e) ACM2 and f) BouLac schemes at 1200 UTC of 15 August 2009.

The WRF-ARW model has simulated accumulated upward latent heat flux (ACLHF) using six schemes at 1200 UTC of 15 August 2009 at the surface and is shown in Fig. 21(a-f). The

YSU, MYNN3, MYJ, ACM2, QNSE and BouLac schemes have simulated the maximum ACLHF in the southern part along the land-ocean boundary and the southeastern region of Bangladesh. The ACM2 scheme has simulated almost 0-6 MJ m⁻² ACLHF in the northwestern to northeastern region, which is the lowest value. The simulated ACLHF by using QNSE (Fig. 21c) schemes is 18-21 MJ m⁻² in the southern region of Bangladesh at the same time. From the figure, it is also observed that the ACLHF is minimum in the northeastern part of Bangladesh for all schemes. On this day the simulated ACLHF is maximum as simulated QNSE scheme.

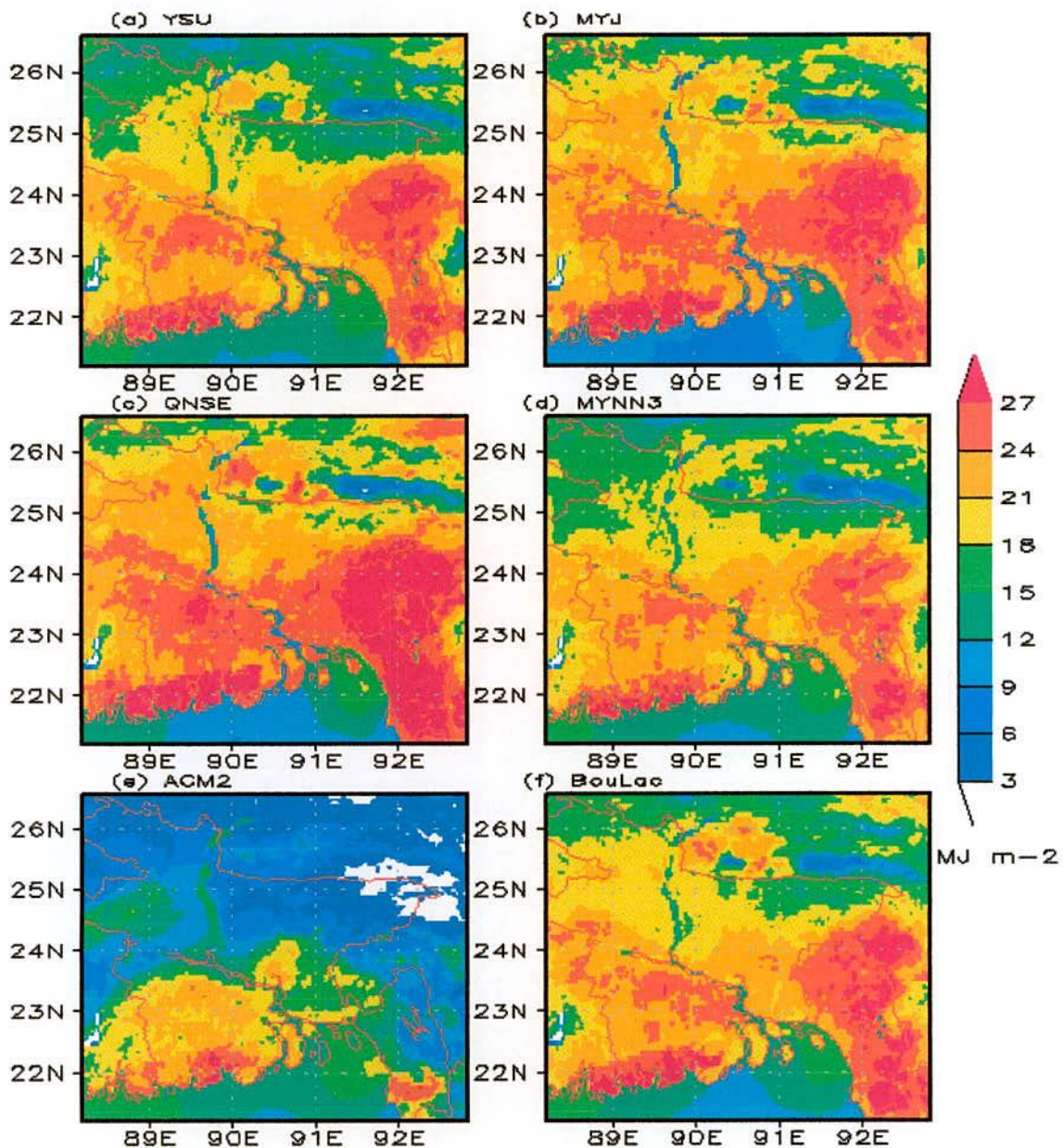


Fig. 22: Spatial distribution of simulated ACLHF using a) YSU, b) MYJ, c) QNSE, d) MYNN3, e) ACM2 and f) BouLac schemes at 1200 UTC of 16 August 2009.

Figure 22(a-f) represents the simulated ACLHF at 1200 UTC on 16 August 2009 at the surface for six different schemes. At 1200 UTC of 16 August 2009, the significant amount of ACLHF has been simulated by YSU, MYJ, QNSE, MYNN3 and BouLac schemes. Out of all PBL schemes QNSE has simulated maximum and ACM2 has simulated minimum ACLHF all over Bangladesh. For all schemes, the northeastern and northwestern regions of Bangladesh have minimum simulated ACLHF and southern and southeastern region have maximum simulated ACLHF. The simulated ACLHF is also significant in the land-ocean boundary of Bangladesh.

4.2.3 Downward Long wave Flux at Ground Surface (GLW)

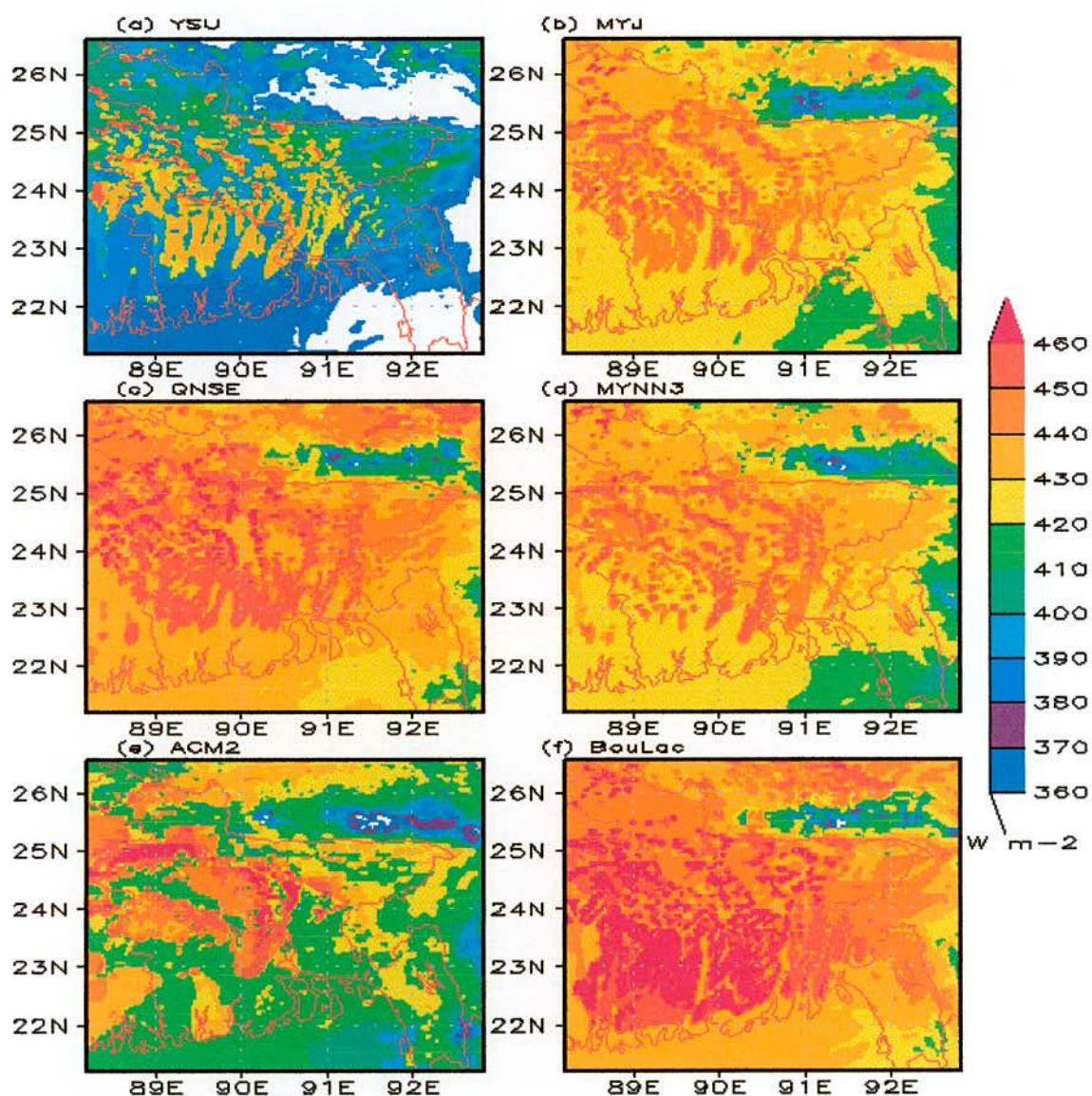


Fig. 23: Spatial distribution of simulated GLW using a) YSU, b) MYJ, c) QNSE, d) MYNN3, e) ACM2 and f) BouLac schemes at 1200 UTC of 15 August 2009.

Figure 23(a-f) shows that the WRF-ARW model simulated the spatial distribution of downward long wave flux ($W m^{-2}$) at the surface using six schemes at 1200 UTC of 15 August 2009. The significant amount of GLW has simulated all over the country by using MYJ, QNSE, MYNN3 and BouLac schemes. The minimum GLW has simulated in the southeastern region of domain D2 for all schemes. From the figure, it is also observed that significant amount of GLW has simulated in the central to western region by YSU and ACM2 schemes.

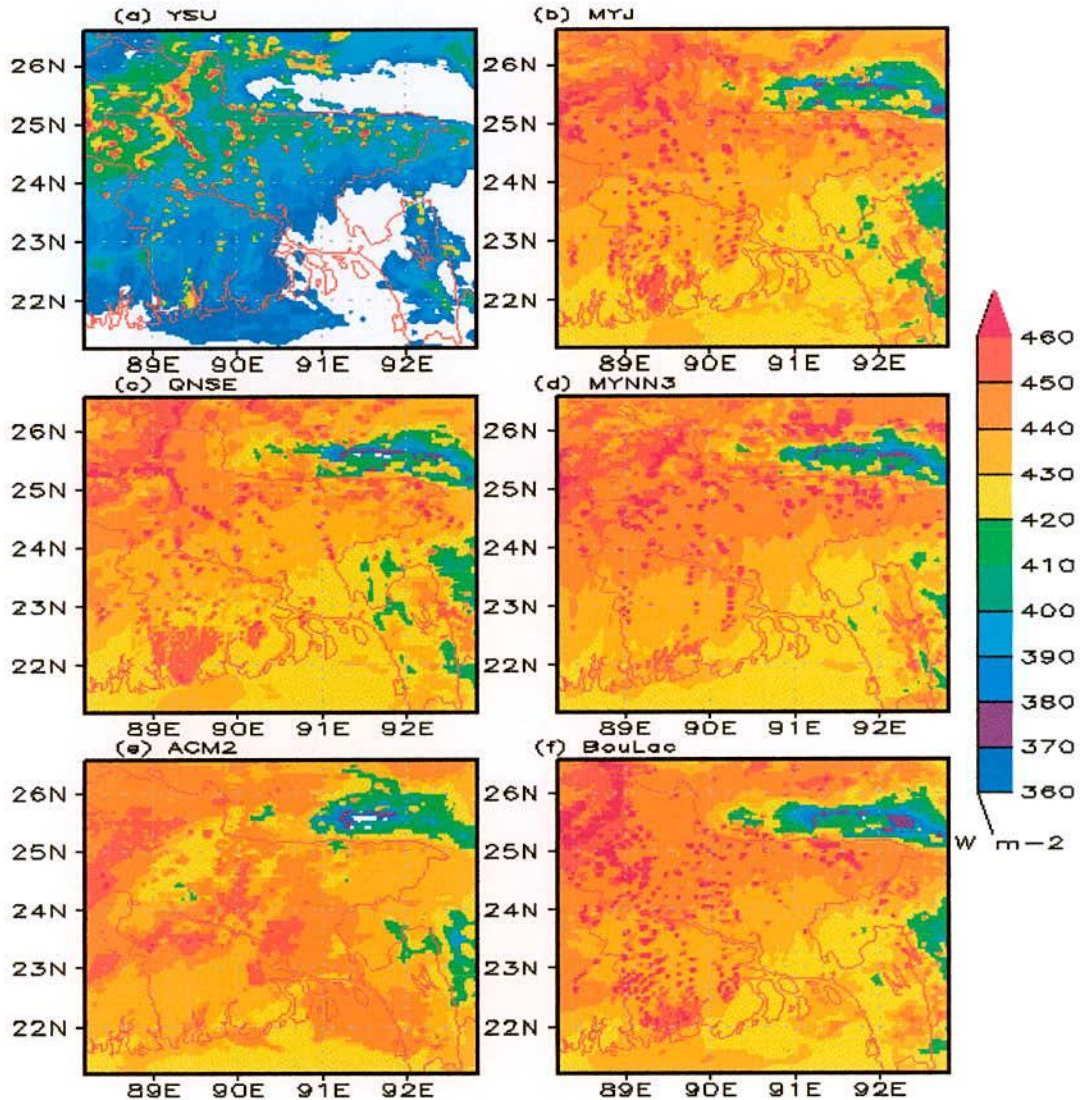


Fig. 24: Spatial distribution of simulated GLW using a) YSU, b) MYJ, c) QNSE, d) MYNN3, e) ACM2 and f) BouLac schemes at 1200 UTC of 16 August 2009.

At 1200 UTC on 16 August 2009, the minimum GLW has simulated in the southeastern and northeastern region of domain D2 (outside Bangladesh) by all schemes. Maximum areas of minimum GLW has simulated by YSU scheme at 1200 UTC of 16 August 2009 in the

southern to southeastern region. The simulated GLW has maximum all over Bangladesh for MYJ, QNSE, MYNN3, ACM2 and BouLac schemes. On this day the simulated GLW is also maximum in the northwestern and southwestern region as simulated by BouLac scheme.

4.2.4 Outgoing Long Wave Radiation (OLR)

WRF Model has simulated outgoing long wave radiation in the domain D2 at 1200 UTC of 15 and 16 August 2009 using different schemes and the results are presented in Figs. 25 & 26. Figure 25(a-f) shows that the simulated the OLR is minimum ($50 - 150 \text{ W/m}^2$) in the southeastern to northern region for all schemes. The OLR has also minimum value in the northeastern region for BouLac (Fig. 25f) and northern region of Bangladesh for MYNN3 (Fig. 25d) schemes.

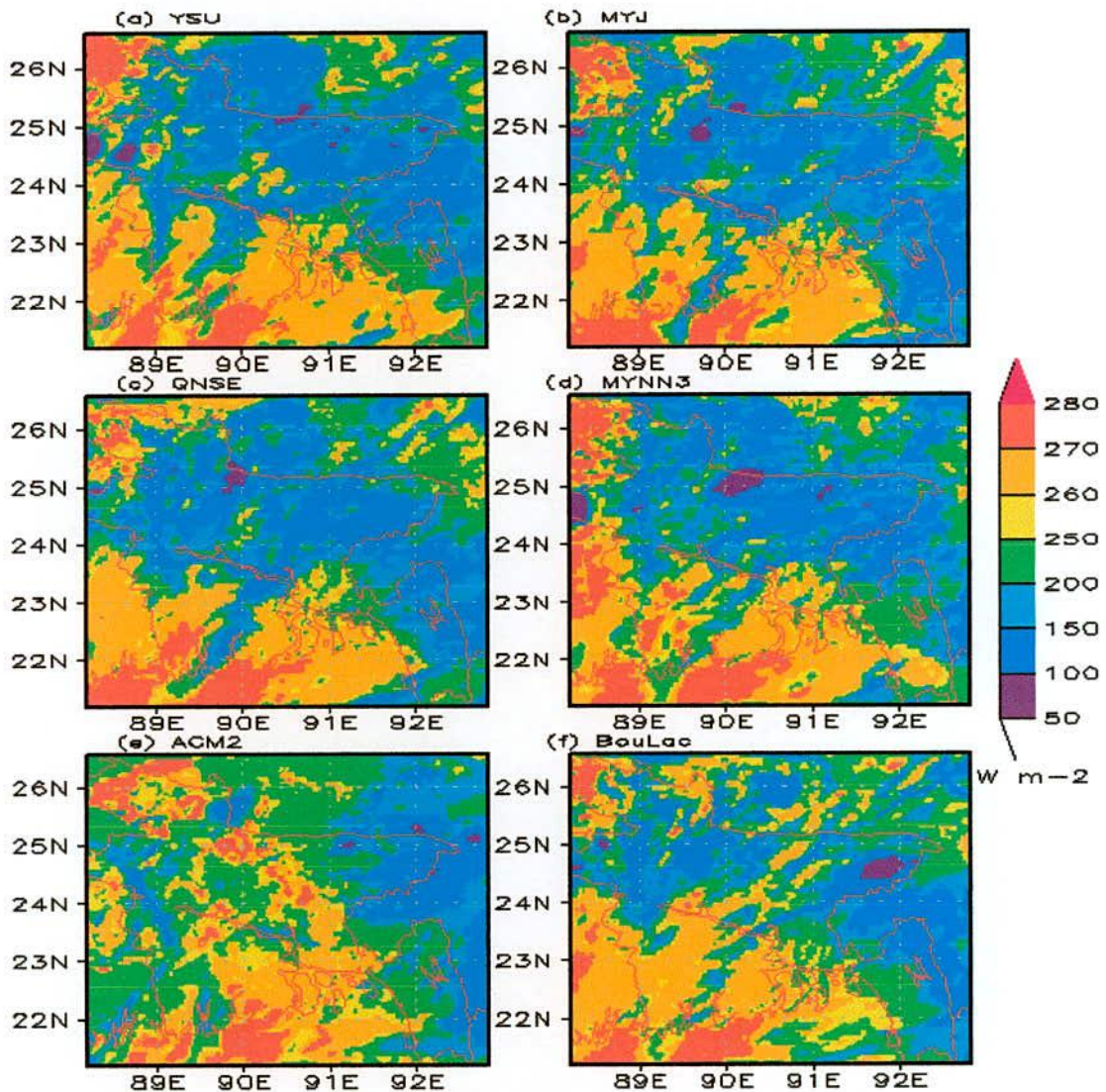


Fig. 25: Spatial distribution of simulated OLR using a) YSU, b) MYJ, c) QNSE, d) MYNN3, e) ACM2 and f) BouLac schemes at 1200 UTC of 15 August 2009.

The maximum OLR is simulated in the northwestern region of Bangladesh by using the six schemes and also the southern (along the boarder line of land-ocean and over the Bay of Bengal) region. On this day, the more OLR is simulated in the southern to northwestern region by ACM2 scheme.

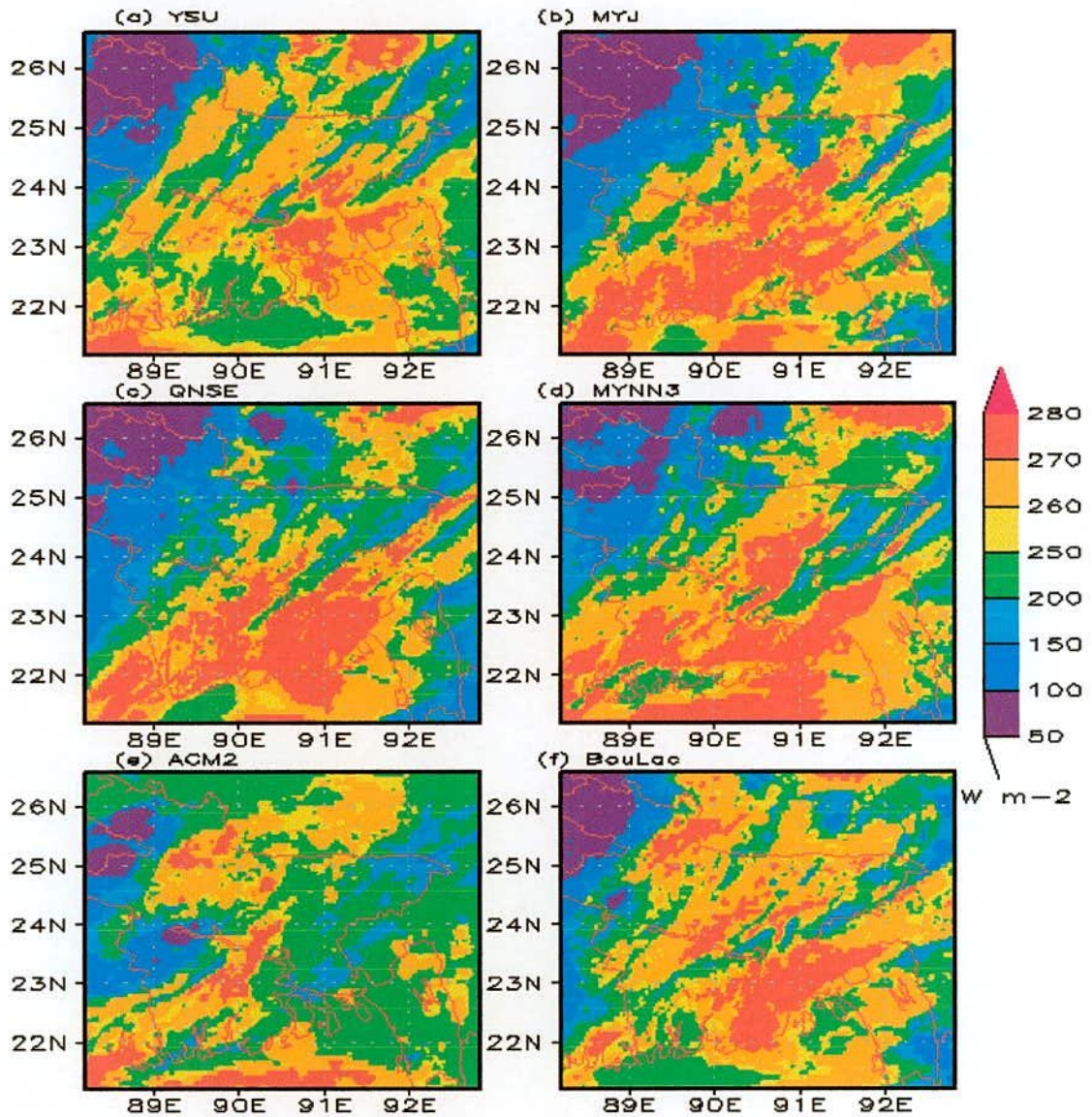


Fig. 26: Spatial distribution of simulated OLR using a) YSU, b) MYJ, c) QNSE, d) MYNN3, e) ACM2 and f) BouLac schemes at 1200 UTC of 16 August 2009.

Figure 26(a-f) shows the OLR at the surface for 1200 UTC of 16 August 2009. The minimum OLR have also been simulated in the northwestern region by YSU, MYJ, QNSE, MYNN3, ACM2 and BouLac schemes. The simulated maximum OLR position has been shifted in the southern most regions to eastern region of Bangladesh for all schemes. The maximum OLR has been simulated in the southern to northern region by using ACM2 scheme.

4.2.5 Variation of Planetary Boundary Layer (PBL)

WRF Model has simulated PBL (meter) of domain D2 at 1200 UTC of 15 and 16 August 2009 by using different schemes and the results are presented in Figs. 27 & 28 respectively. The maximum PBL has been simulated in southern region by using six schemes and the minimum PBL in the northeastern region of Bangladesh. The maximum and significant PBL has been simulated by using QNSE (Fig. 27c) scheme in the southwestern to central region. The simulated minimum PBL position has been shifted in the northern most region of Bangladesh for MYNN3 scheme.

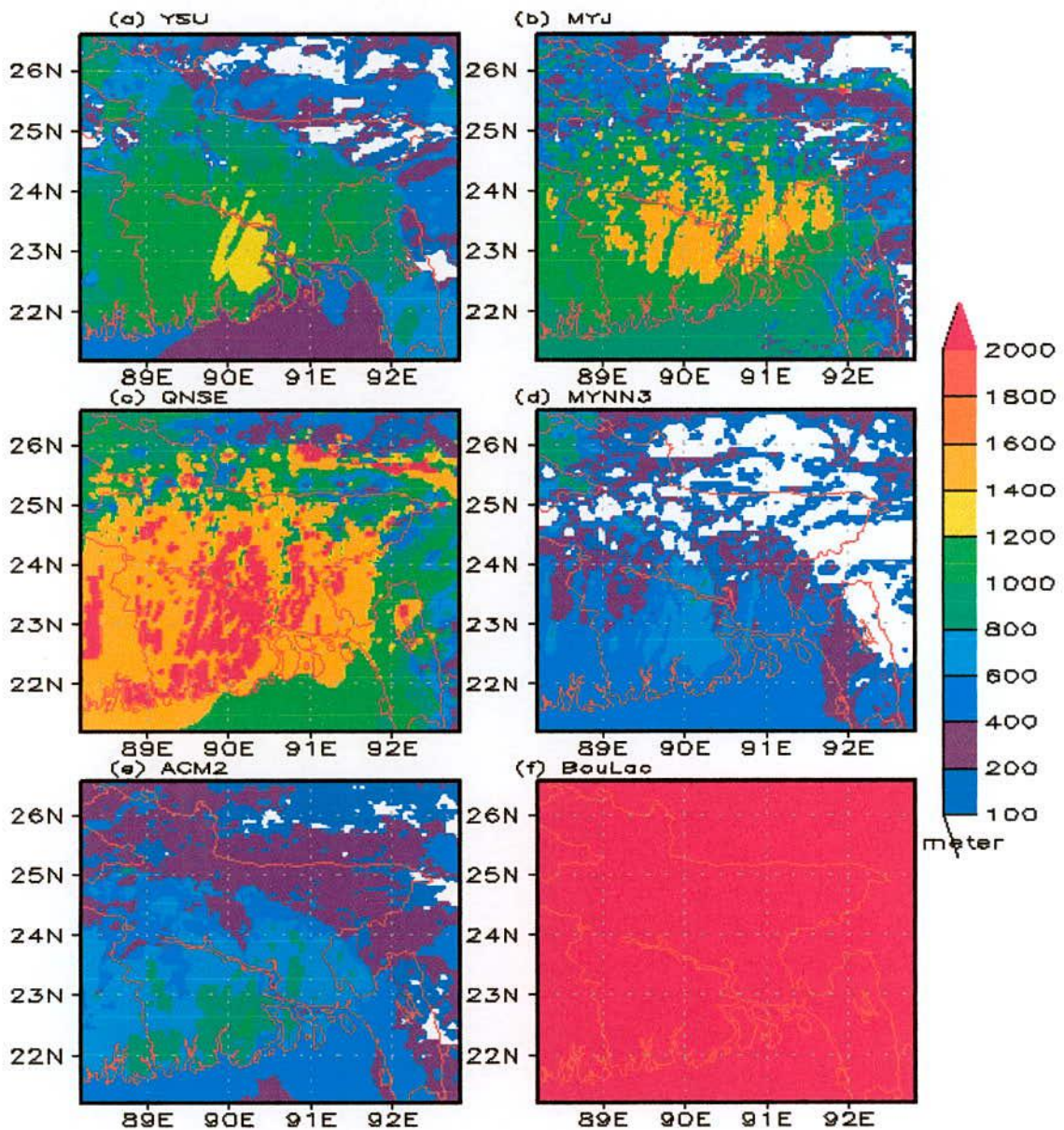


Fig. 27: Spatial distribution of simulated PBL height using a) YSU, b) MYJ, c) QNSE, d) MYNN3, e) ACM2 and f) BouLac schemes at 1200 UTC of 15 August 2009.

Figs. 28(a-f) represent the distribution of PBL simulated by WRF model at 1200 UTC of 16 August 2009. The YSU (Fig. 28a), MYJ (Fig. 28b), MYNN3 (Fig. 28d), and ACM2 (Fig. 28e) schemes have simulated the maximum PBL in the southwestern region. The maximum and significant PBL has been simulated by using QNSE (Fig. 28c) scheme in the southwestern and northwestern region of Bangladesh. The YSU (Fig. 28a) and MYNN3 PBL (Fig. 28d) scheme have simulated the minimum PBL in the northwestern region. The minimum PBL is simulated by using MYJ (Fig. 28b) and QNSE (Fig. 28c) scheme in the northeastern region. The ACM2 (Fig. 28e) scheme has also simulated minimum PBL in the southeastern region. In case of BouLac scheme the constant PBL has been simulated all over the country on 15 and 16 August 2009.

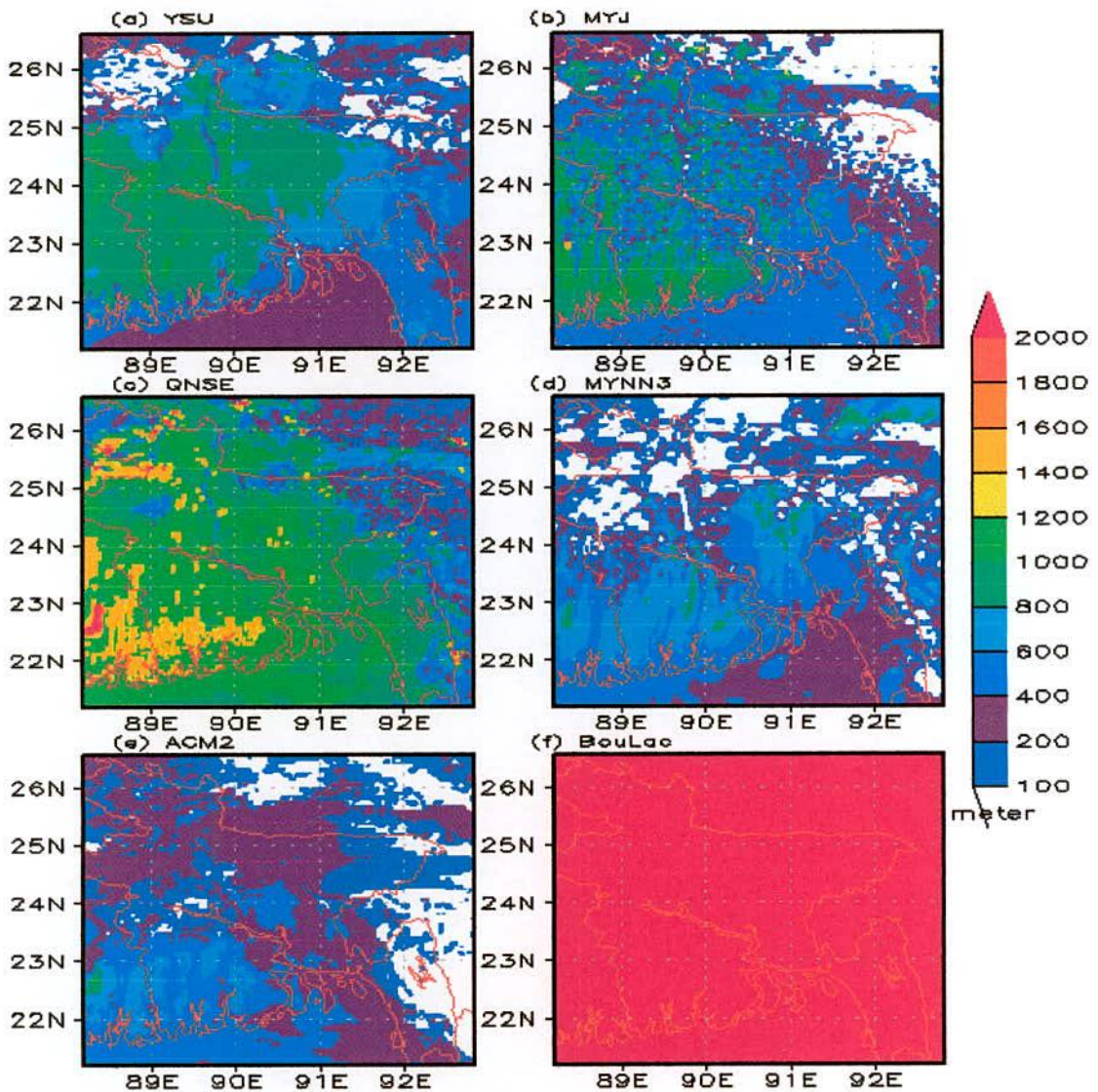


Fig.28: Spatial distribution of simulated PBL height using a) YSU, b) MYJ, c) QNSE, d) MYNN3, e) ACM2 and f) BouLac schemes at 1200 UTC of 16 August 2009.

From the figure, if the simulated rainfalls (mm) are compared with the PBL (meter) it has been found that the maximum PBL indicates minimum rainfall occurring and the minimum PBL (meter) indicates the heavy rainfall occurring in that position i.e. the PBL height decreases during the maximum rainfall.

4.2.6 Reflectivity

Figures 29(a-f) represent the spatial distribution of WRF model simulated reflectivity (shaded) using different schemes at 850 hPa levels at 1200 UTC of 15 August 2009.

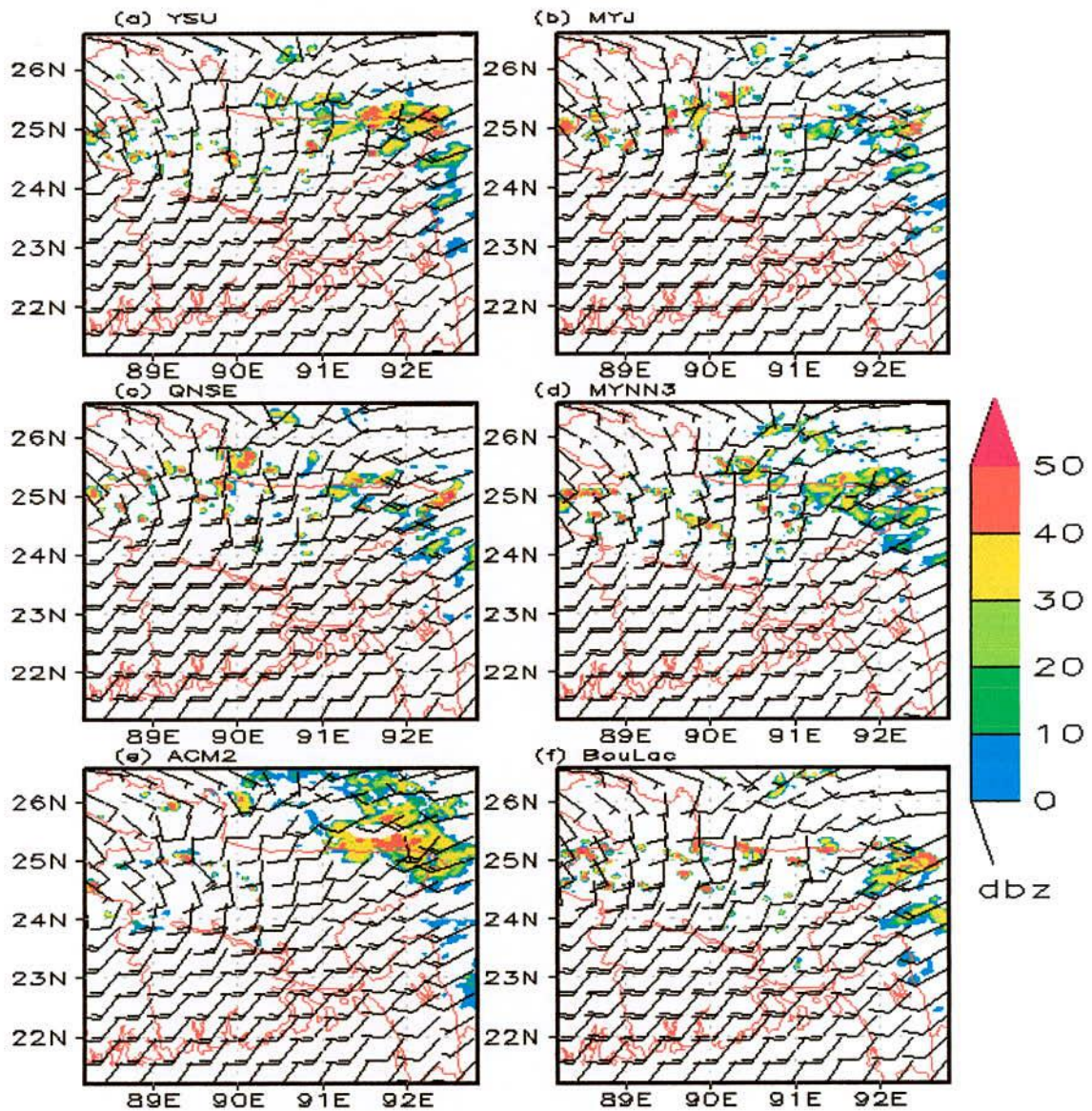


Fig. 29: Spatial distribution of simulated wind speed (m/s) and reflectivity (dBZ) at 850 hPa level using a) YSU, b) MYJ, c) QNSE, d) MYNN3, e) ACM2 and f) BouLac schemes at 1200 UTC of 15 August 2009.

The YSU (Fig. 29a) scheme has simulated significant amount of reflectivity in the western and northeastern region. The MYJ (Fig. 29b), QNSE (Fig. 29c) and BouLac (Fig. 29f) schemes have also simulated significant amount of reflectivity in the western and northern region and MYNN3 (Fig. 29d) scheme has simulated maximum reflectivity in the northeastern region and western region of Bangladesh at the same time. The ACM2 scheme has simulated maximum reflectivity in the northeastern (outside Bangladesh) and western regions.

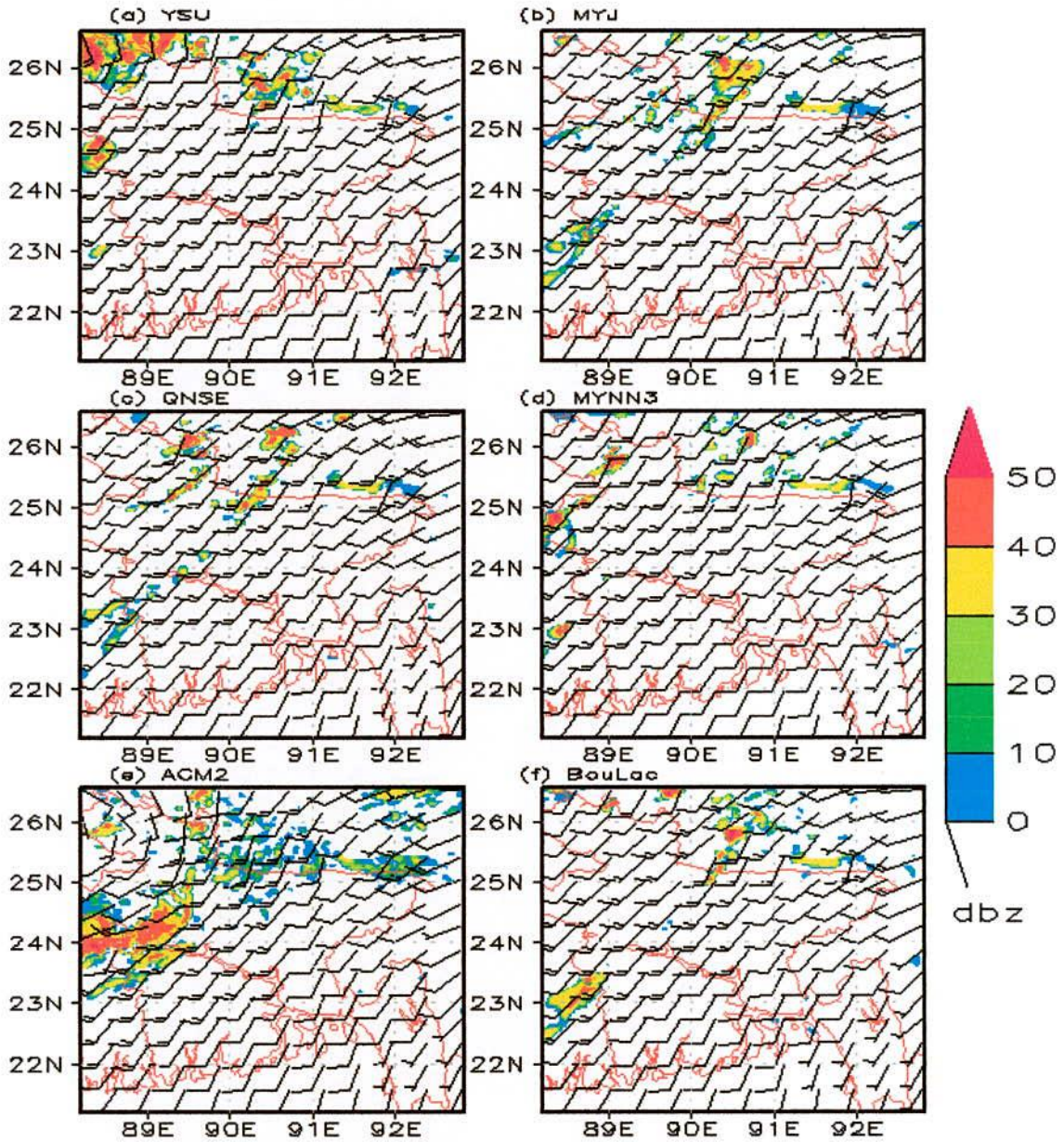


Fig. 30: Spatial distribution of simulated wind speed (m/s) and reflectivity (dBZ) at 850 hPa level using a) YSU, b) MYJ, c) QNSE, d) MYNN3, e) ACM2 and f) BouLac schemes at 0000 UTC of 16 August 2009.

At 0000 UTC of 16 August 2009, the YSU (Fig. 30a) and MYNN3 (Fig. 30d) schemes have simulated significant amount of reflectivity in the northwestern region of Bangladesh. The MYJ (Fig. 30b) and BouLac (Fig. 30f) schemes have also simulated significant amount of reflectivity in the northern region. The QNSE (Fig. 30c) scheme has simulated maximum reflectivity in the northwestern region and the maximum reflectivity has also found in the northern region at the same time. Maximum reflectivity is also simulated by ACM2 scheme in the western region at 850 hPa levels.

From figure (not shown) it has been observed that the ACM2 scheme has simulated the maximum reflectivity in the western and northwestern region and the YSU, MYJ, QNSE, MYNN3, and BouLac schemes have also simulated the maximum reflectivity in the northwestern region at 850 hPa level at 1200 UTC of 16 August 2009.

4.2.7 Wind

The simulated wind speed is maximum in the southwestern and southern region by all schemes. The maximum wind speed 20 m/s is simulated by using YSU, QNSE, MYNN3, ACM2 and BouLac schemes and 20 m/s by using MYJ scheme in the southwestern and southern side of maximum reflectivity. The minimum wind speed has been simulated by all schemes in the northwestern side of maximum reflectivity at 850 hPa level of 1200 UTC on 15 August 2009.

The maximum wind speed has also been simulated in the western region of all schemes at 0000 UTC on 16 August 2009. The maximum wind speed simulated is 20 m/s by using MYNN3 schemes in the southwestern side of maximum reflectivity and 15 m/s by using YSU scheme in the southern and southeastern side of maximum reflectivity and 15 m/s by using BouLac, QNSE and MYJ schemes in the southwestern side of maximum reflectivity and 15 m/s by using ACM2 scheme in the southern and northeastern region of maximum reflectivity. The minimum wind speed has been simulated by all schemes in the southeastern side of maximum reflectivity at 850 hPa level at 0000 UTC on 16 August 2009.

At 1200 UTC on 16 August 2009, the maximum wind speed simulated by all PBL schemes is 10 m/s except YSU scheme in the southern region of maximum reflectivity and 15 m/s by using YSU scheme in the inner side of maximum reflectivity. The minimum wind speed simulated by all schemes is found to lie in the southeastern region of maximum reflectivity.

4.2.8 Relative Humidity (RH)

WRF model has simulated relative humidity (RH) of Domain2 at 850 hPa levels at 1200 UTC on 15 August 2009 and the results are presented in Figures 31(a-f). The YSU, MYJ, QNSE, MYNN3 AND BouLac schemes have simulated maximum RH all over Bangladesh except southwestern and southeastern region. The minimum RH is simulated in the southeastern region and the southwestern region of Bangladesh. In the case of ACM2 scheme, the maximum RH is simulated all over the country except southeastern region.

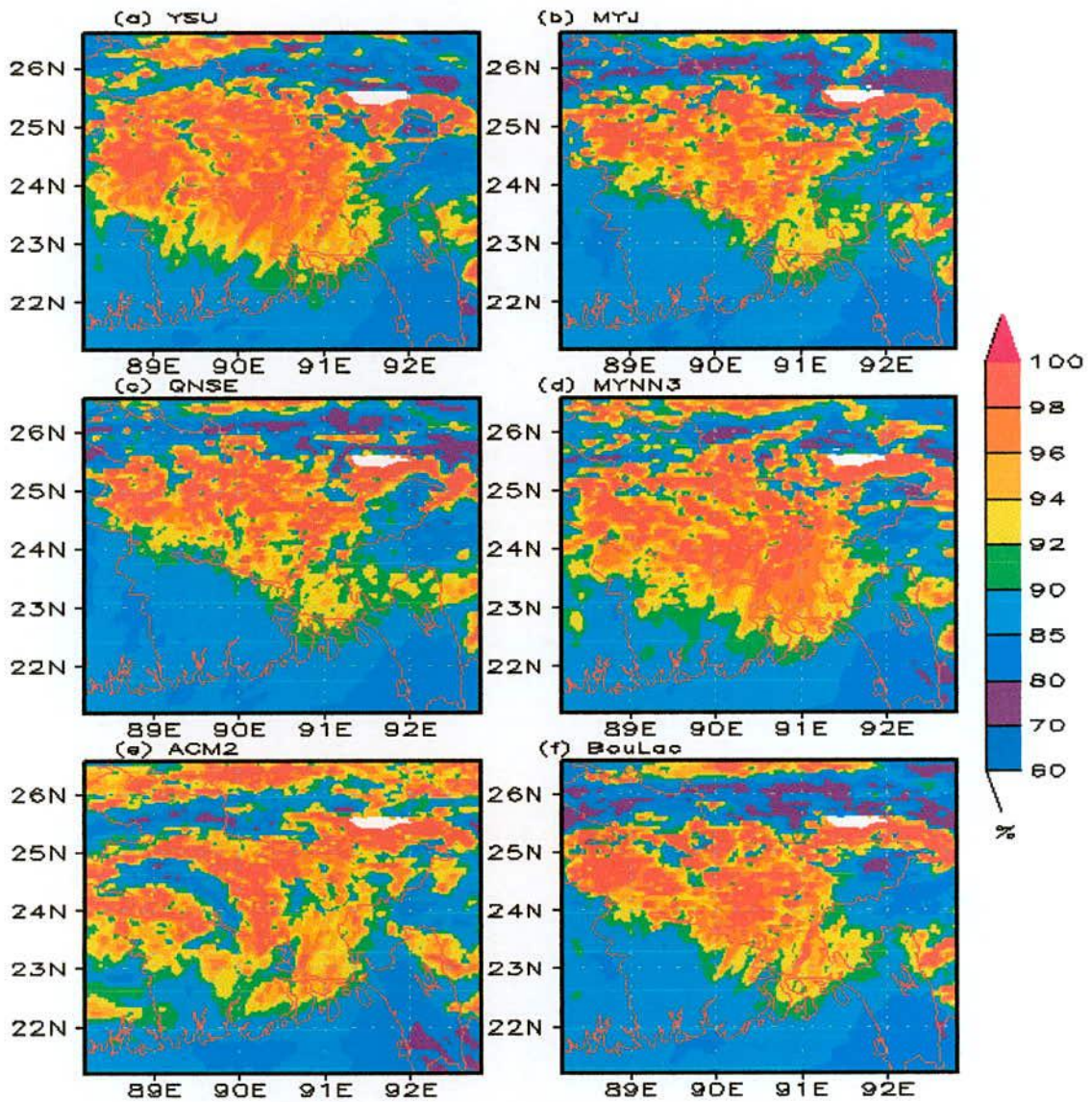


Fig. 31: Spatial distribution of simulated RH using a) YSU, b) MYJ, c) QNSE, d) MYNN3, e) ACM2 and f) BouLac schemes at 1200 UTC of 15 August 2009.

Figure 32 (a-f) shows that the maximum RH in the northern and northwestern region simulated by using all schemes at 1200 UTC on August 16, 2009. Maximum areas of

minimum RH have been simulated by all schemes in the southern to the eastern region of Bangladesh. The simulated maximum RH position has been shifted in the central most regions to northwestern region of Bangladesh for ACM2 scheme.

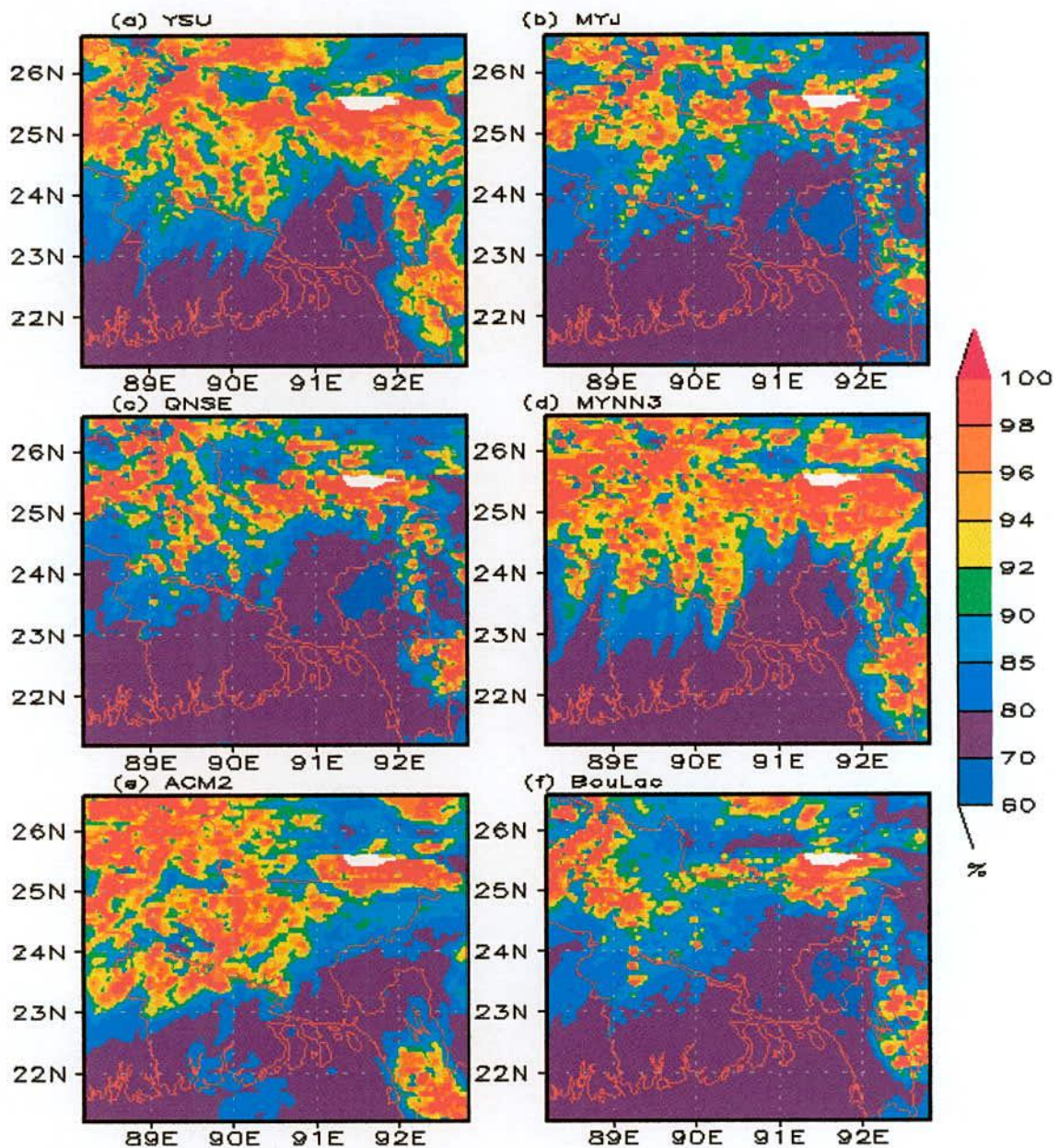


Fig. 32: Spatial distribution of simulated RH using a) YSU, b) MYJ, c) QNSE, d) MYNN3, e) ACM2 and f) BouLac schemes at 1200 UTC of 16 August 2009.

4.2.9 Rainfall

The distribution of BMD and TRMM daily rainfall during 15 – 16 August 2009 are shown in Figs. 33(a & c) and Figs. 33(b & d) respectively. From Figs. 33(a & b)) it is observed that the maximum rainfall occurred at Hatiya (138 mm) and in the south south-eastern region on 15

August 2009. The maximum rainfall occurred in the northwestern region (Rangpur, Dinajpur, and Sayedpur) on 16 August 2009 (Figs. 33c & d). The WRF-ARW Model has simulated rainfall using Lin *et al* microphysics scheme and Kain-Fritsch cumulus parameterization scheme in combination with YSU, MYJ, QNSE, MYNN3, ACM2 and BouLac Planetary Boundary Layer schemes during 15 – 16 August 2009 and the distribution are presented in Figs. 34 - 35 respectively.

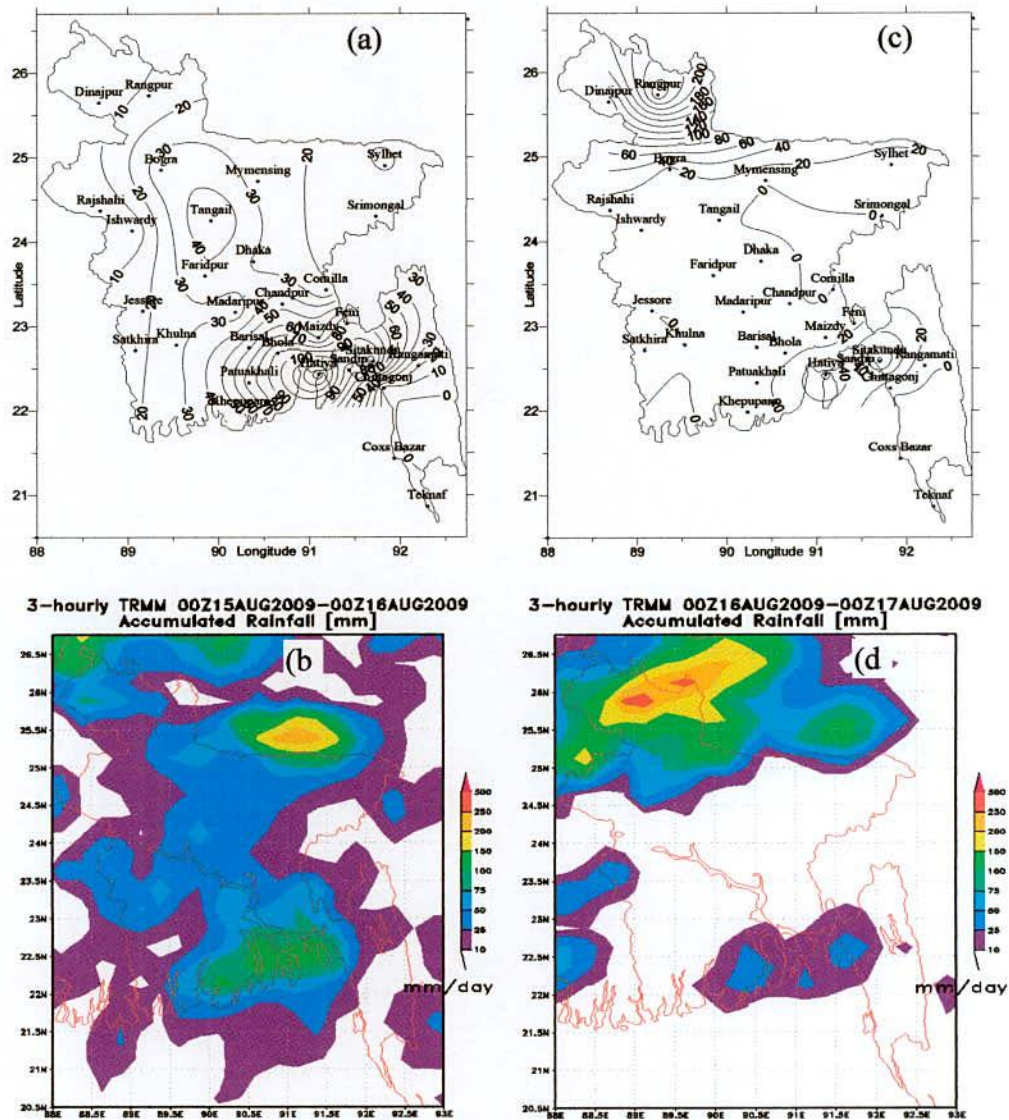


Fig. 33: BMD observed and TRMM daily rainfall in (a-b) 15 August and (c-d) 16 August 2009 respectively.

Figures 34(a-d & f) show the distribution of WRF model simulated rainfall pattern using YSU MYJ, QNSE, MYNN3 and BouLac schemes on 15 August 2009. The All PBL schemes have simulated maximum rainfall at the northern (along the boarder line of Bangladesh) and northwestern (Rangpur, Dinajpur) region and almost no rainfall has been simulated in the

southern and southeastern region (Chittagong, Cox's Bazar, Teknaf). From Fig. 34(e), it has also been found that the ACM2 scheme produces maximum rainfall in the western and northern (Mymensingh) region and almost no rainfall has been simulated in the southern region and southeastern region (Chittagong, Cox's Bazar).

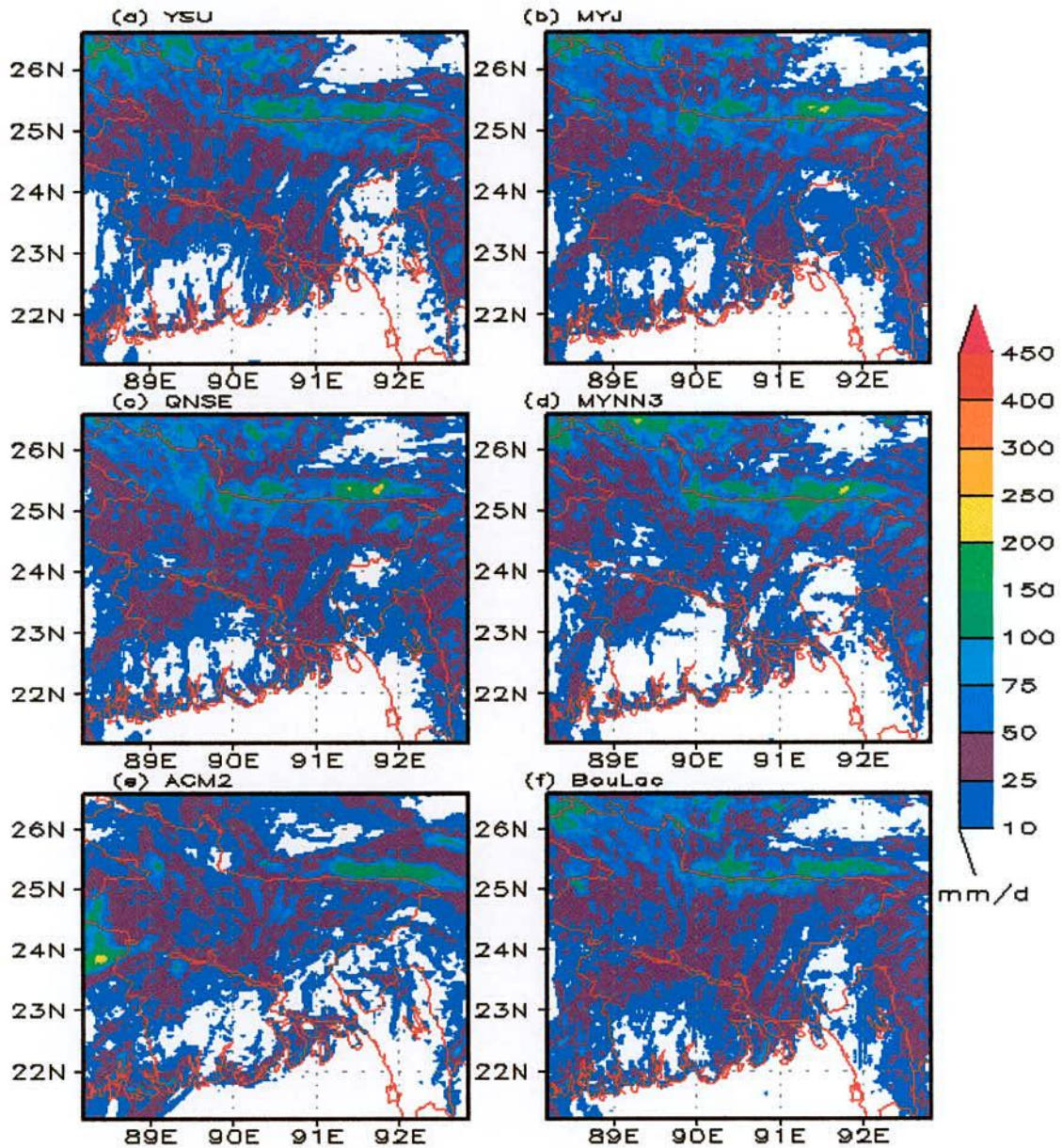


Fig. 34: Spatial distribution of simulated rainfall (mm) using a) YSU, b) MYJ, c) QNSE, d) MYNN3, e) ACM2 and f) BouLac schemes at 15 August 2009.

Figure 35(a – f) shows the distribution of WRF model simulated rainfall pattern on 16 August 2009 using different schemes. The All six schemes have simulated maximum rainfall at the northwestern (Rangpur, Dinajpur, and Ponchogor) region and almost no rainfall has

simulated in the eastern (over Comilla) and southeastern (Chittagong, Cox's Bazar, Teknaf) region. The YSU, MYJ, MYNN3, QNSE, ACM2 and BouLac schemes have simulated 200 to 250 mm rain over Rangpur, Dinajpur and Ponchogor region.

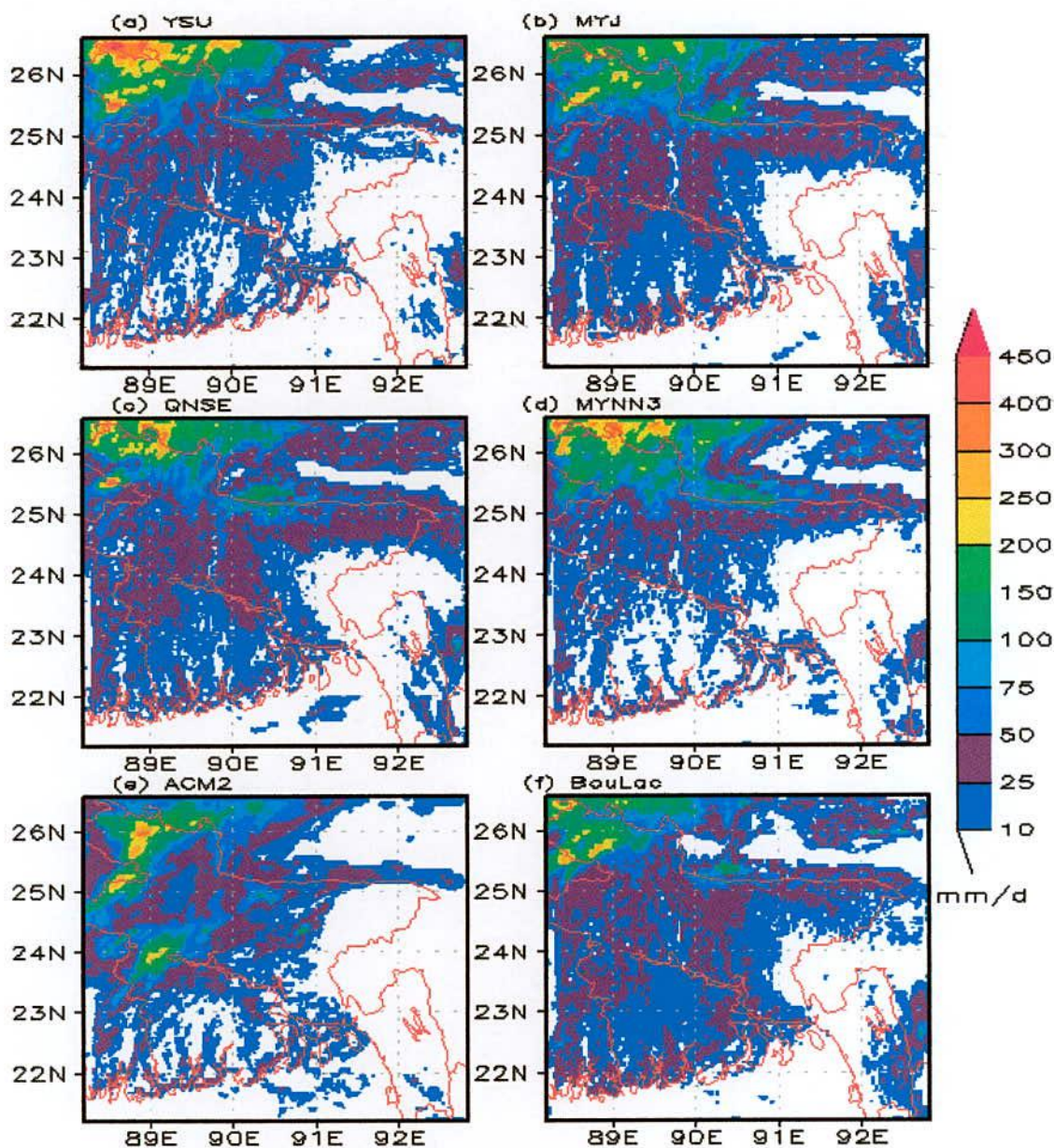


Fig. 35: Spatial distribution of simulated rainfall (mm) using a) YSU, b) MYJ, c) QNSE, d) MYNN3, e) ACM2 and f) BouLac schemes at 16 August 2009.

The simulated 24-h heavy rainfall (mm) obtained using (a) YSU, (b) MYJ, (c) QNSE, (d) MYNN3, (e) ACM2 and (f) BouLac schemes have compared with the 24-hour rainfall observed by BMD rain-gauge and TRMM daily rainfall on 15 - 16 August 2009. On 15 August 2009, the YSU and ACM2 schemes have simulated rain of 100 to 150 over Hatiya. Out of six PBL schemes, only the rainfall simulated by using YSU and ACM2 schemes are

almost closest to the values of observed rainfall of BMD and TRMM daily rainfall. The YSU and ACM2 schemes have simulated 200 to 300 mm rain over Rangpur region on 16 August 2009. The maximum (256 mm) rainfall occurred in the northwestern region (Rangpur) on 16 August 2009 [Fig. 33(c & d)] as recorded by BMD and TRMM daily rainfall. So out of six schemes, the YSU and ACM2 schemes are comparatively better than others.

4.2.10 Summary

The YSU, ACM2 and BouLac schemes have simulated 100 to 150 mm, 75 to 100 mm and 25 to 50 mm rain respectively but the observed rainfall was 138 mm over Hatiya region on 15 August 2009. The ACM2, YSU and BouLac schemes have simulated 250 to 300 mm, 200 to 250 mm and 150 to 200 mm rain respectively over Rangpur region on 16 August 2009 whereas the observed rain was 256 mm over Rangpur. The ACM2 scheme has simulated minimum ACHFX in the southeastern region (Hatiya) on 15 August 2009 and also simulated minimum ACHFX in the northwestern region on 16 August 2009 where maximum actual rainfall has been observed. The QNSE scheme has simulated maximum ACLHF over Hatiya and Rangpur region on 15 and 16 August 2009 respectively where maximum rainfall observed. The result shows that where the ACLHF is maximum (minimum) the rainfall is also maximum (minimum) in that region. The simulated PBL is minimum by ACM2 and MYNN3 schemes at the position where the rainfall is maximum on 15 and 16 August 2009. The YSU scheme has simulated maximum rainfall over Hatiya and Rangpur region where the simulated GLW minimum on 15 and 16 August 2009. On 15 and 16 August 2009, the ACM2 scheme has simulated minimum OLR over Hatiya and Rangpur region where maximum rainfall is observed. The maximum reflectivity simulated in the northwestern region by ACM2 scheme on 15 and 16 August 2009. The ACM2 scheme has simulated maximum wind speed at 850 hPa in the southern region 1200 UTC of 15 August 2009 and also simulated maximum wind speed in the northwestern region on 16 August 2009. The relative humidity simulated by ACM2 scheme is 98 to 100% in the southern and northwestern region on 15 and 16 August 2009 respectively.

4.3 Heavy rainfall event of 26-27 June 2010 using WRF model

4.3.1 Accumulated Upward Heat Flux (ACHFX) at the surface

WRF model has simulated accumulated upward heat flux (ACHFX) at 1200 UTC of 26 June 2010 at the surface is shown in Figs. 36(a-f). The ACHFX is maximum in the southeastern, western and northwestern regions for YSU (Fig. 36a), MYJ (Fig. 36b), QNSE (Fig. 36c), MYNN3 (Fig. 36d) and BouLac (Fig. 36f) schemes. On this day, the ACHFX has also found maximum in the western region (outside Bangladesh) for ACM2 ((Fig. 36e) scheme. From the figure, it is also observed that the ACHFX is minimum in the northeastern to southern region and the ACM2 scheme simulated the minimum ACHFX in the northwestern region.

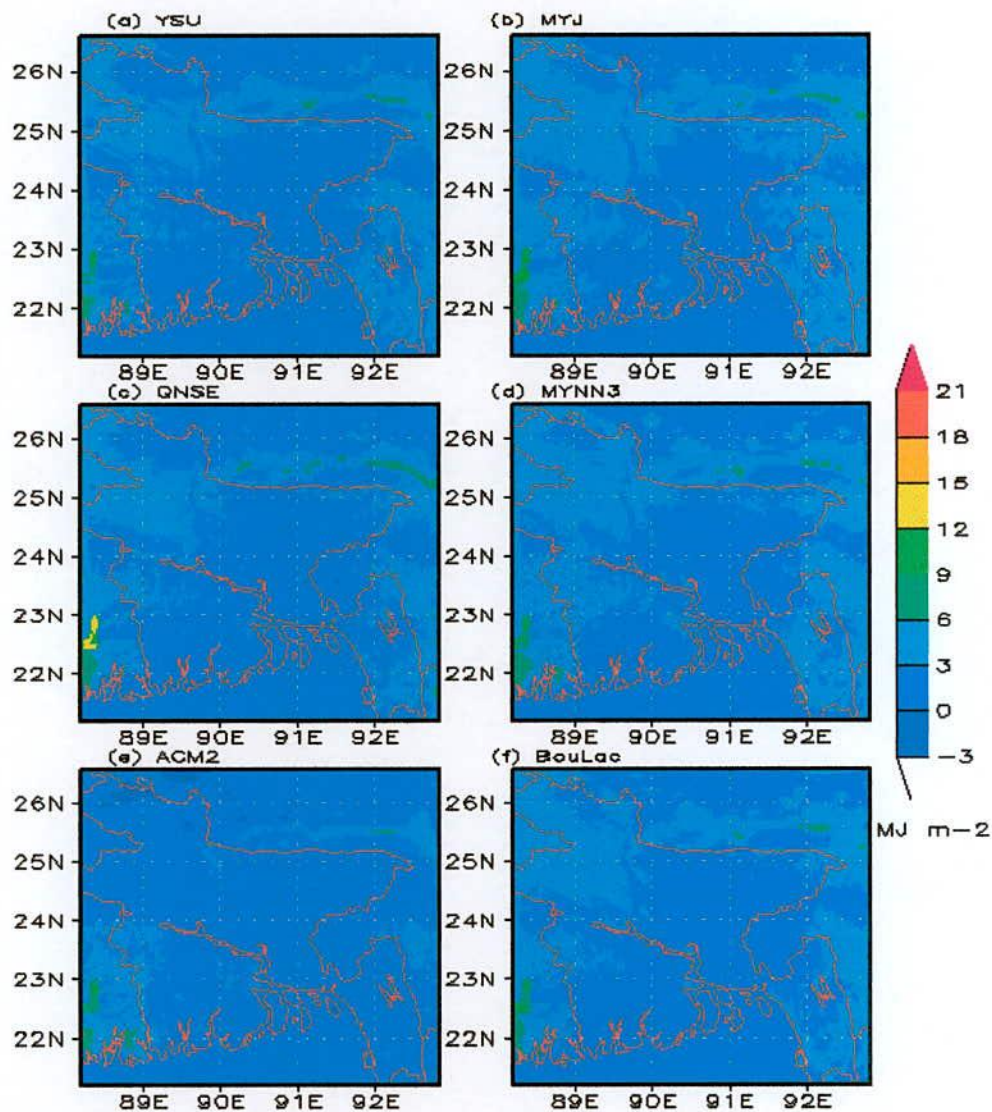


Fig. 36: Spatial distribution of simulated ACHFX using a) YSU, b) MYJ, c) QNSE, d) MYNN3, e) ACM2 and f) BouLac schemes at 1200 UTC of 26 June 2010.

Figure 37 (a-f) shows the spatial distribution of ACHFX using different schemes at 1200 UTC on 27 June 2010. It has been found that the maximum ACHFX is simulated in the southeastern and northwestern region by YSU (Fig. 37a), MYJ (Fig. 37b), QNSE (Fig. 37c), MYNN3 (Fig. 37d) and BouLac (Fig. 37f) schemes and also maximum ACHFX has been simulated in the southeastern region for ACM2 ((Fig. 37e) scheme. From the figure it is also observed that the ACHFX simulated minimum in the southern (along the land boundary) and eastern region for YSU, QNSE and BouLac schemes. The MYJ and MYNN3 schemes have simulated minimum ACHFX in the southern region (along the land boundary). The minimum ACHFX is simulated in the northwestern region and southern region (along the land boundary) in case of ACM2 scheme.

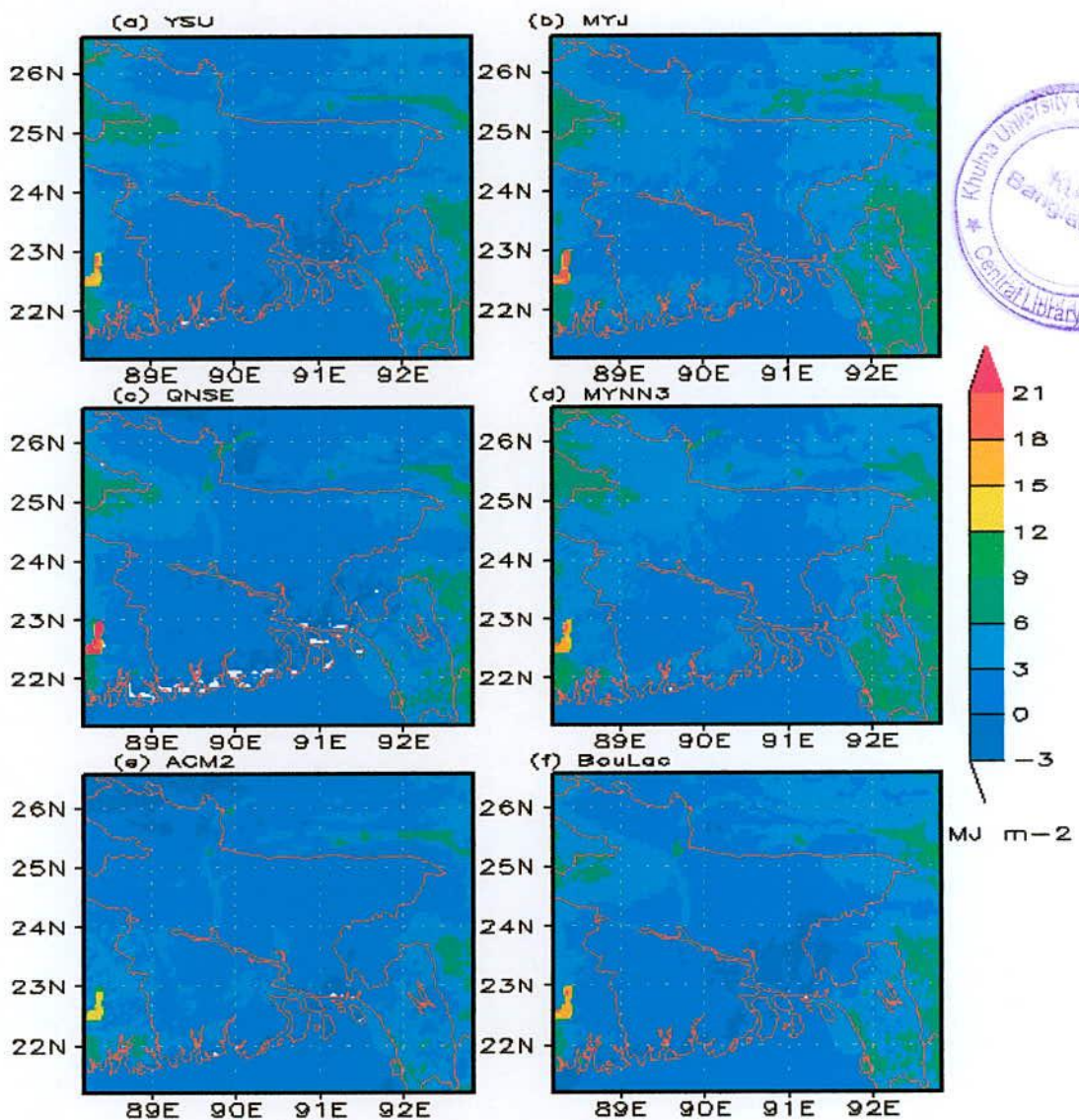


Fig. 37: Spatial distribution of simulated ACHFX using a) YSU, b) MYJ, c) QNSE, d) MYNN3, e) ACM2 and f) BouLac schemes at 1200 UTC of 27 June 2010.

Minimum ACHFX has been simulated at D2, where the location is relatively covered by a cloud sky during the 24-h period of interest and the maximum ACHFX is found over the less rainfall area in that location. From figure it has been found that the ACHFX is minimum in the northwestern, southern region and the model has also simulated maximum rainfall in that region by all schemes.

4.3.2 Accumulated Upward Latent Heat Flux (ACLHF) at the surface

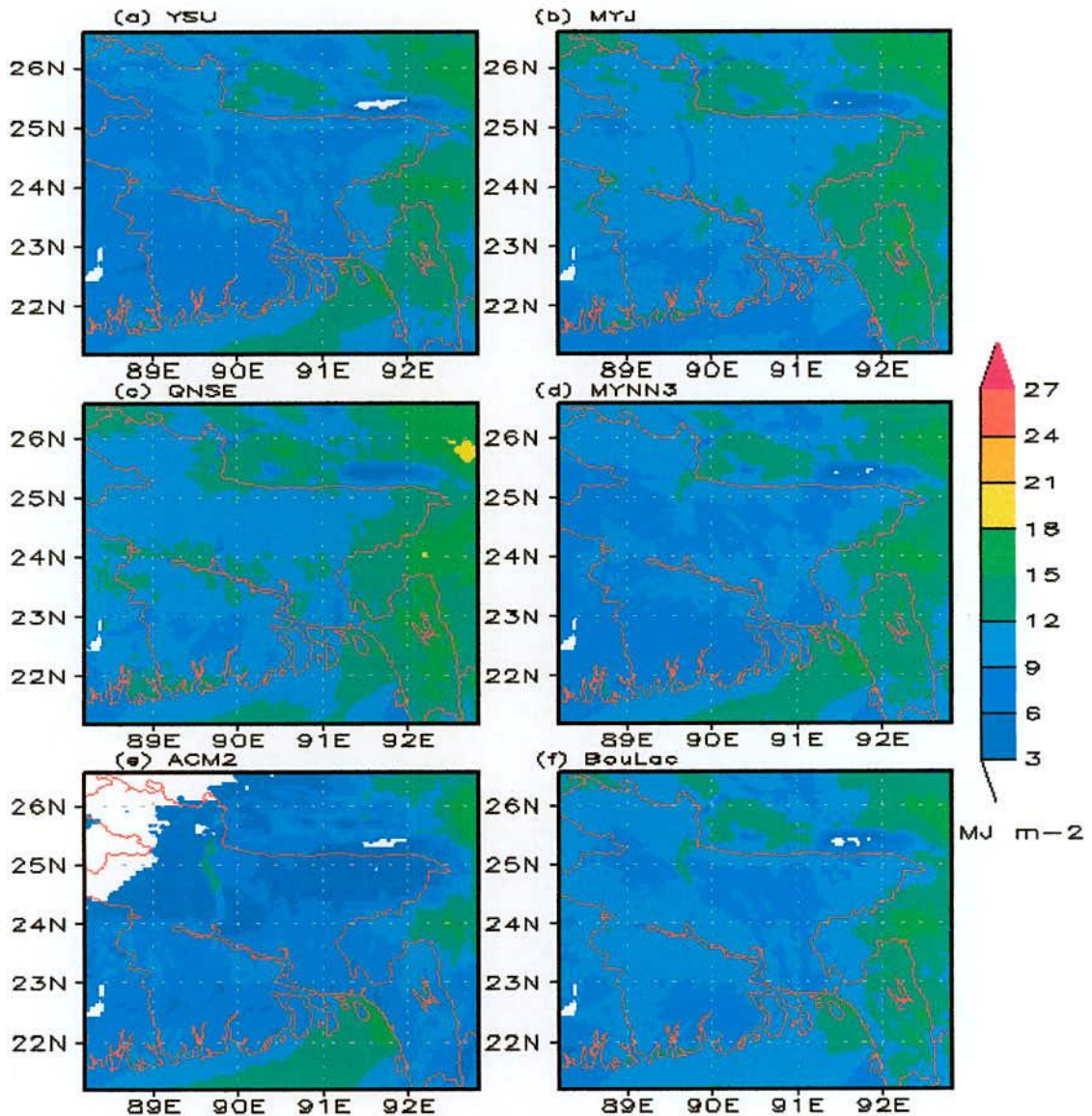


Fig. 38: Spatial distribution of simulated ACLHF using a) YSU, b) MYJ, c) QNSE, d) MYNN3, e) ACM2 and f) BouLac schemes at 1200 UTC of 26 June 2010.

WRF-ARW model has simulated accumulated upward latent heat flux (ACLHF) at 1200 UTC on 26 June 2010 at the surface and the distributions are presented in Figs. 38(a-f) and

39(a-f). The YSU (Fig. 38a), MYJ (Fig. 38b), MYNN3 (Fig. 38d) and BouLac (Fig. 38f) schemes have simulated maximum ACLHF in the southeastern region. The ACM2 (Fig. 38e) scheme has simulated maximum ACLHF in southern (over ocean) region. The minimum and maximum ACLHF are simulated all over Bangladesh by QNSE and ACM2 schemes respectively on 26 June. From the figure, it can also be observed that the ACLHF is minimum in the southwestern part for all schemes. The YSU, MYNN3, MYJ, QNSE and BouLac schemes have simulated the minimum ACLHF in the southwestern. The ACM2 scheme has simulated almost no ACLHF in the northwestern region.

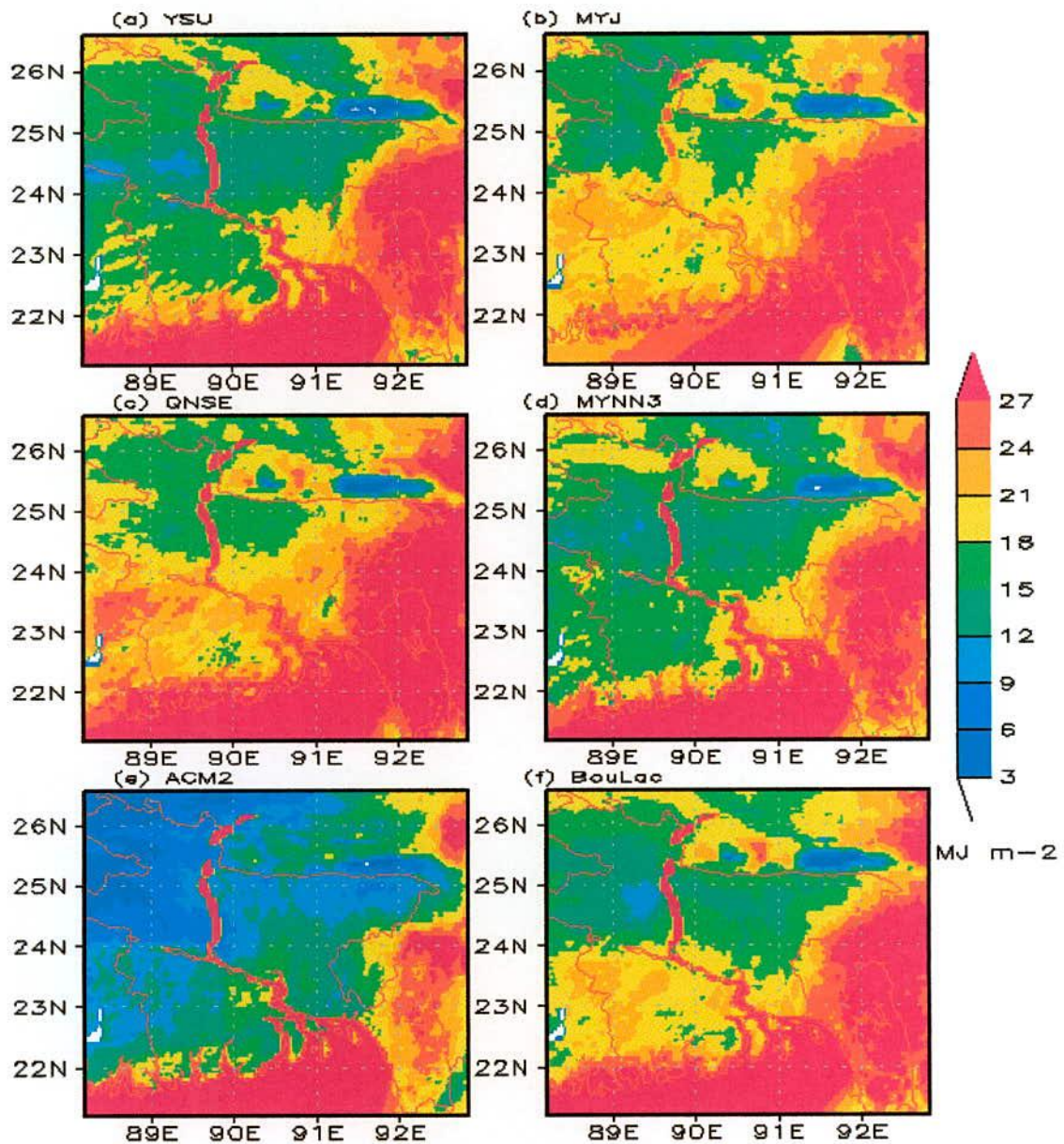


Fig. 39: Spatial distribution of simulated ACLHF using a) YSU, b) MYJ, c) QNSE, d) MYNN3, e) ACM2 and f) BouLac schemes at 1200 UTC of 27 June 2010.

Figure 39(a-f) represent the simulated ACLHF at the surface at 1200 UTC on 27 June 2010 obtained by using different schemes. The maximum ACLHF has simulated in the southern (along the boarder line of land-ocean and Bay of Bengal), southeastern and eastern (outside Bangladesh) region for all schemes. The minimum ACLHF is simulated in the northwestern region by MYJ, QNSE and BouLac schemes and minimum ACLHF is also simulated in the western to northern region using YSU and MYNN3 schemes. The simulated minimum ACLHF position has been shifted in the northwestern most region of Bangladesh for ACM2 scheme.

4.3.3 Downward Long wave Flux at Ground Surface (GLW)

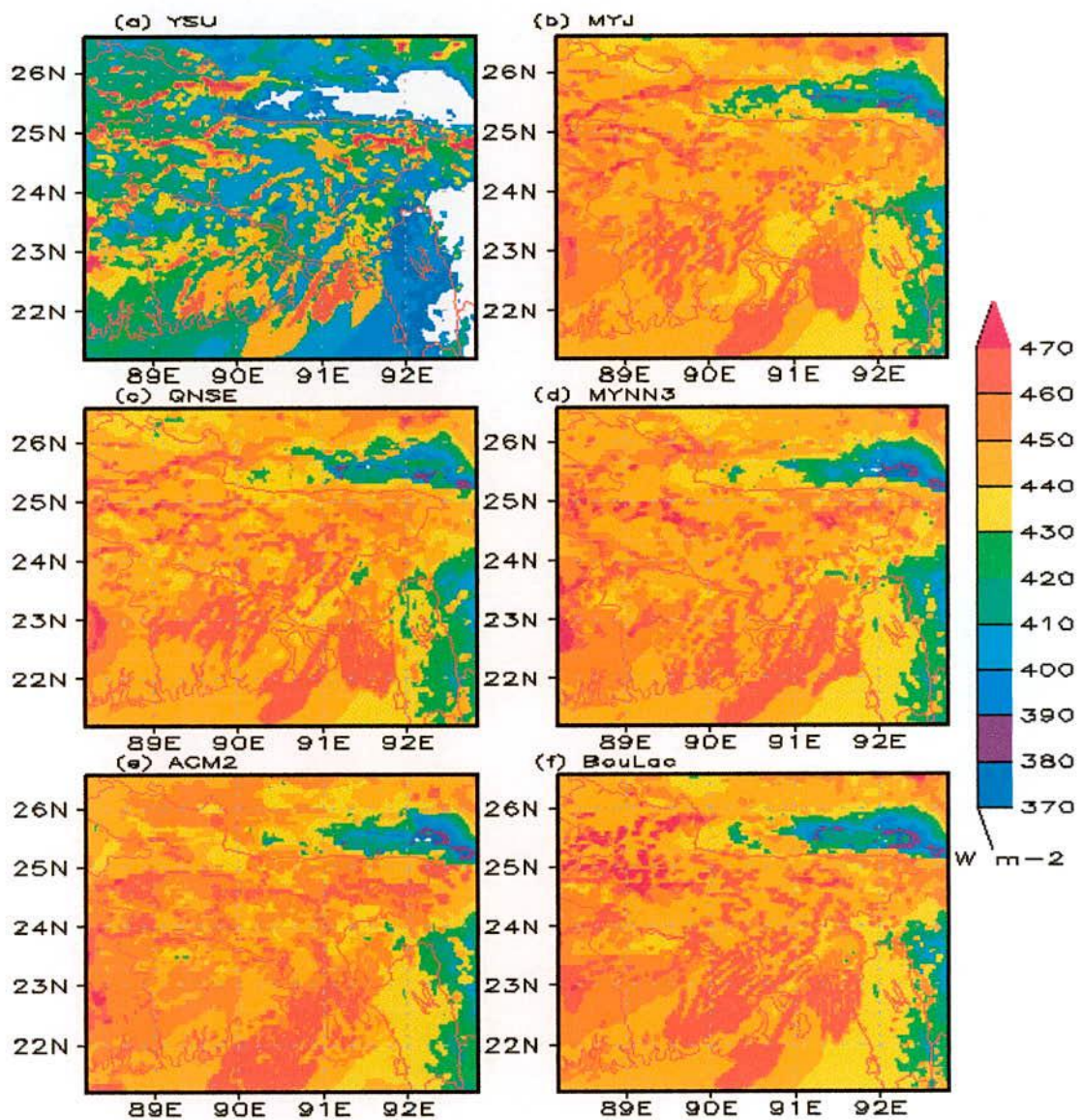


Fig. 40: Spatial distribution of simulated GLW using a) YSU, b) MYJ, c) QNSE, d) MYNN3, e) ACM2 and f) BouLac schemes at 1200 UTC of 26 June 2010.

Figure 40(a-f) shows the spatial distribution of model simulated downward long wave flux ($W m^{-2}$) at the surface using six schemes at 1200 UTC on 26 June 2010. The maximum and significant amount of GLW has been simulated all over the country except southeastern region by all schemes. At the same time, it is observed that the downward long wave flux is minimum in the southeastern region. Figure 40a shows that the simulated GLW is minimum ($00 - 380 W/m^2$) in the southeastern region in case of YSU schemes.

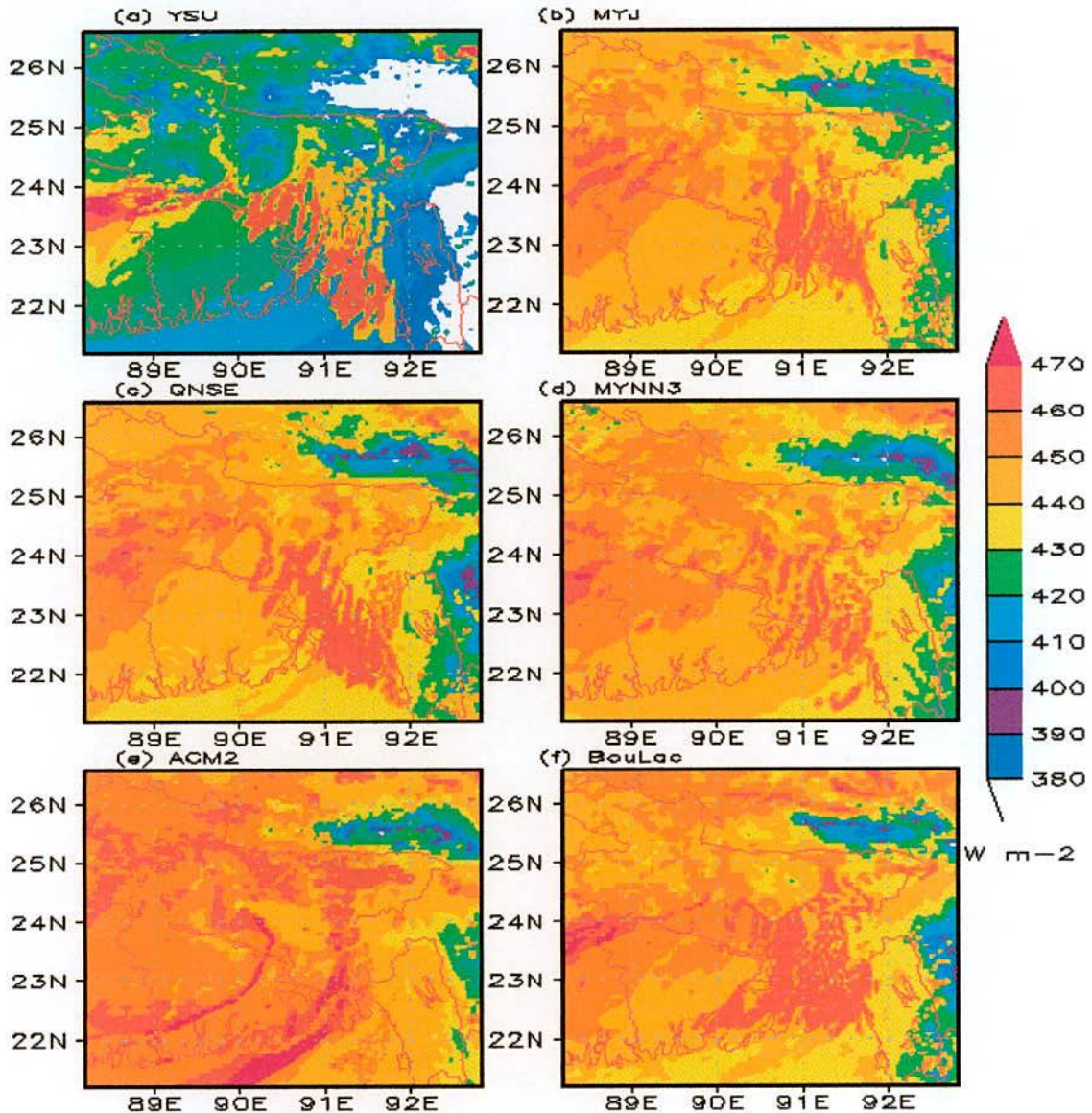


Fig. 41: Spatial distribution of simulated GLW using a) YSU, b) MYJ, c) QNSE, d) MYNN3, e) ACM2 and f) BouLac schemes at 1200 UTC of 27 June 2010.

At 1200 UTC on 27 June 2010, the GLW has been simulated and is found to be minimum in the southeastern region of domain D2 for all schemes. The simulated GLW has been maximum all over Bangladesh as simulated by all schemes. The simulated GLW is also

maximum in the southern and southwestern region as obtained by ACM2 scheme. On this day, the YSU (Fig. 41a) scheme has simulated maximum GLW in the western side and the QNSE (Fig. 41c) scheme has also simulated GLW in the eastern and northwestern part of Chittagong region. The MYJ (Fig. 41b) scheme has also simulated significant amount of GLW in the western, eastern and northwestern parts of Chittagong. The maximum GLW is simulated in the eastern and northwestern parts of Chittagong by using MYNN3 (Fig. 41d) scheme. The BouLac (Fig. 41f) scheme has also simulated significant amount of GLW in the western, eastern and northwestern parts of Chittagong region.

4.3.4 Outgoing Long wave Radiation (OLR)

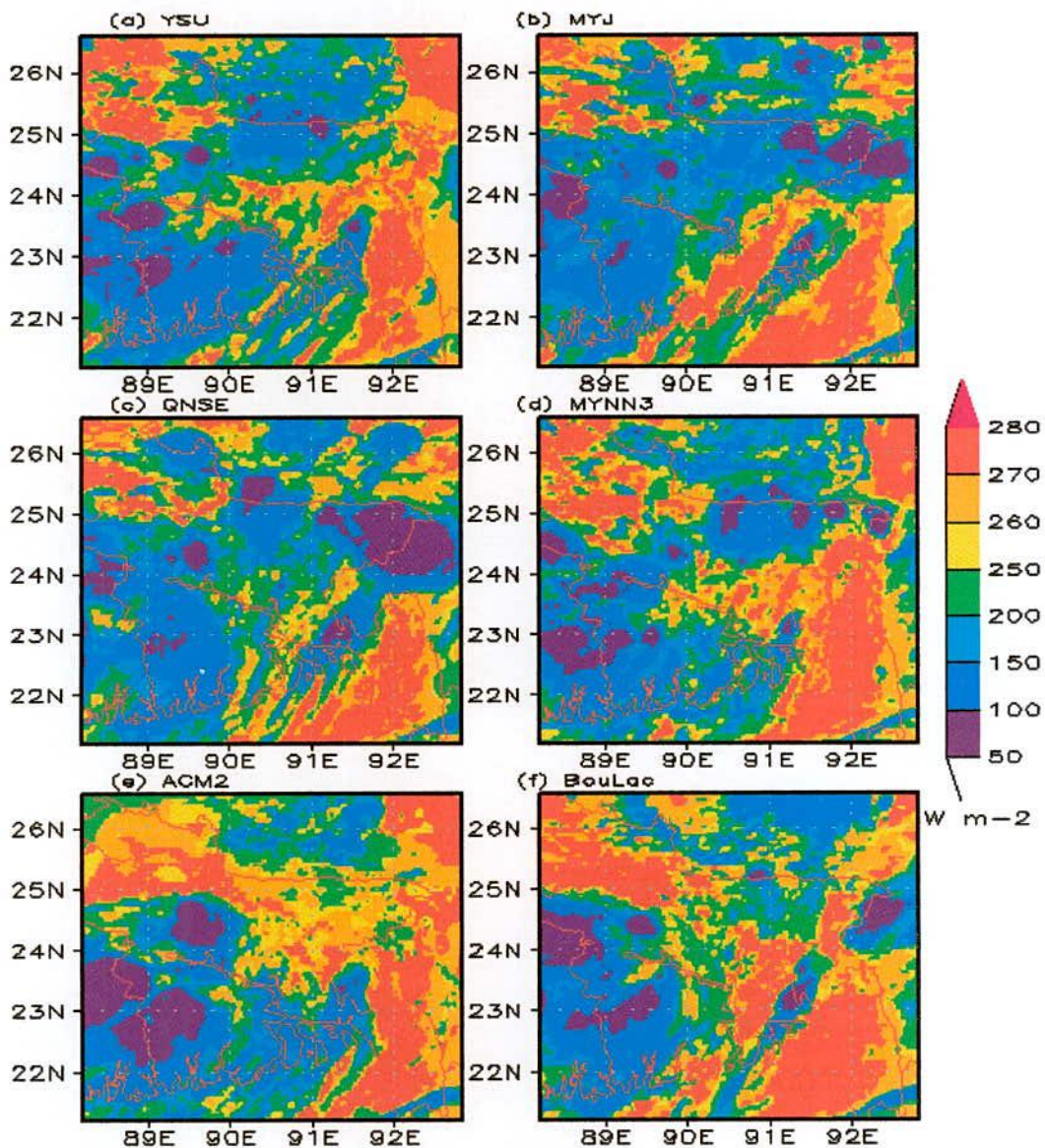


Fig. 42: Spatial distribution of simulated OLR using a) YSU, b) MYJ, c) QNSE, d) MYNN3, e) ACM2 and f) BouLac schemes at 1200 UTC of 26 June 2010.

WRF Model has simulated outgoing long wave radiation of domain D2 at 1200 UTC on 26 and 27 June 2010 using different schemes and the distributions are presented in Figs.42 & 43. The maximum OLR has been simulated in the northwestern and southeastern regions of Bangladesh by using six PBL schemes. The OLR is found minimum in the western region for all schemes and also minimum in the northeastern region for MYJ, QNSE and MYNN3 schemes. The maximum and significant amount of OLR is simulated in the southeastern to northwestern region of Bangladesh for ACM2 and BouLac schemes.

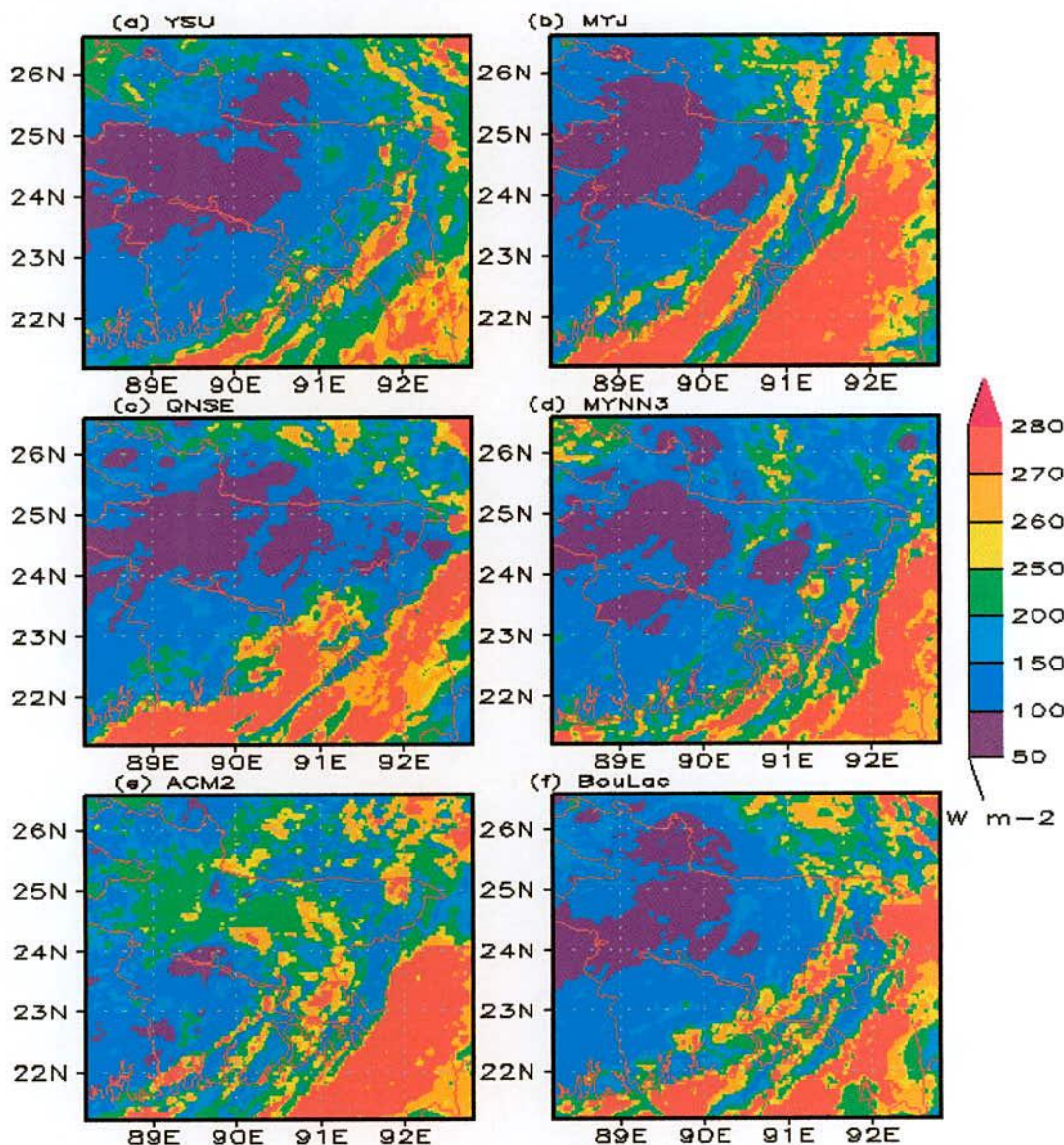


Fig. 43: Spatial distribution of simulated OLR using a) YSU, b) MYJ, c) QNSE, d) MYNN3, e) ACM2 and f) BouLac schemes at 1200 UTC of 27 June 2010.

On 27 June 2010, the significant amount of OLR has been simulated in the southeastern region by using six schemes. The YSU, MYNN3, ACM2 and BouLac schemes have

simulated maximum OLR in the southeastern region. From Figures 43(b & c), it has been found that the significant amount of OLR is in the southeastern and southern region. Maximum areas of minimum OLR has also simulated in the central to the western region by all PBL schemes. From Figure 43(e) shows minimum OLR in the southwestern region of Bangladesh for ACM2 scheme.

4.3.5 Variations of Planetary Boundary Layer (PBL)

WRF Model has simulated PBL (meter) of domain D2 at 1200 UTC on 26 and 27 June 2010 using different schemes and the distributions are presented in Figs. 44 & 45 respectively.

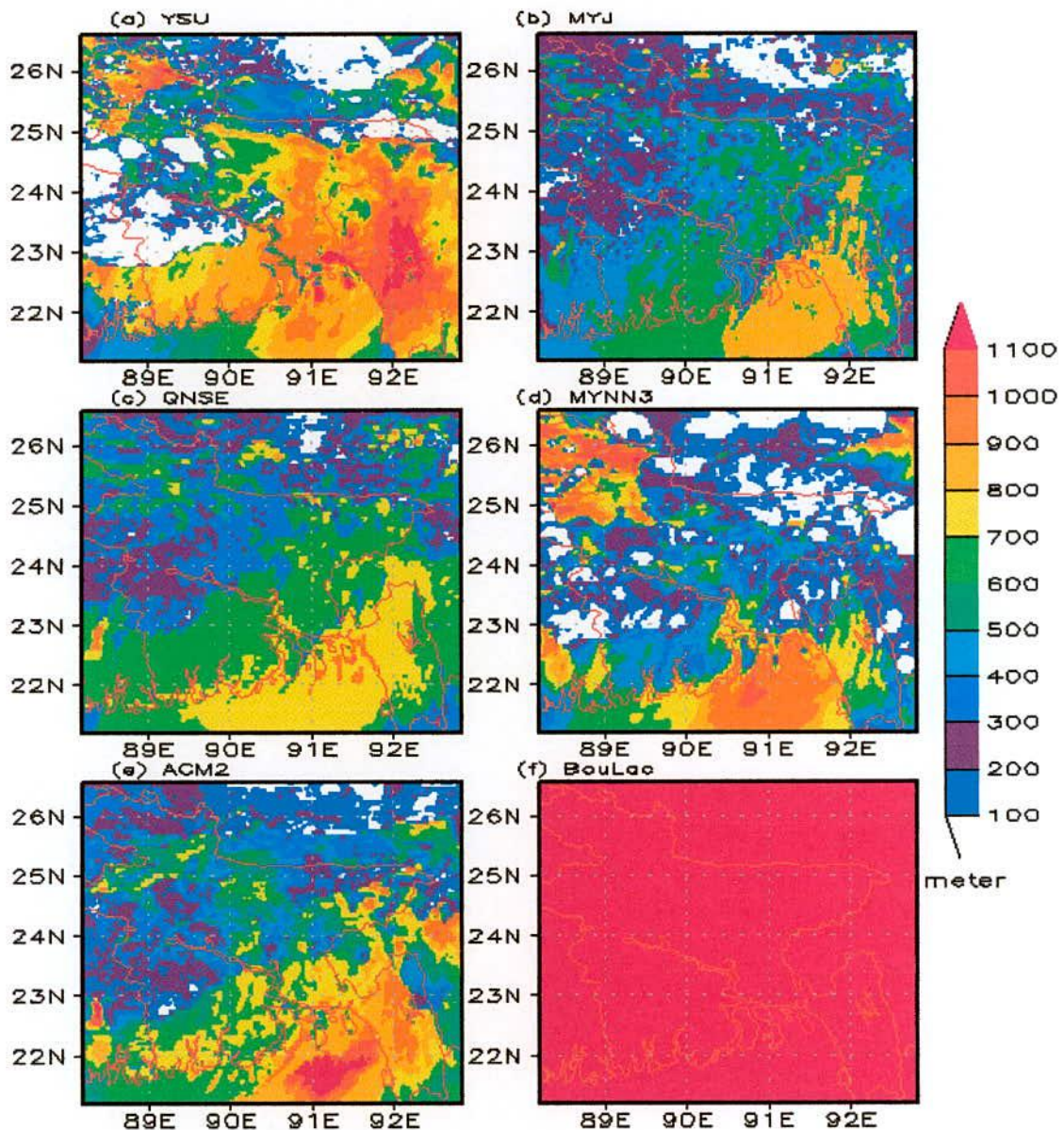


Fig. 44: Spatial distribution of simulated PBL height using a) YSU, b) MYJ, c) QNSE, d) MYNN3, e) ACM2 and f) BouLac schemes at 1200 UTC of 26 June 2010.

The YSU scheme has simulated maximum PBL in the southeastern and northwestern regions and almost no PBL has been simulated in the western region. The maximum PBL is simulated in the southeastern region by MYJ, QNSE and ACM2 schemes and the minimum PBL has been simulated in the western region. Figure 44(d) shows maximum simulated PBL in the northwestern region and minimum PBL in the western to northeastern region.

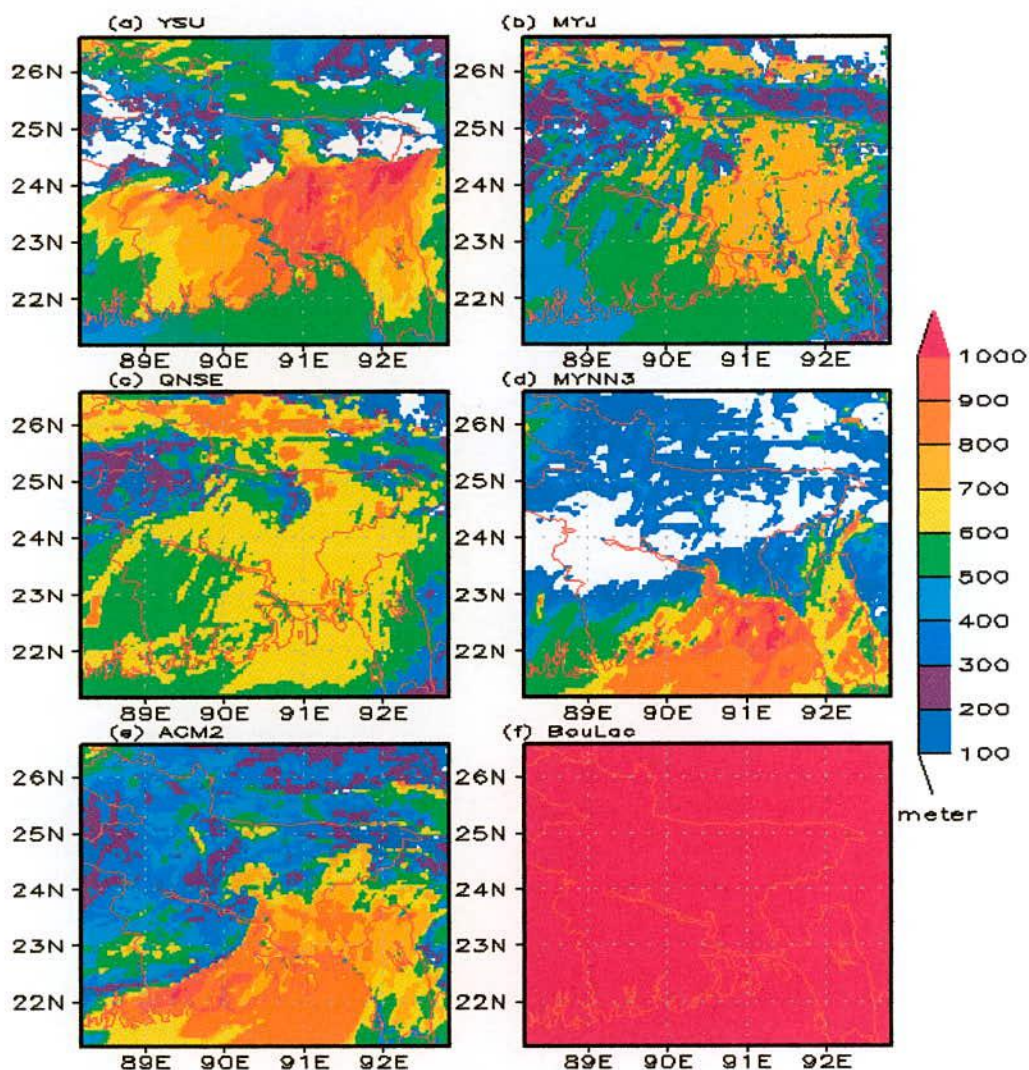


Fig. 45: Spatial distribution of simulated PBL height using a) YSU, b) MYJ, c) QNSE, d) MYNN3, e) ACM2 and f) BouLac schemes at 1200 UTC of 27 June 2010.

Figure 45 represents the spatial distribution of WRF model simulated PBL at 1200 UTC on 27 June 2010. The YSU (Fig. 45a) scheme has simulated maximum PBL in the eastern region and the minimum PBL in the western to northeastern region. Significant PBL is simulated by MYJ scheme in the eastern region and the minimum PBL is simulated in the northwestern region. The maximum PBL is simulated by using QNSE (Fig. 45c) scheme in the

northeastern region of Bangladesh and the minimum PBL in the northwestern region. The MYNN3 (Fig. 45d) scheme has simulated maximum PBL in the southern (over the Bay of Bengal) region and almost no PBL in the western to northeastern region (Jessore, Iswardy, Sylhet, Dhaka, Jhenaidah). The maximum PBL is simulated by using ACM2 scheme (Fig. 45e) in the southeastern region (over Mongla) and minimum PBL is simulated in the northeastern part (Sylhet) of Bangladesh. In case of BouLac scheme, constant PBL has been simulated all over the country on 26 and 27 June 2010.

From the figure, if the simulated rainfalls (mm) are compared with the PBL (meter), it has been found that the maximum PBL lies over the area of minimum rainfall and the minimum PBL (meter) over the area of heavy rainfall.

4.3.6 Reflectivity

Figure 46(a-f) represents the spatial distribution of WRF model simulated reflectivity (shaded) using different schemes at 850 hPa levels at 1200 UTC on 26 June 2010. The YSU (Fig. 46a) scheme has simulated significant reflectivity in the western region. The MYJ (Fig. 46b), MYNN3 (Fig. 46d) and BouLac (Fig. 46f) schemes have simulated significant amount of reflectivity in small area in the western, northeastern (along the boarder line of Bangladesh) and southeastern regions and QNSE (Fig. 46c) scheme has also simulated maximum reflectivity in the northeastern region of Bangladesh at the same time. The maximum reflectivity is simulated by ACM2 scheme in the western region.

At 1200 UTC on 27 June 2010, WRF model simulated reflectivity (shaded) using different PBL schemes. The YSU (Fig. 47a), QNSE (Fig. 47c), MYNN3 (Fig. 47d), MYJ (Fig. 47b) and BouLac (Fig. 47f) schemes have simulated maximum and significant amount of reflectivity in the northern to the northwestern region. The ACM2 scheme has also simulated maximum reflectivity in the central and northwestern region at 850 hPa level.

It has been observed that the YSU, MYJ, and QNSE scheme have simulated maximum reflectivity in the northern region and the BouLac scheme also has simulated maximum reflectivity in the northwestern region at 850 hPa level at 1800 UTC on 27 June 2010(not shown by figure). The maximum reflectivity is simulated in the northwestern part of Dhaka by using MYNN3 scheme. The ACM2 scheme has simulated maximum reflectivity in the northeastern region.

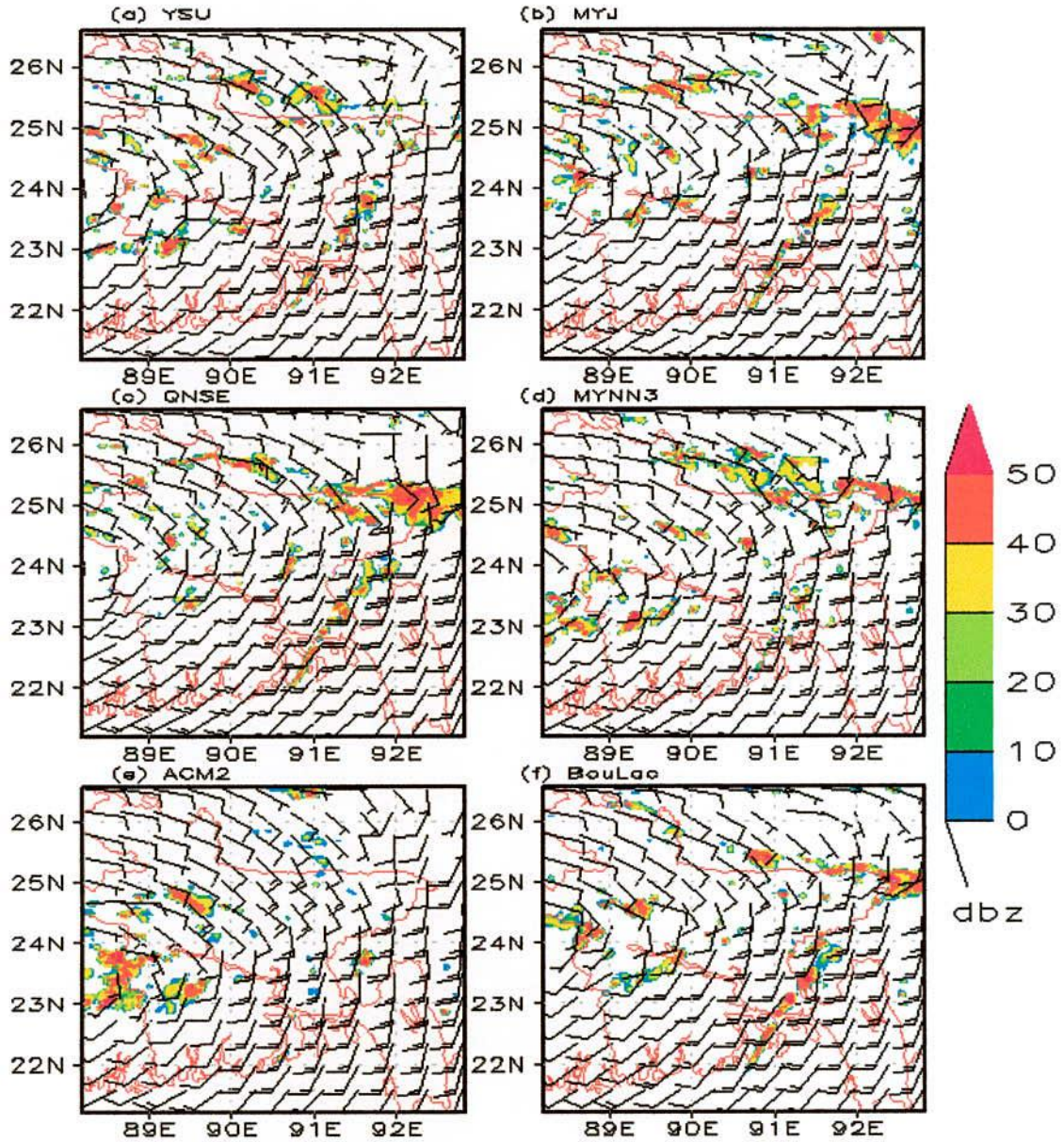


Fig. 46: Spatial distribution of simulated wind speed (m/s) and reflectivity (dBZ) at 850 hPa level using a) YSU, b) MYJ, c) QNSE, d) MYNN3, e) ACM2 and f) BouLac schemes at 1200 UTC of 26 June 2010.

4.3.7 Wind

The maximum wind speed has been simulated in the eastern and southeastern region by all schemes at this time. The maximum wind speed of 20 m/s is simulated by using YSU, QNSE, MYJ, ACM2, MYNN3 and BouLac schemes in the southeastern region. The minimum wind speed is simulated by all schemes in the northwestern side of maximum reflectivity at 850 hPa level at 1200 UTC on 26 June 2010.

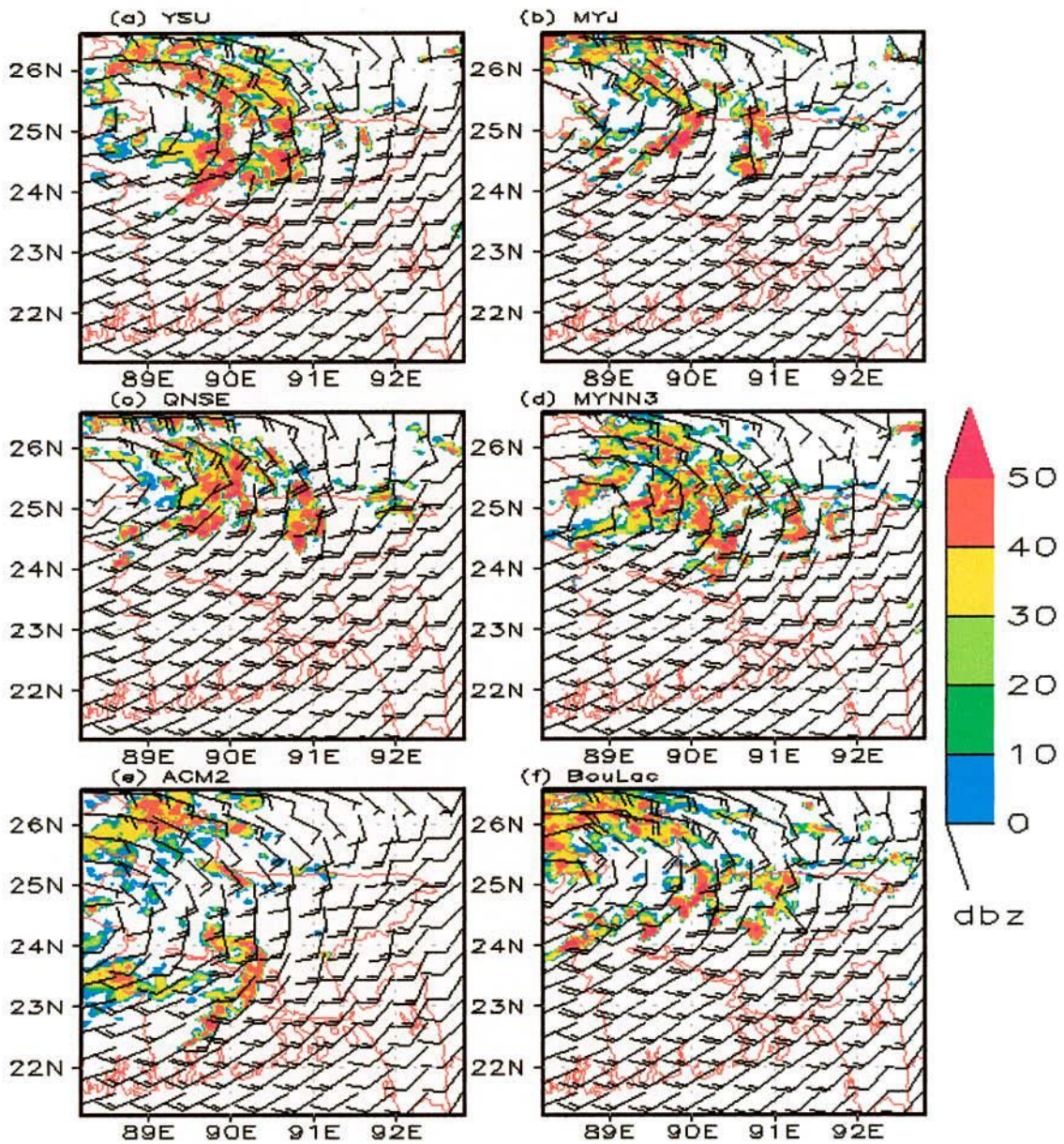


Fig. 47: Spatial distribution of simulated wind speed (m/s) and reflectivity (dBZ) at 850 hPa level using a) YSU, b) MYJ, c) QNSE, d) MYNN3, e) ACM2 and f) BouLac schemes at 1200 UTC of 27 June 2010.

On 27 June 2010, maximum wind speed is simulated all over the country except northwestern region by using all schemes. The maximum wind speed of 20 m/s is simulated by using all schemes in the southwestern, southern and southeastern side of maximum reflectivity. The minimum wind speed is simulated by QNSE and MYNN3 schemes in the inner portion of maximum reflectivity. The simulated wind speed is minimum in the northwestern region of maximum reflectivity as obtained by using MYJ, YSU and BouLac schemes. The ACM2

scheme has also simulated minimum wind speed in the northwestern region of maximum reflectivity at 850 hPa levels.

4.3.8 Relative Humidity (RH)

WRF model has simulated the spatial distribution of relative humidity at 850 hPa levels at 1200 UTC on 26 June 2010 and is presented as in Figs. 48(a-f). The maximum and significant amount (98-100)% of relative humidity simulated all over the Domain except over a small area in the southeastern region by using YSU, MYNN3 and ACM2 schemes and the maximum relative humidity has also been simulated all over Bangladesh except the southwestern region of the country by MYJ, QNSE and BouLac schemes.

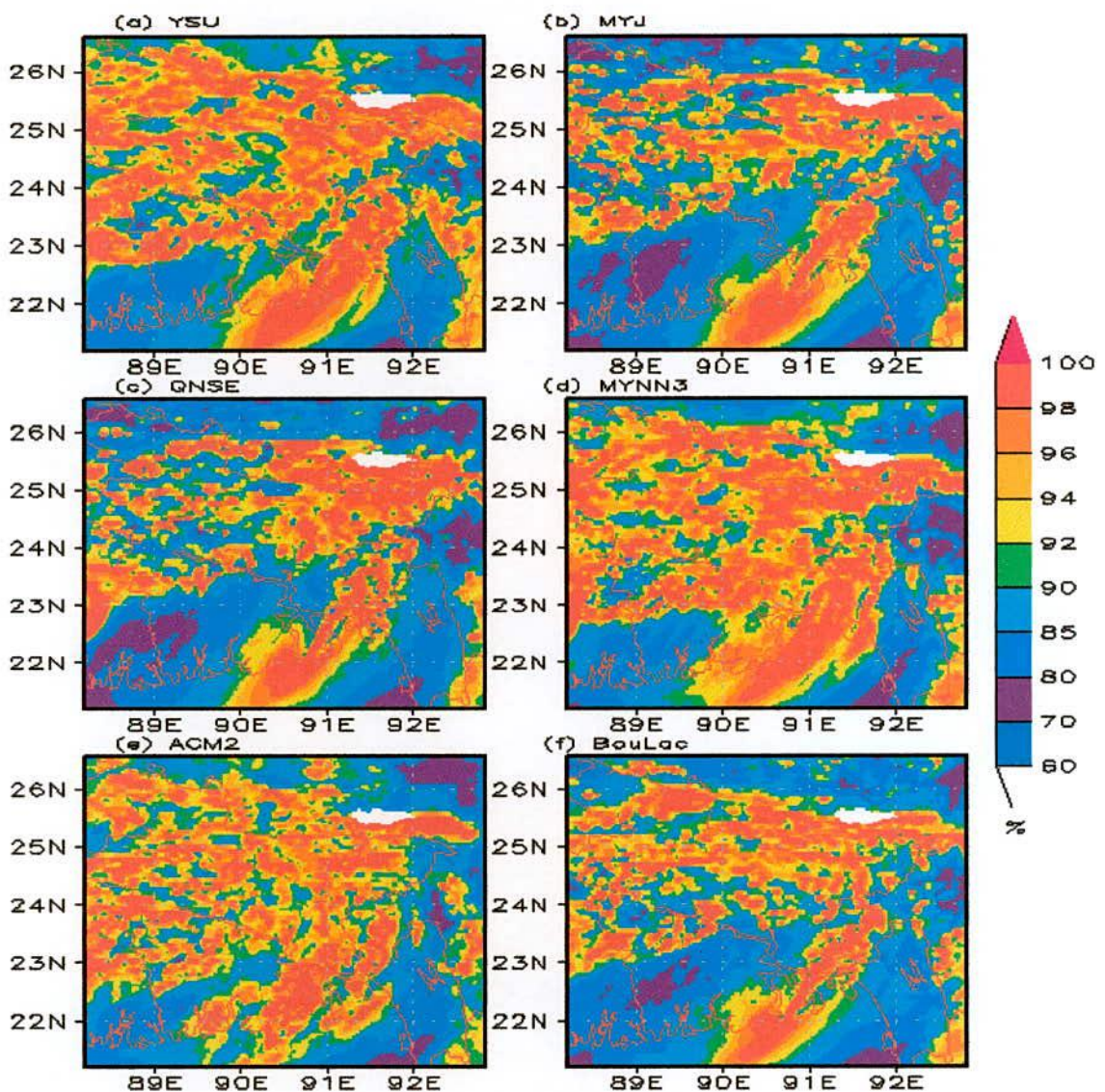


Fig. 48: Spatial distribution of simulated RH at 850 hPa level using a) YSU, b) MYJ, c) QNSE, d) MYNN3, e) ACM2 and f) BouLac schemes at 1200 UTC of 26 June 2010.

From another study, it has been found that the maximum relative humidity has been simulated all over country except southeastern by using all PBL schemes at 1800 UTC on 26 June 2010. The relative humidity is minimum in the southeastern region for all PBL schemes.

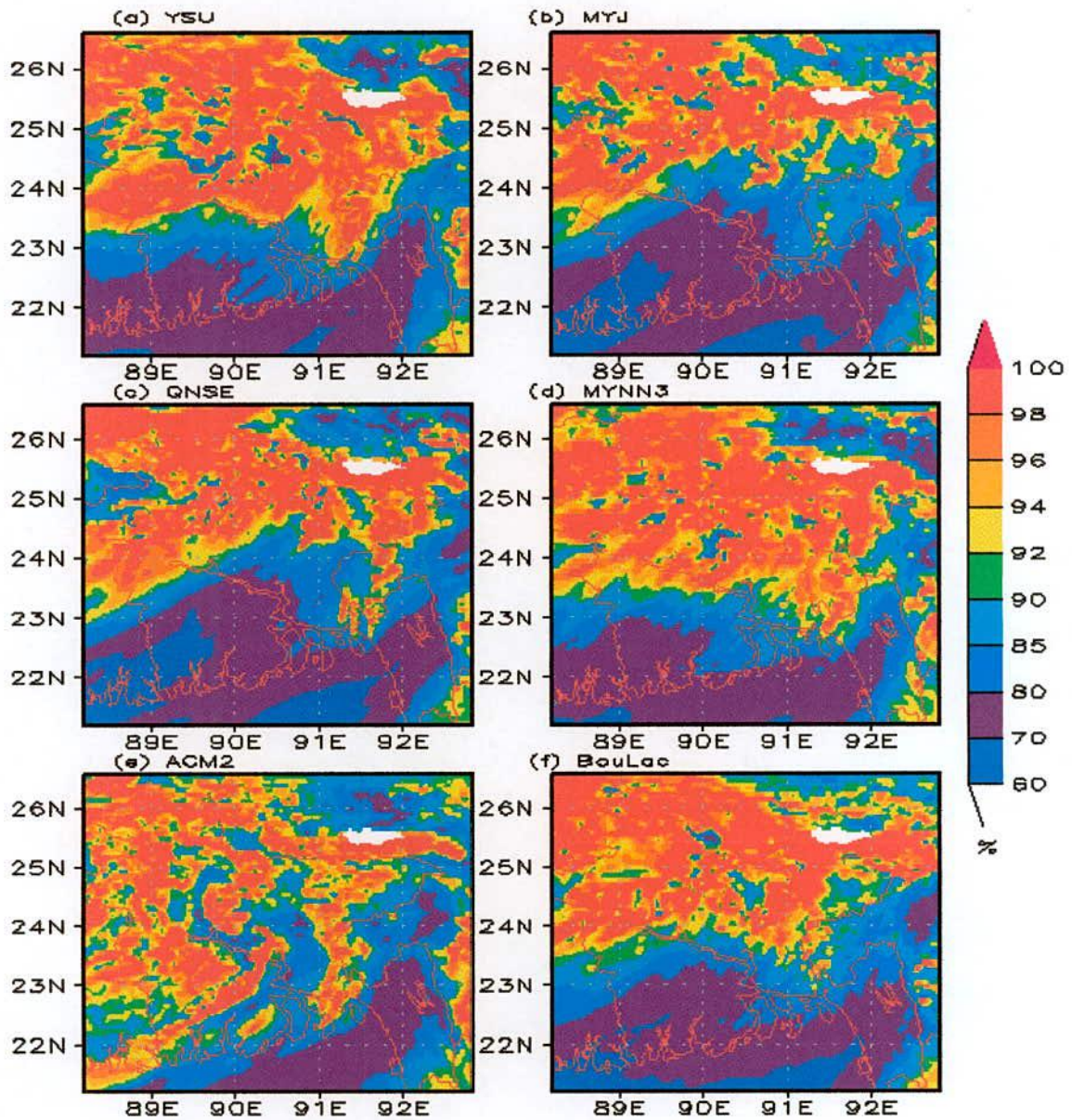


Fig. 49: Spatial distribution of simulated RH at 850 hPa level using a) YSU, b) MYJ, c) QNSE, d) MYNN3, e) ACM2 and f) BouLac schemes at 1200 UTC of 27 June 2010.

Figure 49(a-f) shows the distribution pattern of WRF model simulated relative humidity obtained by using different schemes at 1200 UTC on 27 June 2010. The maximum relative humidity has been simulated all over the domain by YSU, MYJ, QNSE, MYNN3, ACM2 and

BouLac schemes. Maximum areas of minimum relative humidity is simulated in the southern, southwestern and southeastern region for YSU, MYJ, QNSE, MYNN3 and BouLac schemes but the ACM2 scheme has simulated minimum relative humidity in a small area in the southeastern region of Bangladesh at 850 hPa levels.

4.3.9 Rainfall

The analysis of BMD observed and TRMM daily rainfall during 26-27 June 2010 are shown in Figs. 50(a & c) and Figs. (b & d) respectively. From Figs. 50(a & b) it is observed that the maximum rainfall is found at M. Court station (113 mm) in the south-eastern region on 26 June 2010. The maximum rainfall is also found at Sayedpur and Dinajpur stations (311 & 174 mm) in the northeastern region on 27 June 2010 [Figs. 50(c & d)].

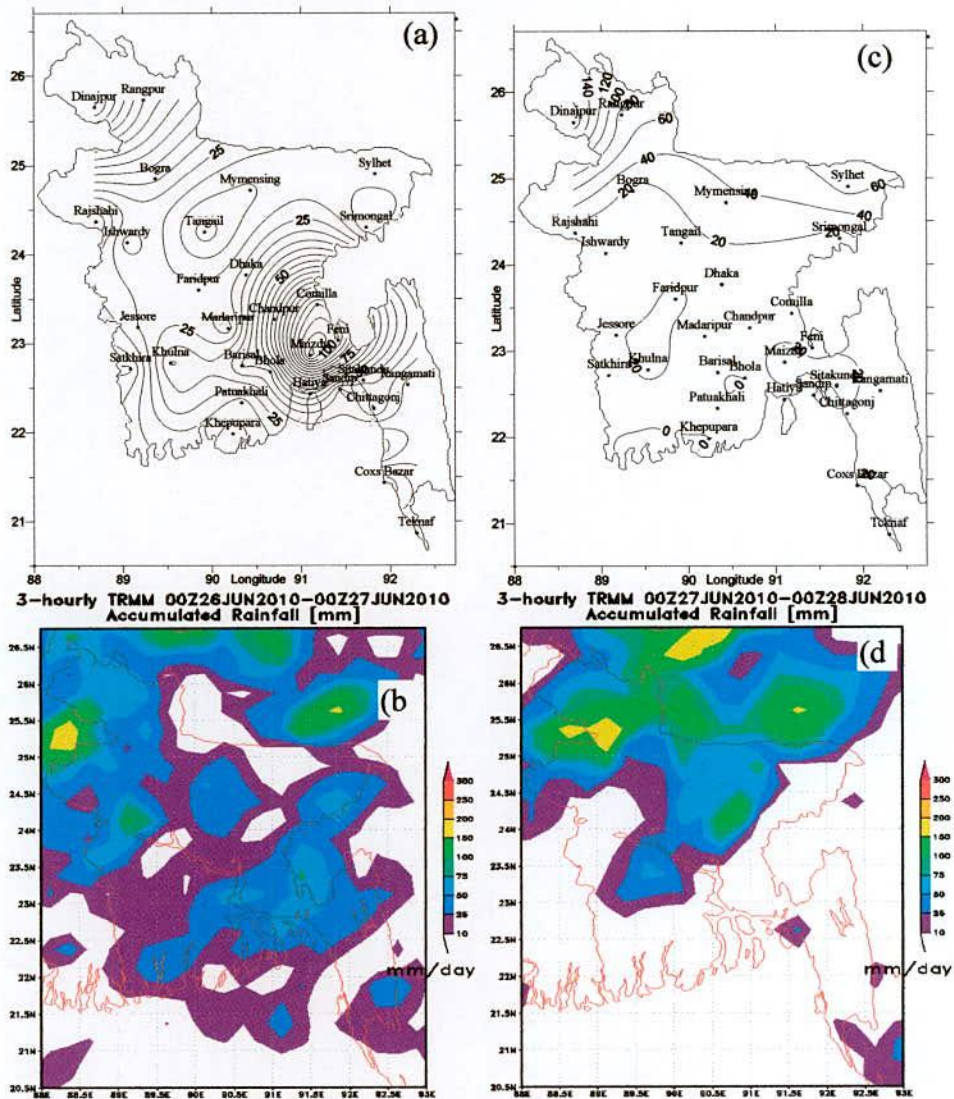


Fig. 50: BMD observed and TRMM daily rainfall in (a-b) 26 June, and (c-d) 27 June 2010 respectively.

The WRF-ARW Model has simulated rainfall using Lin *et al.* microphysics scheme and Kain-Fritsch cumulus parameterization scheme in combination with YSU, MYJ, QNSE, MYNN3, ACM2 and BouLac Planetary Boundary Layer schemes during 26-27 June 2010 are presented in Figs. 51 and 52 respectively.

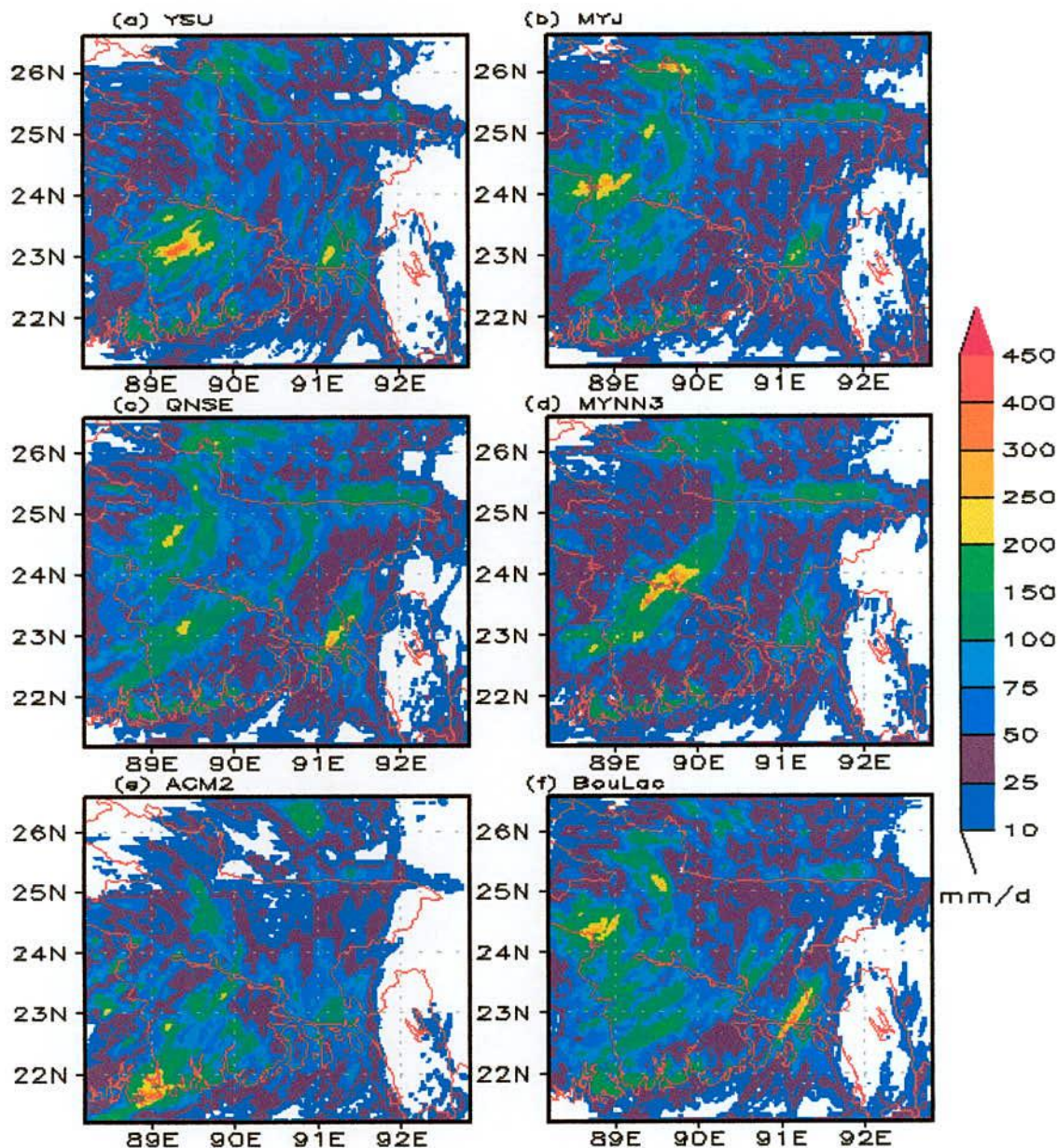


Fig. 51: Spatial distribution of simulated rainfall (mm) using a) YSU, b) MYJ, c) QNSE, d) MYNN3, e) ACM2 and f) BouLac schemes at 26 June 2010.

Figure 51a shows the distribution of WRF model simulated rainfall pattern using YSU schemes. The YSU scheme has produced maximum rainfall over southwestern (Jessore, Khulna) region and almost no rainfall has been simulated in the southeastern region (Chittagong, Cox's Bazar). From Fig. 51b, it has also been found that the MYJ scheme

produces maximum rainfall in the western region (Ishurdi) and almost no rainfall has been simulated in the southeastern region (Chittagong, Cox's Bazar). The BouLac (Fig. 51f) scheme has also simulated maximum rainfall in the western region and the northwestern part of Chittagong (Feni, M. Court) and almost no rainfall is simulated in the southeastern region (Chittagong).

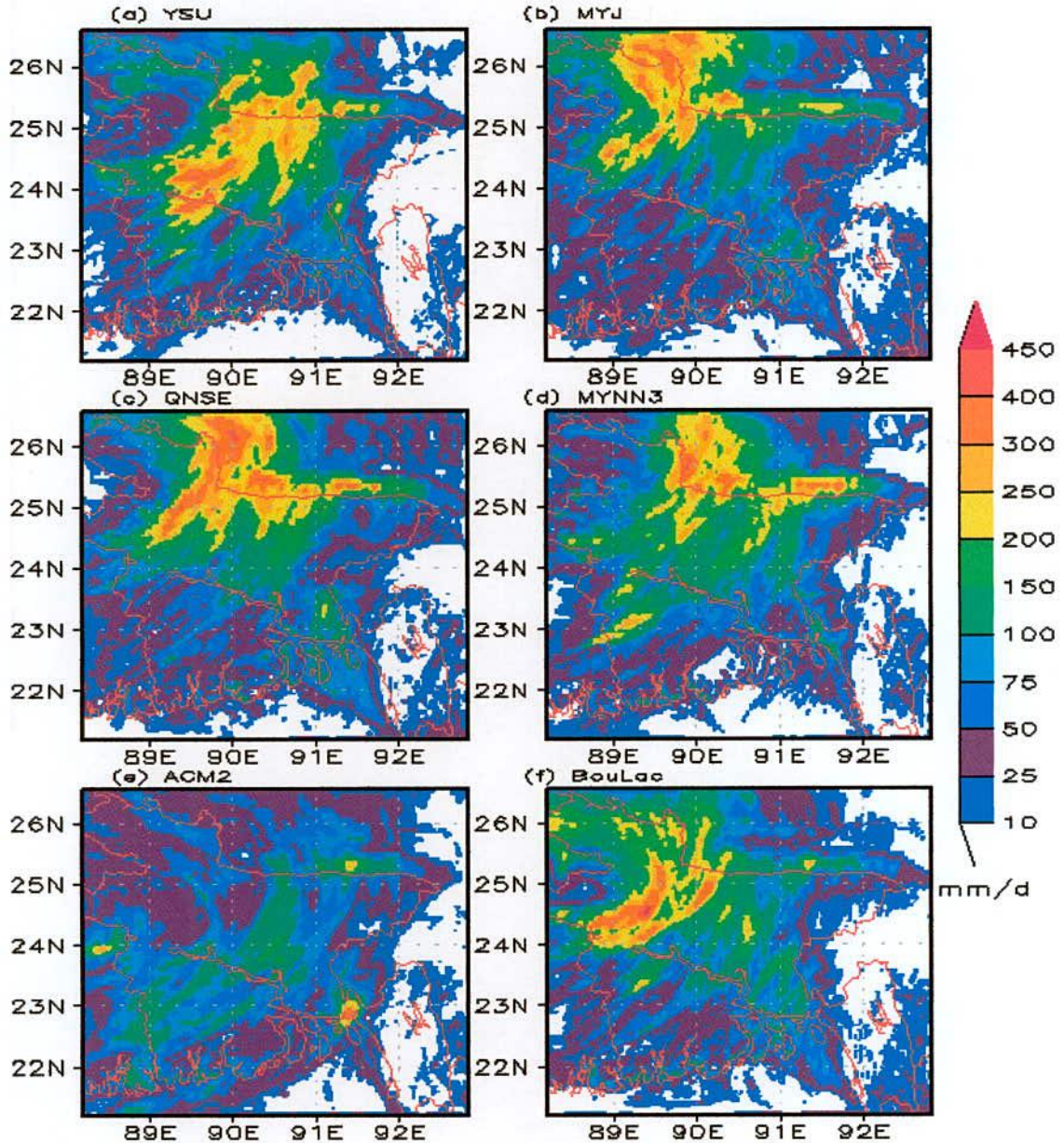


Fig. 52: Spatial distribution of simulated rainfall (mm) using a) YSU, b) MYJ, c) QNSE, d) MYNN3, e) ACM2 and f) BouLac schemes at 27 June 2010.

The ACM2 scheme (Fig. 51e) has simulated maximum rainfall in the southwestern (along the boarder line of land-ocean) region. The minimum rainfall is simulated in the northwestern

and southeastern regions. The MYNN3 (Fig. 51d) has simulated maximum rainfall in the central region. Figure 51c shows the maximum rainfall in the western region and northwestern parts of Chittagong (Feni, M. Court) and almost no rainfall has been simulated in the southeastern region (Chittagong, Cox's-Bazar). The YSU, QNSE and BouLac schemes have simulated rainfall over M.Court region from 200 to 250 mm and the MYJ, MYNN3 and ACM2 schemes have simulated rainfall 100 to 150 mm over M. Court region.

Figure 52(a – f) shows the distribution of WRF model simulated rainfall on 27 June 2010 obtained by using different schemes. The YSU (Fig. 52a) scheme has simulated maximum rainfall in the central (Tangail) to northern (Mymensingh) region and the minimum rainfall have been simulated in southeastern region. From (Fig. 52d), it has also been found that the MYNN3 scheme produces maximum rainfall in the northern (along the boarder line of Bangladesh and the minimum rainfall has been simulated in the southeastern (Chittagong, Cox's Bazar) region. The ACM2 scheme (Fig. 52e) has simulated significant amount of rainfall in the northwestern part of Chittagong (Feni, M. Court).

The maximum rainfall is simulated by using QNSE (Fig. 52c) scheme in the northern region and the minimum rainfall developed in the southeastern region. The MYJ (Fig. 52b) scheme also simulated maximum rainfall in the northwestern region. Figure 52 shows the significant amount of rainfall in the western to northern region for BouLac scheme and the minimum rainfall has been simulated in the southeastern region. The YSU, MYJ and BouLac schemes have simulated 150 to 200 mm rainfall over Sayedpur and Dinajpur region.

4.3.10 Summary

The MYJ, ACM2 and MYNN3 schemes have simulated 150 to 200 mm, 100 to 150 mm and 100 to 150 mm rain respectively but the observed rainfall was 113 mm over M. Court region on 26 June 2010. The BouLac, MYJ and YSU scheme have simulated 150 to 200 mm, 150 to 200 mm and 100 to 150 mm rain respectively over Sayedpur and Dinajpur region whereas the observed rainfall was 311 mm over Sayedpur and 174 mm over Dinajpur region on 27 June 2010. The ACM2 scheme has simulated minimum ACHFX in the southeastern and northwestern region whereas maximum rainfall was observed on 26 and 27 June 2010. The MYNN3 and QNSE schemes have simulated maximum ACLHF over M. Court and Sayedpur regions where maximum rainfall is observed on 26 and 27 June 2010. The result shows that where the ACLHF is maximum (minimum) the rainfall is maximum (minimum). The simulated PBL is found minimum at the position where the rainfall is maximum. The MYJ

and MYNN3 schemes is simulated minimum PBL over M. Court and Sayedpur regions on 26 and 27 June 2010. The YSU scheme has simulated maximum rainfall over M. Court and Sayedpur regions where the simulated GLW is minimum on 26 and 27 June 2010 respectively. The ACM2 and MYJ schemes have simulated minimum OLR over M. Court and Sayedpur regions whereas the rainfall is maximum on 26 and 27 June 2010. The maximum reflectivity has been simulated over M. Court and Sayedpur regions by the BouLac and ACM2 schemes on 26 and 27 June 2010 respectively. All schemes have simulated maximum wind speed at 850 hPa in the eastern and southeastern regions on 26 and 27 June 2010. The relative humidity simulated by all scheme is 98 to 100% over M. Court and Sayedpur regions.

4.4 Heavy rainfall event of 7-8 September 2011 using WRF model

4.4.1 Accumulated Upward Heat Flux (ACHFX) at the surface

WRF model has simulated accumulated upward heat flux (ACHFX) at 1200 UTC of 7 September 2011 at the surface is shown in Figs. 53(a-f). The ACHFX is maximum in the northeastern region for all schemes. From the figure, it is also observed that the ACHFX is minimum in the southern region. The MYJ and BouLac schemes have simulated more ACHFX all over the domain except southwestern region than other schemes. The minimum ACHFX is also simulated by using ACM2 (Fig. 53e) scheme in the southeastern region.

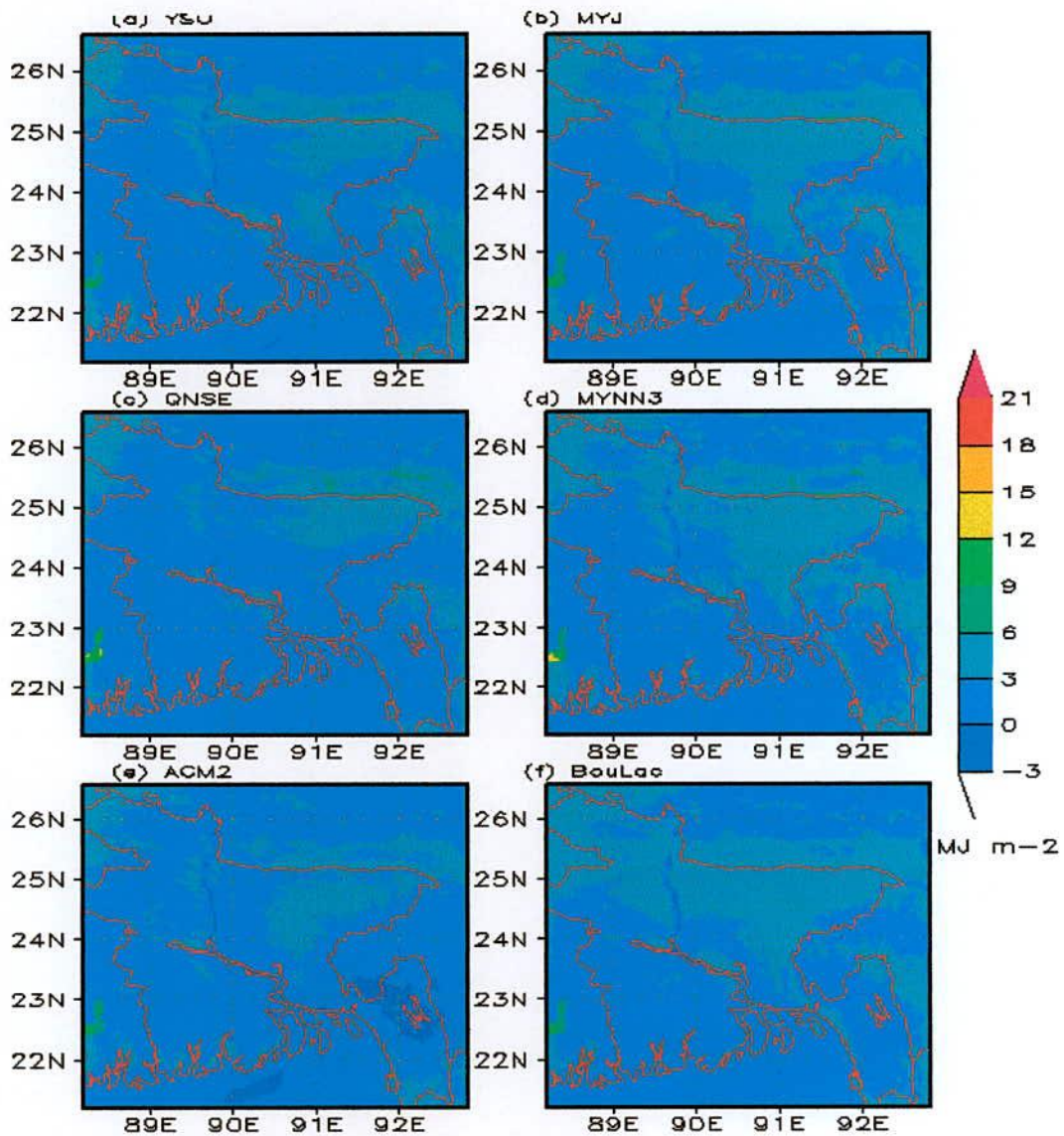


Fig. 53: Spatial distribution of simulated ACHFX using a) YSU, b) MYJ, c) QNSE, d) MYNN3, e) ACM2 and f) BouLac schemes at 1200 UTC of 7 September 2011.

Figure 54(a-f) shows the spatial distribution of ACHFX simulated by different schemes at 1200 UTC on 8 September 2011. The YSU (Fig. 54a), MYJ (Fig. 54b), QNSE (Fig. 54c), MYNN3 (Fig. 54d) and BouLac (Fig. 54f) schemes have simulated maximum and significant amount of ACHFX in the northeastern and northwestern regions. Out of all PBL schemes, the ACM2 scheme has simulated maximum ACHFX in the northeastern region of Bangladesh. On this day, the minimum ACHFX has been simulated in the southwestern region by YSU, MYJ, QNSE, MYNN3 and BouLac schemes. Maximum areas of minimum ACHFX has also simulated all over Bangladesh except northeastern region by ACM2 scheme.

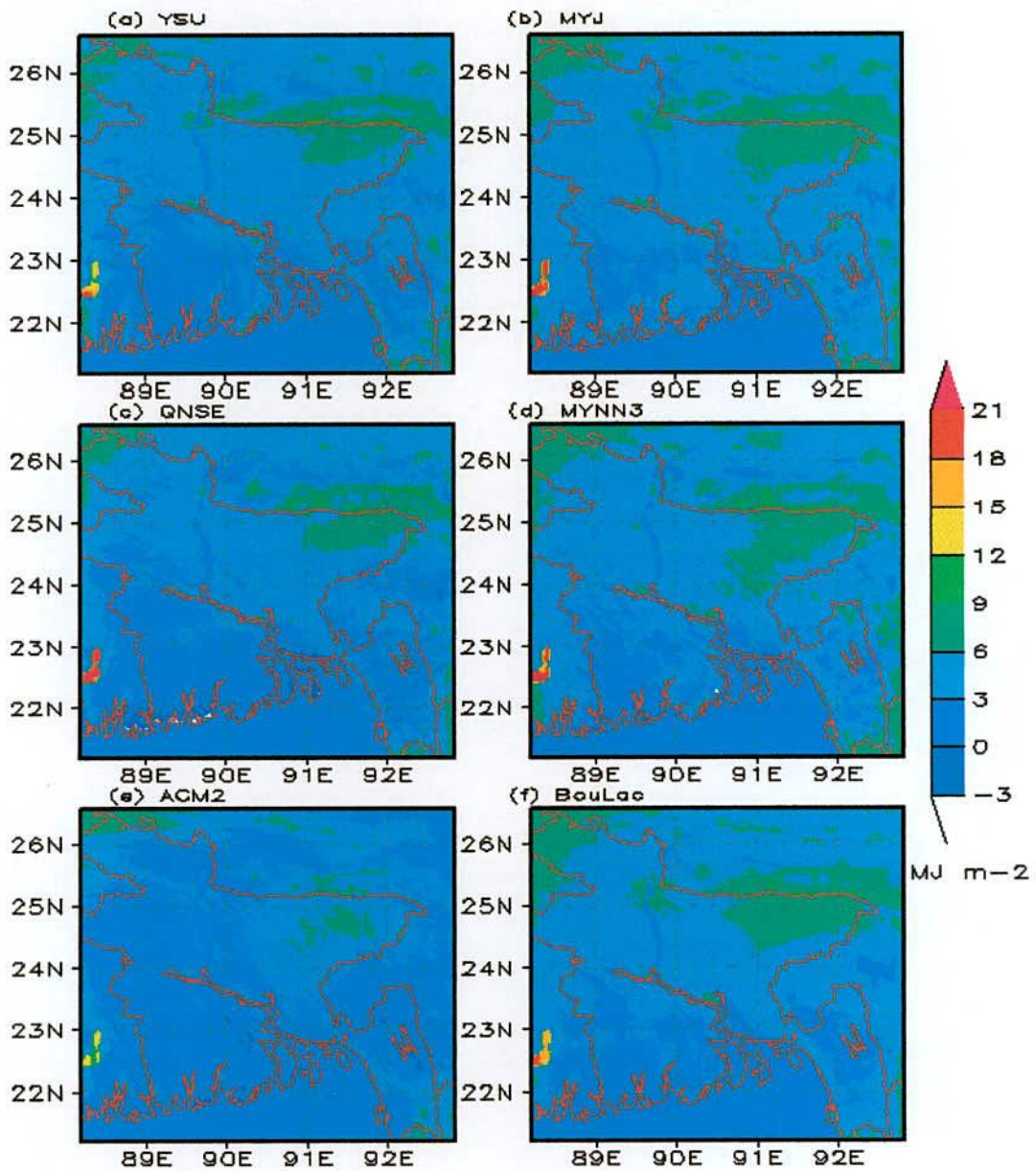


Fig. 54: Spatial distribution of simulated ACHFX using a) YSU, b) MYJ, c) QNSE, d) MYNN3, e) ACM2 and f) BouLac schemes at 1200 UTC of 8 September 2011.

Minimum ACHFX has been simulated at D2, the location is relatively covered by a cloud sky during the 24-h period of interest and the maximum ACHFX is found over area of less rainfall. From figure, it has been found that the ACHFX minimum in the southwestern region and the model also has simulated maximum rainfall in that region for all schemes.

4.4.2 Accumulated Upward Latent Heat Flux (ACLHF) at the surface

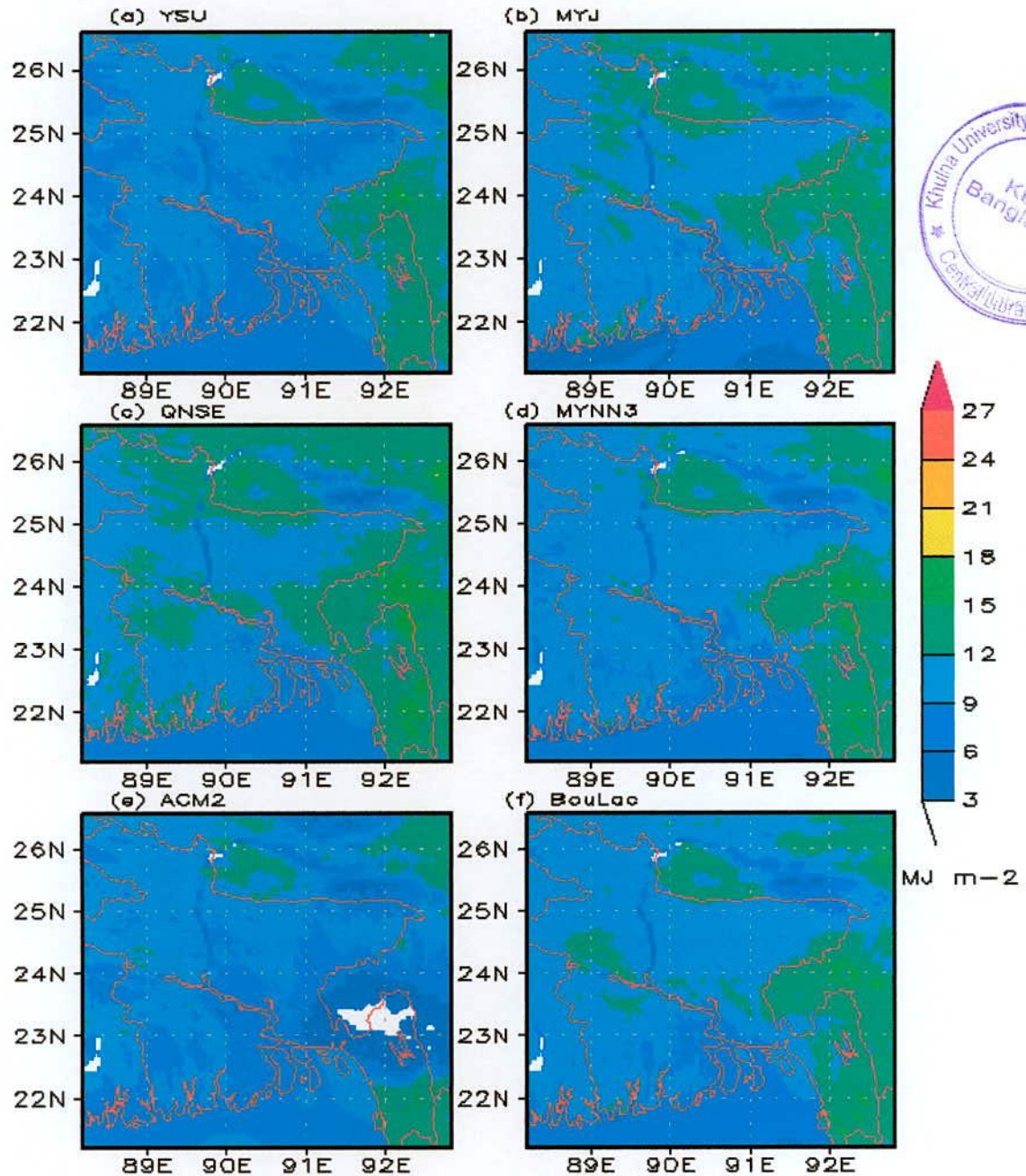


Fig. 55: Spatial distribution of simulated ACLHF using a) YSU, b) MYJ, c) QNSE, d) MYNN3, e) ACM2 and f) BouLac schemes at 1200 UTC of 7 September 2011.

WRF model has simulated accumulated upward latent heat flux (ACLHF) for 1200 UTC of 7 September 2011 at the surface and the distribution is shown in Figs. 55(a-f). The YSU, QNSE and ACM2 schemes have simulated maximum ACLHF in the southeastern region of Bangladesh. The maximum ACLHF is also simulated by using MYJ, MYNN3 and BouLac schemes in the southeastern region at the same time. From the figure it is also observed that the ACLHF is minimum in the southern region for all schemes. The YSU, MYNN3, ACM2 and BouLac schemes have simulated minimum ACLHF in the southern region of Bangladesh. The ACM2 scheme has simulated almost 0-3 MJm^{-2} ACLHF in the northern region of maximum ACLHF which is the lowest value.

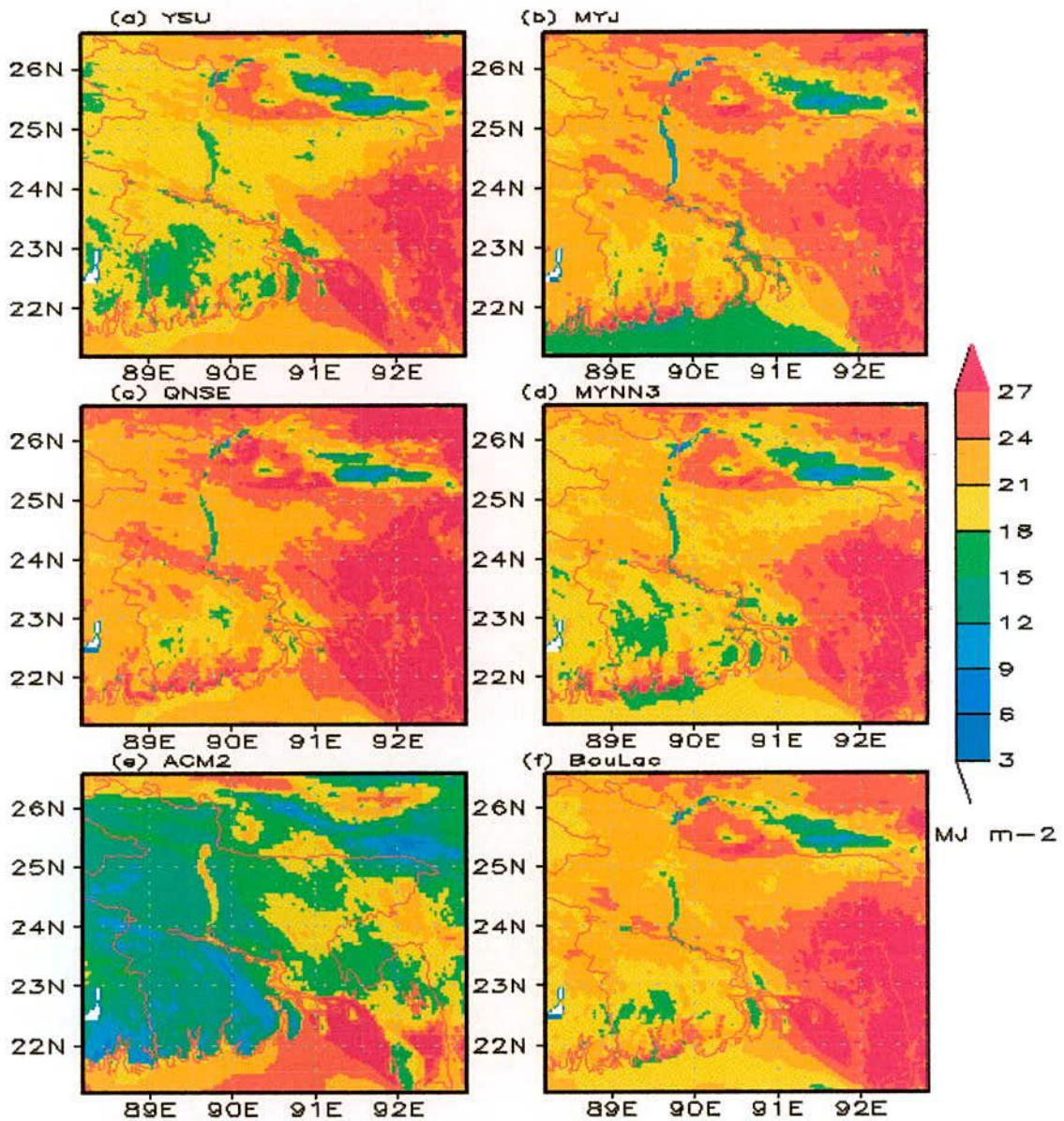


Fig. 56: Spatial distribution of simulated ACLHF using a) YSU, b) MYJ, c) QNSE, d) MYNN3, e) ACM2 and f) BouLac schemes at 1200 UTC of 8 September 2011.

Figures 56(a-f) represent the spatial distribution of WRF model simulated ACLHF at 1200 UTC on 8 September 2011 at the surface for six different schemes. The maximum ACLHF has been simulated by all schemes in the southeastern region. The minimum ACLHF has been simulated in the southwestern region for YSU (Fig. 56a), MYNN3 (Fig. 56d) and BouLac (Fig. 56f) schemes and the southern (along the boarder line of land ocean). The ACM2 (Fig. 56e) has simulated minimum ACLHF in southwestern and western region. The minimum ACLHF has been simulated by using QNSE (Fig. 56c) and MYJ (Fig. 56b) scheme in the small area of southwestern region at the same time.

4.4.3 Downward Long wave Flux at Ground Surface (GLW)

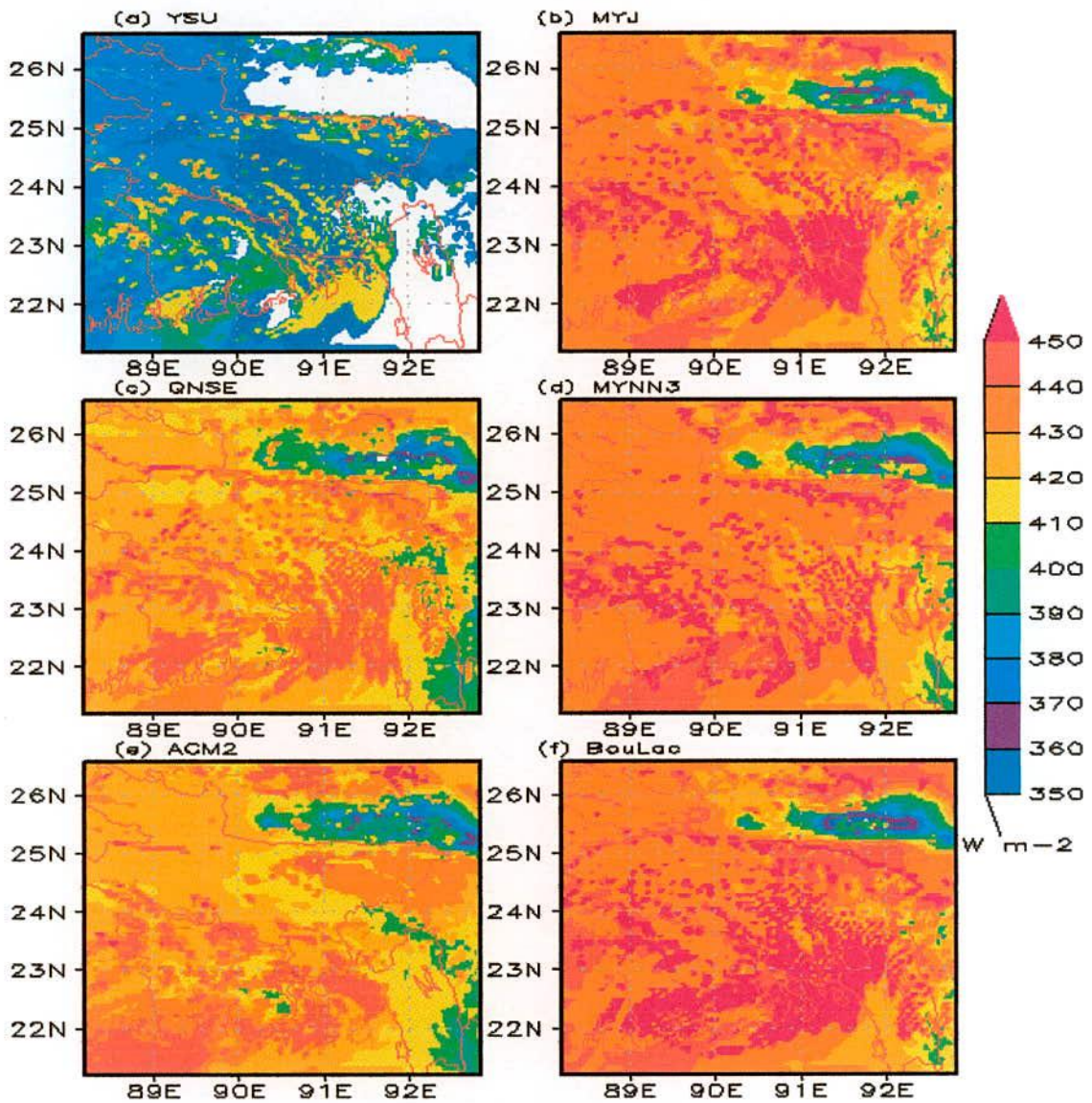


Fig. 57: Spatial distribution of simulated GLW using a) YSU, b) MYJ, c) QNSE, d) MYNN3, e) ACM2 and f) BouLac schemes at 1200 UTC of 7 September 2011.

WRF model has simulated the spatial distribution of downward long wave flux ($W m^{-2}$) at the surface by using six different schemes at 1200 UTC of 7 September 2011. The MYJ, QNSE, MYNN3, ACM2 and BouLac schemes have simulated maximum and significant amount of GLW all over the domain except in small area in the southeastern region. The maximum GLW is also simulated by YSU scheme in the northeastern and southern region at this time. On this day, the YSU scheme has simulated almost 0-350 $W m^{-2}$ in the southeastern region which is the lowest value.

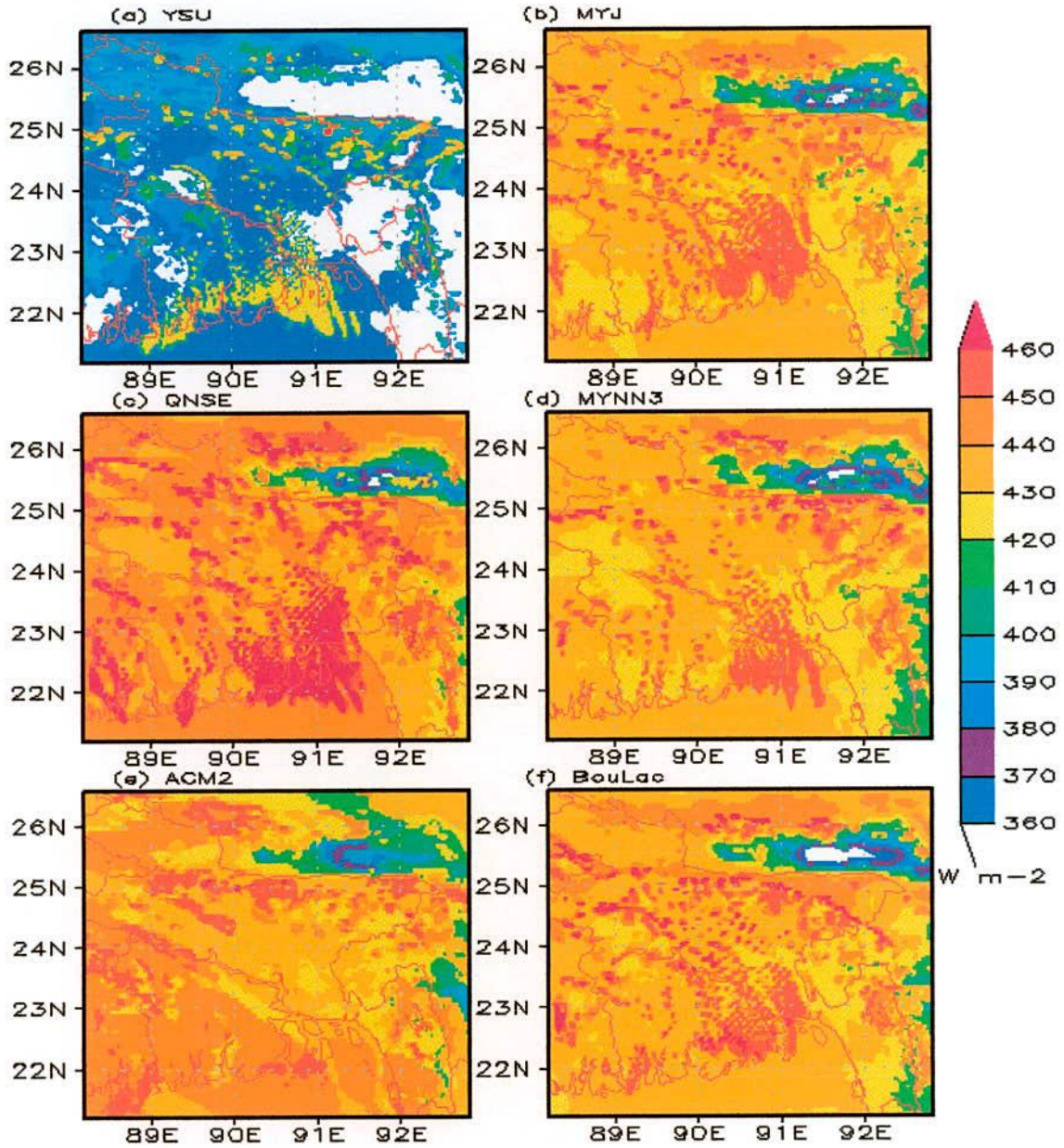


Fig. 58: Spatial distribution of simulated GLW using a) YSU, b) MYJ, c) QNSE, d) MYNN3, e) ACM2 and f) BouLac schemes at 1200 UTC of 8 September 2011.

On 8 September 2011, the MYJ (Fig. 58b), MYNN3 (Fig. 58d), ACM2 (Fig. 58e) and BouLac (Fig. 58f) schemes have simulated more GLW all over the country. The significant GLW is simulated maximum areas of Bangladesh by using ACM2 scheme. More GLW is simulated by using YSU scheme in the southern region and western part of Sylhet and the minimum ($0-360 \text{ Wm}^{-2}$) GLW has been simulated in the southeastern region by YSU scheme. On this day, the minimum GLW is also simulated in small area in southeastern region by MYJ, QNSE, MYNN3, ACM2 and BouLac schemes.

4.4.4 Outgoing Long wave Radiation (OLR)

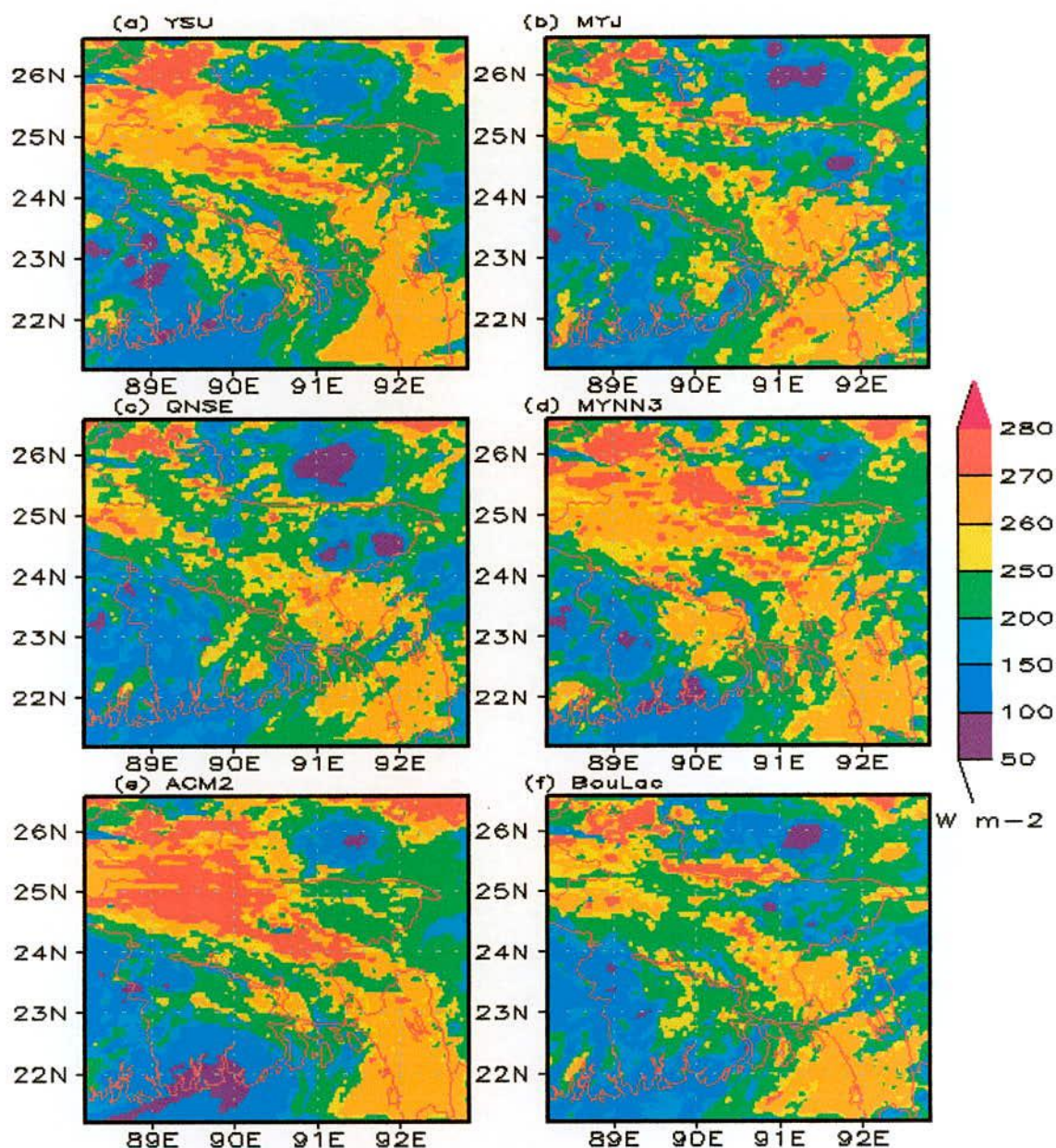


Fig. 59: Spatial distribution of simulated OLR using a) YSU, b) MYJ, c) QNSE, d) MYNN3, e) ACM2 and f) BouLac schemes at 1200 UTC of 7 September 2011.

Figures 59 (a-f) show the spatial distribution of outgoing long wave radiation ($W m^{-2}$) at the ground surface at 1200 UTC on 7 September 2011 simulated by different schemes. The maximum OLR is simulated in the eastern to northwestern region of Bangladesh by using YSU, MYNN3 and ACM2 schemes. The MYJ, QNSE and BouLac schemes have simulated more OLR in the eastern and northwestern regions of Bangladesh at the same time. On this day, the OLR is minimum in the western and southwestern regions as obtained by ACM2 (Fig. 59e), YSU (Fig. 59a) and MYNN3 (Fig. 59d) schemes. The MYJ (Fig. 59b), BouLac (Fig. 59f) and QNSE (Fig. 59c) schemes have simulated minimum OLR in the northeastern and western regions of Bangladesh.

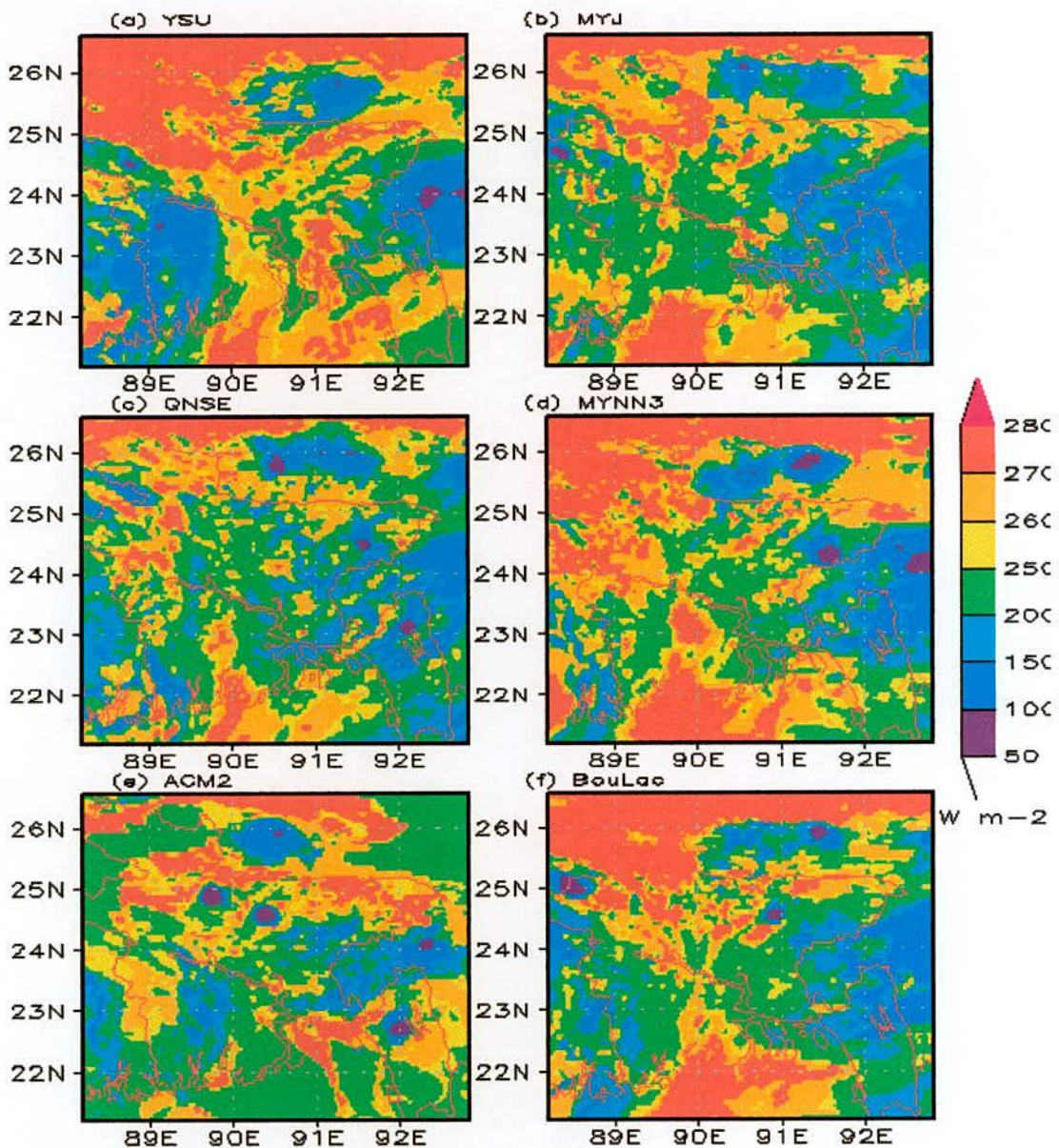


Fig. 60: Spatial distribution of simulated OLR using a) YSU, b) MYJ, c) QNSE, d) MYNN3, e) ACM2 and f) BouLac schemes at 1200 UTC of 8 September 2011.

WRF model has simulated the OLR at the ground surface at 1200 UTC on 8 September 2011 by using all schemes. The maximum and significant OLR has simulated in the northwestern and southern (over the Bay of Bengal) regions by using six schemes. The YSU (Fig. 60a) and ACM2 (Fig. 60e) have also simulated maximum OLR in the northeastern region. The minimum OLR is simulated in the western region by the MYJ (Fig. 60b) scheme. The minimum OLR is also simulated in the northeastern region by using QNSE (Fig. 60c) and MYNN3 (Fig. 60d) schemes. On this day, the ACM2 (Fig. 60e) scheme has also simulated minimum OLR in small area in the northern and southeastern regions of Bangladesh.

4.4.5 Variation of Planetary Boundary Layer (PBL)

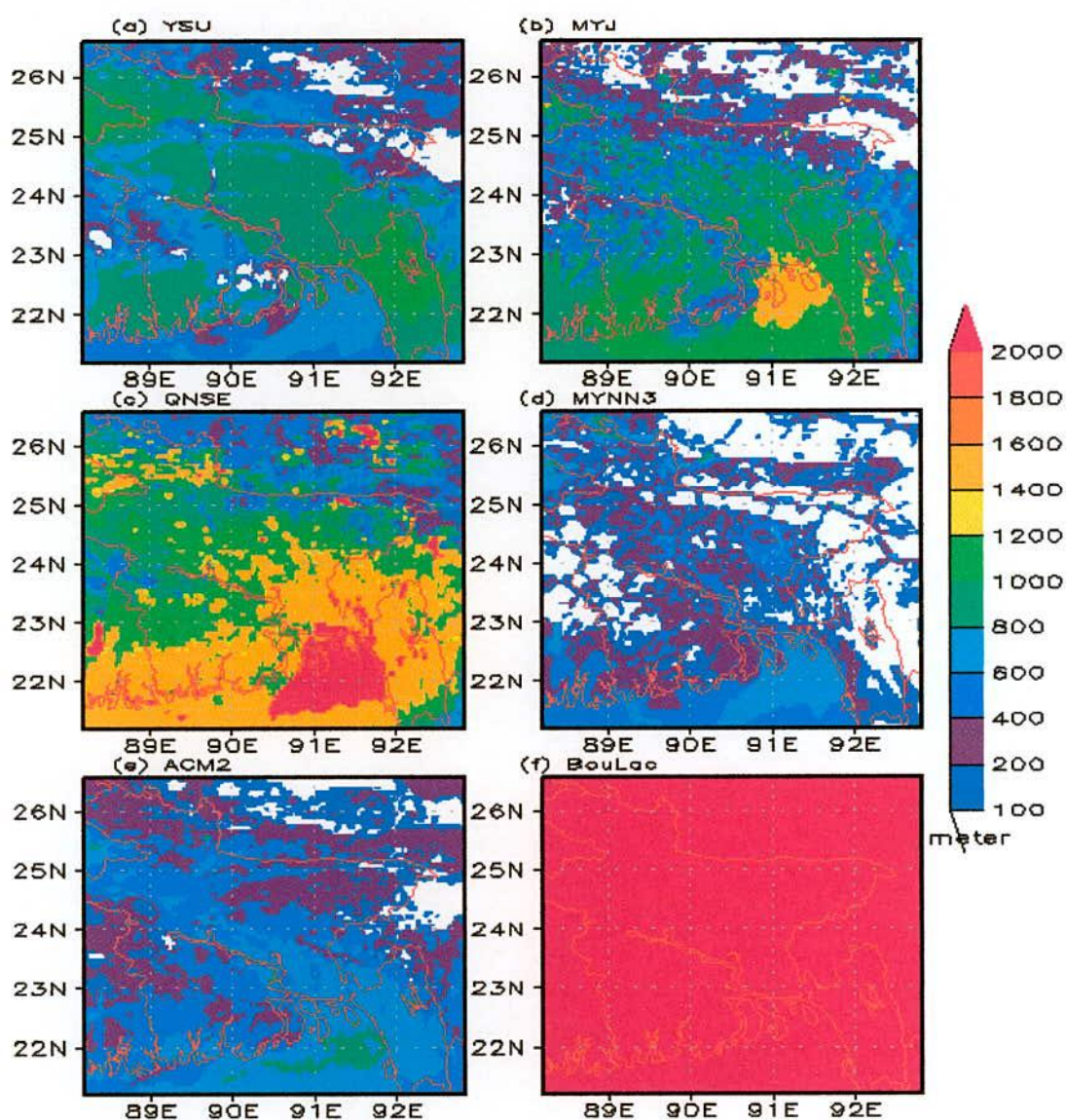


Fig. 61: Spatial distribution of simulated PBL height using a) YSU, b) MYJ, c) QNSE, d) MYNN3, e) ACM2 and f) BouLac schemes at 1200 UTC of 7 September 2011.

WRF model has simulated PBL (meter) pattern by using all schemes at 1200 UTC on 7 September 2011 are presented as in Figs.61 (a-d) and 62(a-f). The YSU scheme has simulated maximum PBL in the southeastern region and the minimum PBL in the northeastern region. The maximum PBL is simulated in the southeastern region (over Sandwip, Hatiya) by using MYJ, MYNN3 and ACM2 schemes and the minimum PBL has been simulated in the northeastern region (over Sylhet). The significant PBL is simulated by using QNSE (Fig. 61c) scheme in the southeastern region (Sandwip, Hatiya) and the minimum PBL in the western region. Maximum areas of minimum PBL has simulated by using MYNN3 scheme all over the domain than that of all other schemes.

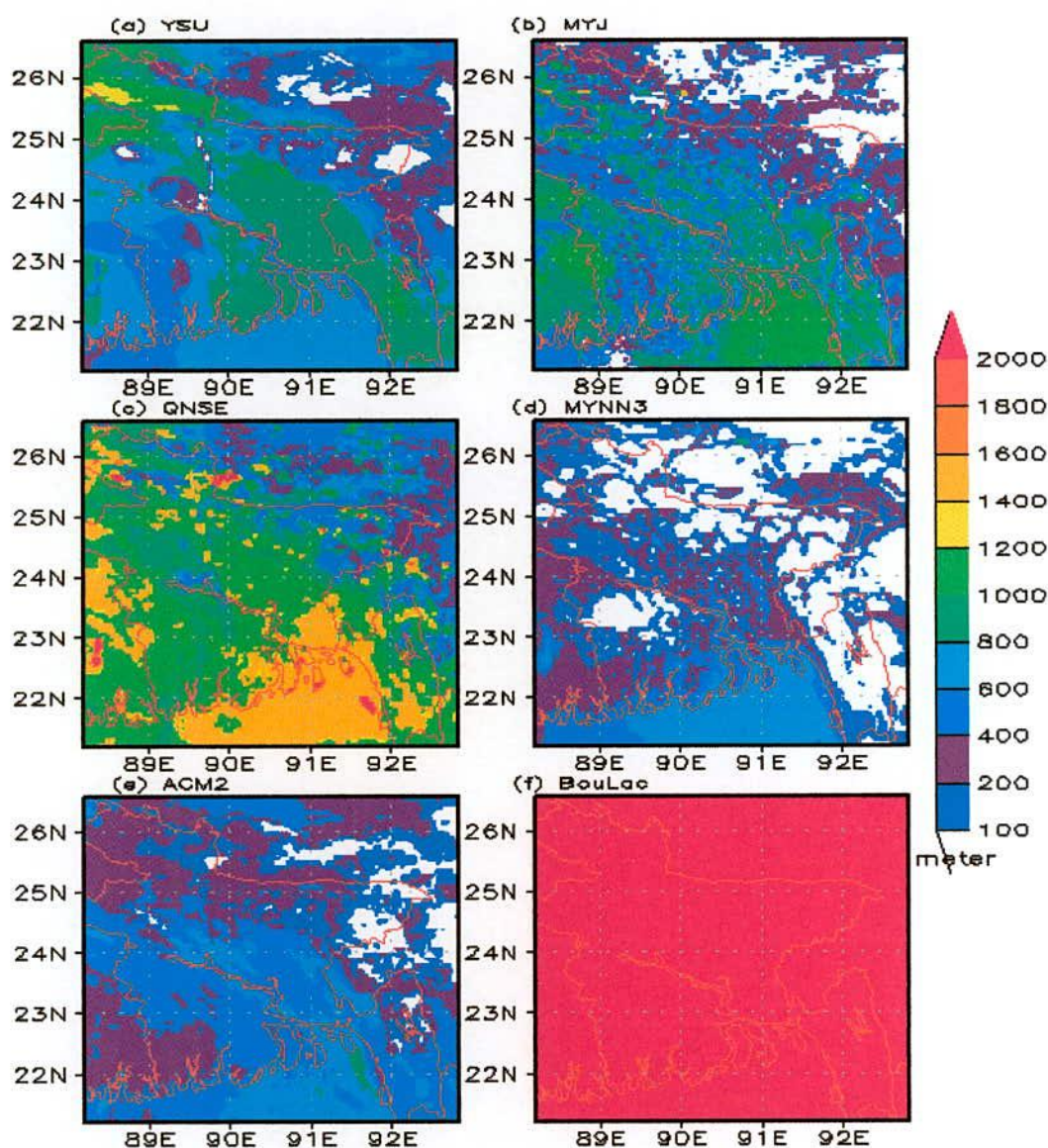


Fig. 62: Spatial distribution of simulated PBL height using a) YSU, b) MYJ, c) QNSE, d) MYNN3, e) ACM2 and f) BouLac schemes at 1200 UTC of 8 September 2011.

At 1200 UTC on 8 September 2011, the YSU (Fig. 62a) scheme has (1200-1400m) simulated maximum PBL in the northwestern region. The significant amount of PBL has simulated by using MYJ scheme in the southeastern region. The maximum PBL is simulated by using ACM2 (Fig. 62e) scheme in the southeastern region. The QNSE (Fig. 62c) scheme has simulated maximum and significant PBL all over the country. Maximum areas of minimum PBL have been simulated by using MYNN3 scheme all over the domain than that of all other schemes. In case of BouLac scheme, simulated PBL is seen to be constant all over the country on 7 and 8 September 2011.

From the figure, if the simulated rainfalls (mm) are compared with the PBL (meter) it has been found that the maximum PBL lies over minimum rainfall area and vice versa.

4.4.6 Reflectivity

Figures 63(a-f) represent spatial distribution of WRF model simulated reflectivity (shaded) using different schemes at 850 hPa level on 1200 UTC of 7 September 2011. The YSU and MYNN3 schemes have simulated significant amount of reflectivity in the western and southern region of Bangladesh. On this day, the maximum and significant amount of reflectivity has been simulated by using MYJ, QNSE and BouLac schemes in the southern and northeastern regions. The ACM2 scheme has simulated maximum reflectivity in the western and southwestern regions.

At 1200 UTC on 8 September 2011, WRF model simulated reflectivity (shaded) using different schemes at 850 hPa level. The YSU (Fig. 64a) and MYJ (Fig. 64b) schemes have simulated significant amount of reflectivity in the northeastern and western regions. Maximum reflectivity has also been simulated by MYNN3 scheme in the southwestern part of Sylhet at the same time. The QNSE (Fig. 64c) and BouLac (Fig. 64f) schemes have simulated significant amount of reflectivity in the northeastern region and the northeastern part of Chittagong. The ACM2 scheme has also simulated maximum reflectivity in the northern region and northeastern part of Chittagong.

On 7 September 2011, WRF model has simulated reflectivity (shaded) using different schemes at 850 hPa levels. The YSU, MYJ and MYNN3 schemes have simulated significant amount of reflectivity in the southwestern part of Sylhet. The maximum reflectivity is also simulated by using QNSE and BouLac schemes in the eastern region and the southwestern part of Sylhet. The ACM2 scheme has also simulated maximum reflectivity in the eastern region at 1800 UTC on 7 September 2011.

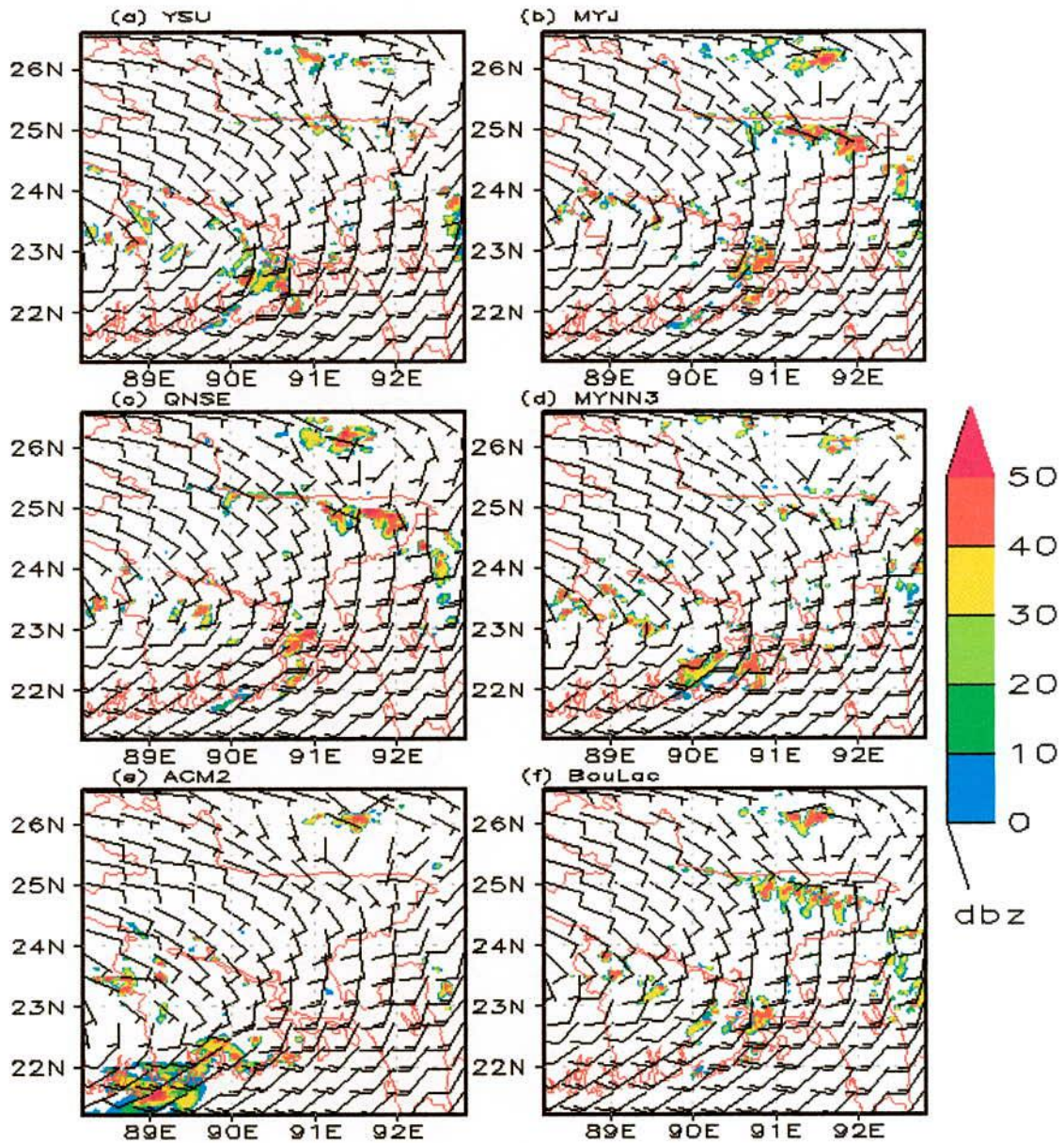


Fig. 63: Spatial distribution of simulated wind speed (m/s) and reflectivity (dBZ) at 850 hPa level using a) YSU, b) MYJ, c) QNSE, d) MYNN3, e) ACM2 and f) BouLac schemes at 1200 UTC of 7 September 2011.

4.4.7 Wind

The maximum wind speed of 20 m/s is simulated by using YSU and MYJ schemes in the southern side of maximum reflectivity and 15 m/s by using ACM2 schemes in the southern and southeastern sides of maximum reflectivity. The QNSE, MYNN3 and BouLac schemes have also simulated 20 m/s wind speed in the inner portion of maximum reflectivity. The maximum simulated wind speed is in the southern region as obtained by all schemes. The minimum wind speed is simulated by all schemes in the northwestern side of maximum reflectivity at 850 hPa level at 1200 UTC on 7 September 2011.

On 8 September 2011, the maximum wind speed is simulated in the southern and southeastern region by all schemes. The maximum wind speed of 15 m/s is simulated by using all schemes in the southern and southeastern side of maximum reflectivity. The minimum wind speed simulated by all schemes in the northwestern side of maximum reflectivity at 850 hPa level at 1200 UTC on 8 September 2011.

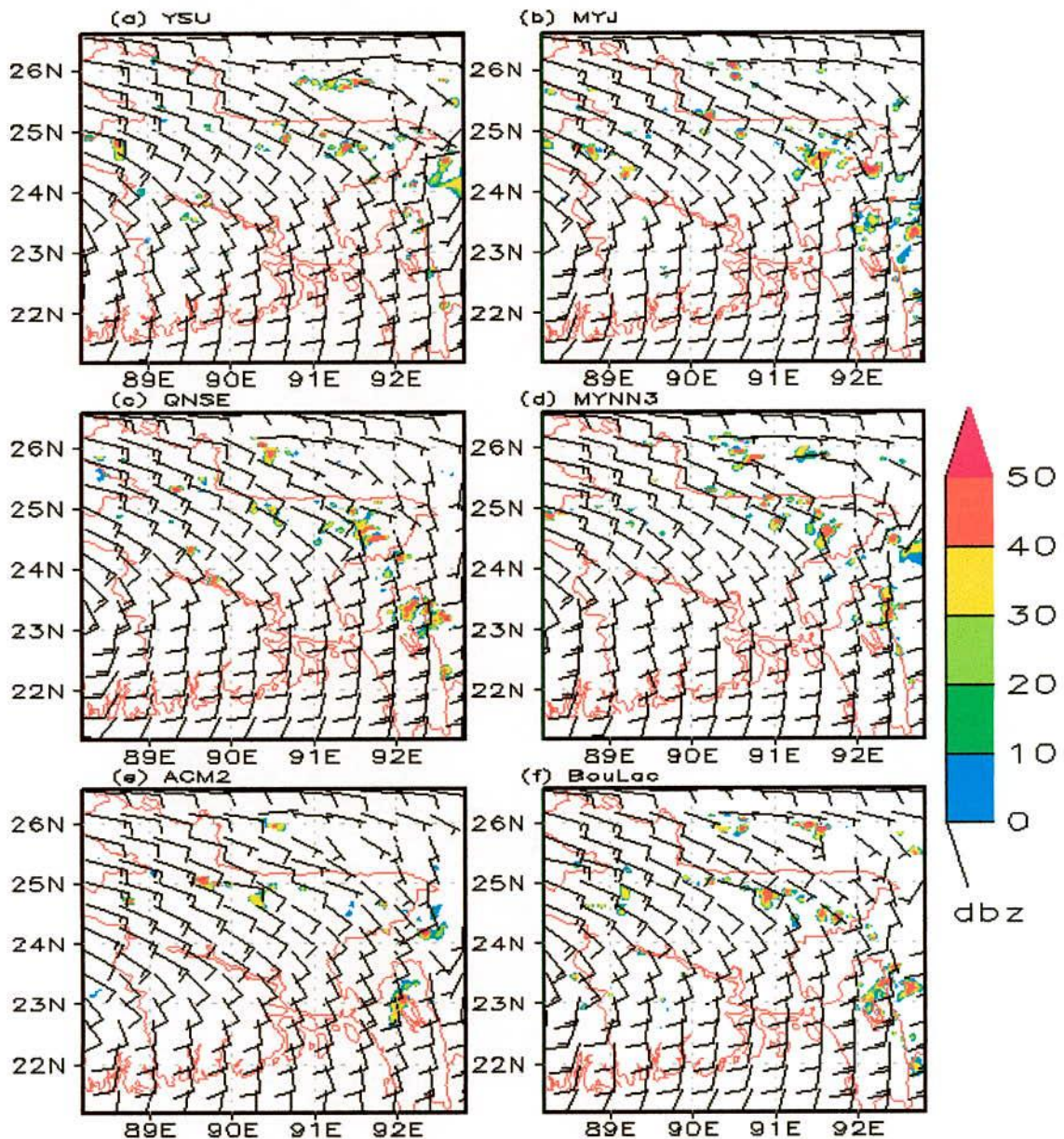


Fig. 64: Spatial distribution of simulated wind speed (m/s) and reflectivity (dBZ) at 850 hPa level using a) YSU, b) MYJ, c) QNSE, d) MYNN3, e) ACM2 and f) BouLac schemes at 1200 UTC of 8 September 2011.

The maximum wind speed has been simulated in the southern and southeastern regions by all schemes. The maximum wind speed of 20 m/s is simulated by using MYNN3 schemes in the

southern side of maximum reflectivity and 15 m/s by using YSU, MYJ, QNSE, ACM2 and BouLac schemes in the southern and southeastern side of maximum reflectivity. The minimum wind speed is simulated by all schemes in the northwestern side of maximum reflectivity at 850 hPa level at 1800 UTC on 7 September 2011.

4.4.8 Relative Humidity (RH)

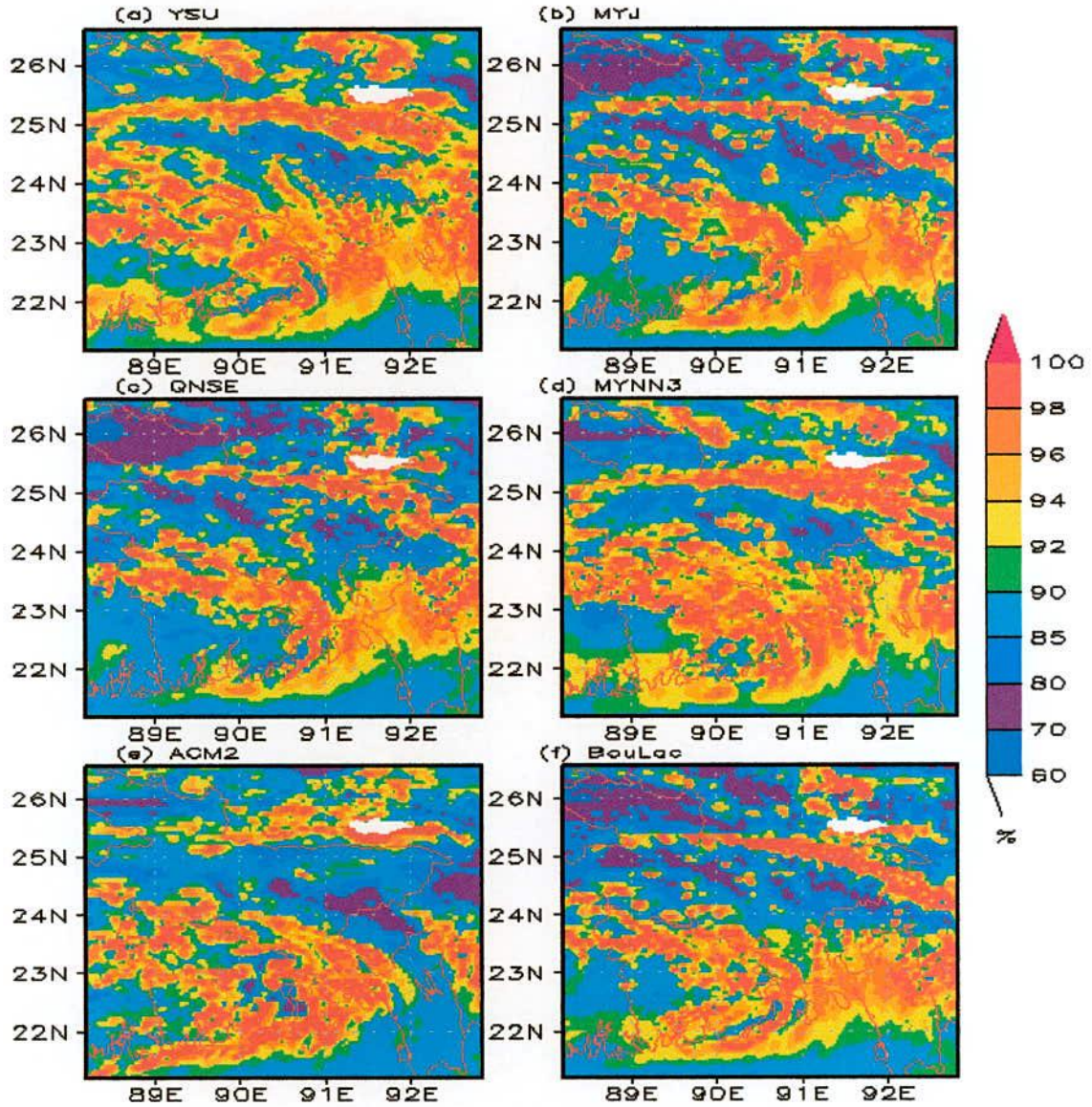


Fig. 65: Spatial distribution of simulated RH at 850 hPa level using a) YSU, b) MYJ, c) QNSE, d) MYNN3, e) ACM2 and f) BouLac schemes at 1200 UTC of 7 September 2011.

WRF model has simulated spatial distribution of relative humidity at 850 hPa levels at 1200 UTC of 7 September 2011 is presented in Figures 65(a-f). The maximum and significant

amount of RH has been simulated by using YSU and MYNN3 schemes all over the domain. The MYJ, QNSE and BouLac schemes have also simulated more RH in the western to the southeastern region and the relative humidity of (60-70) % is simulated in the northwestern region of Bangladesh, which is the lowest value. On this day, the ACM2 scheme has simulated significant amount of RH in the western to the southeastern region including southwestern region and the minimum RH is simulated in small area in the northeastern and northwestern regions.

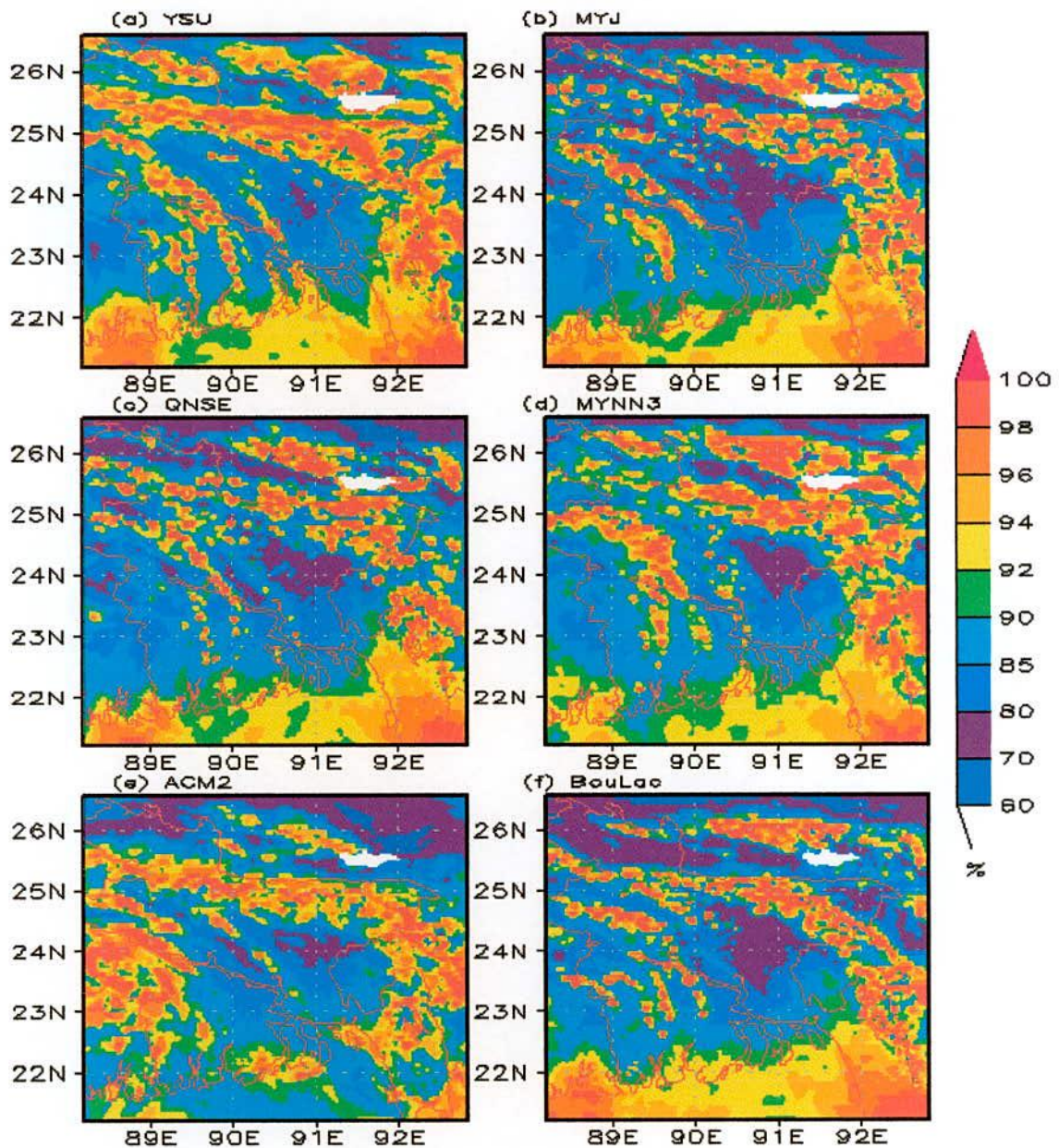


Fig. 66: Spatial distribution of simulated RH at 850 hPa level using a) YSU, b) MYJ, c) QNSE, d) MYNN3, e) ACM2 and f) BouLac schemes at 1200 UTC of 8 September 2011.

The YSU scheme has simulated significant amount of RH all over the country except in small area of the eastern region at 1200 UTC of 8 September 2011. Maximum areas of minimum RH have also been simulated by MYJ, QNSE and BouLac schemes in the eastern and northwestern region and more RH simulated in the southeastern, northeastern and western regions. The MYNN3 scheme has simulated maximum RH all over the domain except eastern region at the same time. The significant amount of RH is simulated by ACM2 scheme in the western, northeastern and northern regions and the minimum RH is also simulated in small area in northwestern and eastern regions.

4.4.9 Rainfall

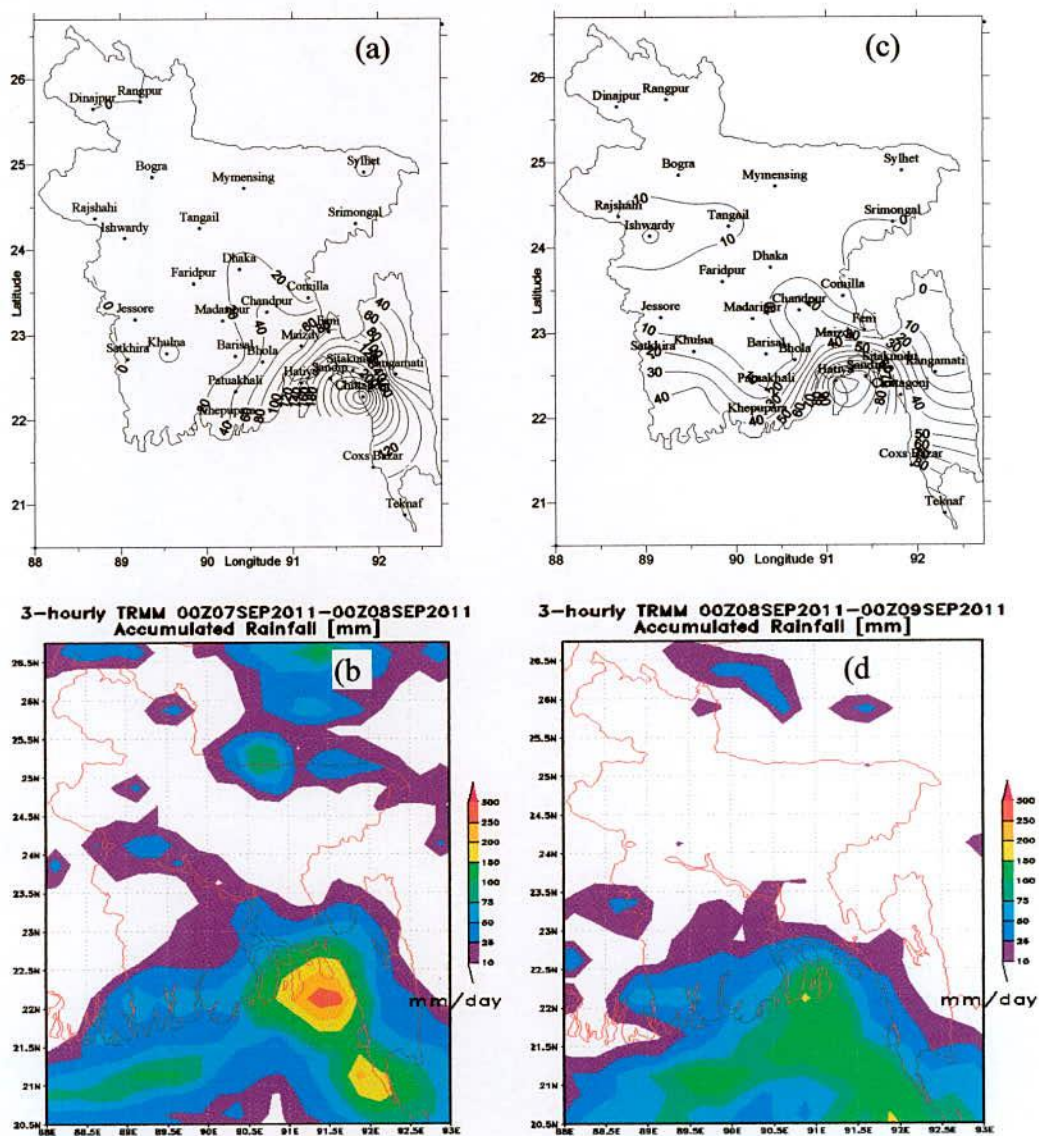


Fig.67: BMD observed and TRMM daily rainfall in (a-b) 7 and (c-d) 8 September 2011 respectively.

The distribution patterns of BMD observed rainfall and TRMM daily rainfall during 7 - 8 September 2011 are shown in Fig. 67(a & c) and Fig. 67(b & d) respectively. From Figs. 67(a & b), it is observed that the maximum rainfall occurred at Chittagong and Sandwip station (331 mm and 226 mm respectively) and in the south southeastern region on 7 September 2011. The maximum rainfall occurred in the southeastern region (Hatiya) on 8 September 2011 [Figs. 67(c & d)]. The WRF-ARW Model has simulated rainfall using Lin *et al* microphysics scheme and Kain-Fritsch cumulus parameterization scheme in combination with YSU, MYJ, QNSE, MYNN3, ACM2 and BouLac Planetary Boundary Layer schemes during 7-8 September 2011, and the results are presented in Figs. 68 - 69 respectively.

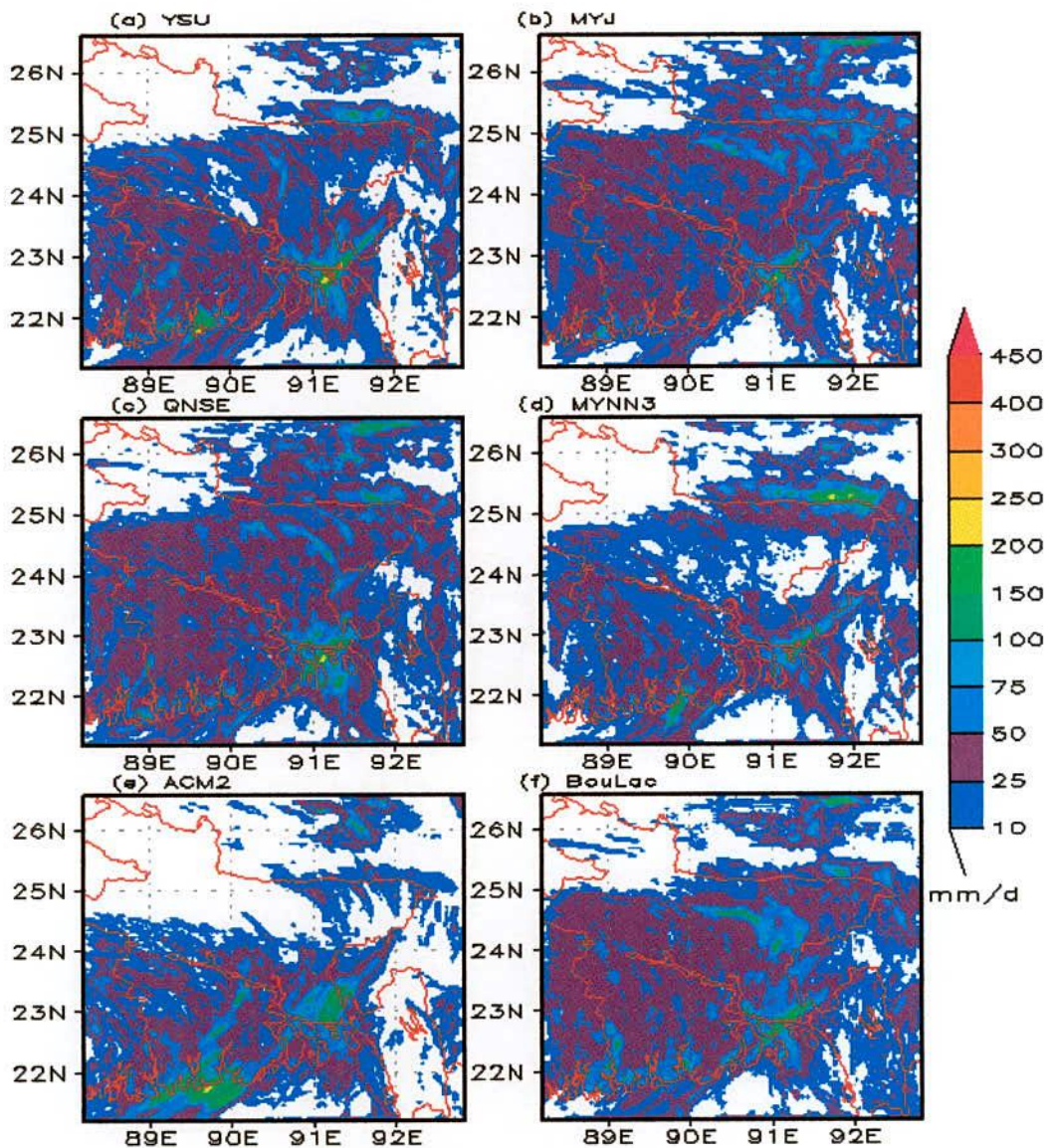


Fig. 68: Spatial distribution of simulated rainfall using a) YSU, b) MYJ, c) QNSE, d) MYNN3, e) ACM2 and f) BouLac schemes on 7 September 2011.

Figure 68 (a-f) shows the distribution of WRF model simulated rainfall pattern on 7 September 2011 using different schemes. The YSU (Fig. 68a) and ACM2 (Fig. 68e) schemes have simulated maximum rainfall at southeastern (Hatiya, Sandwip) and southern regions (along the boarder line of land-ocean) and almost no rainfall has been simulated in the northwestern region (Rangpur, Dinajpur, Sayedpur). From Figs. 68(b-d & f) it has also been found that the MYJ, QNSE, MYNN3 and BouLac schemes has simulated maximum rainfall in the southeastern region (Hatiya, Sandwip) and almost no rainfall has been simulated in the northwestern region (Rangpur, Dinajpur and Sayedpur). All schemes have simulated 150 to 200 mm rainfall over Hatiya region.

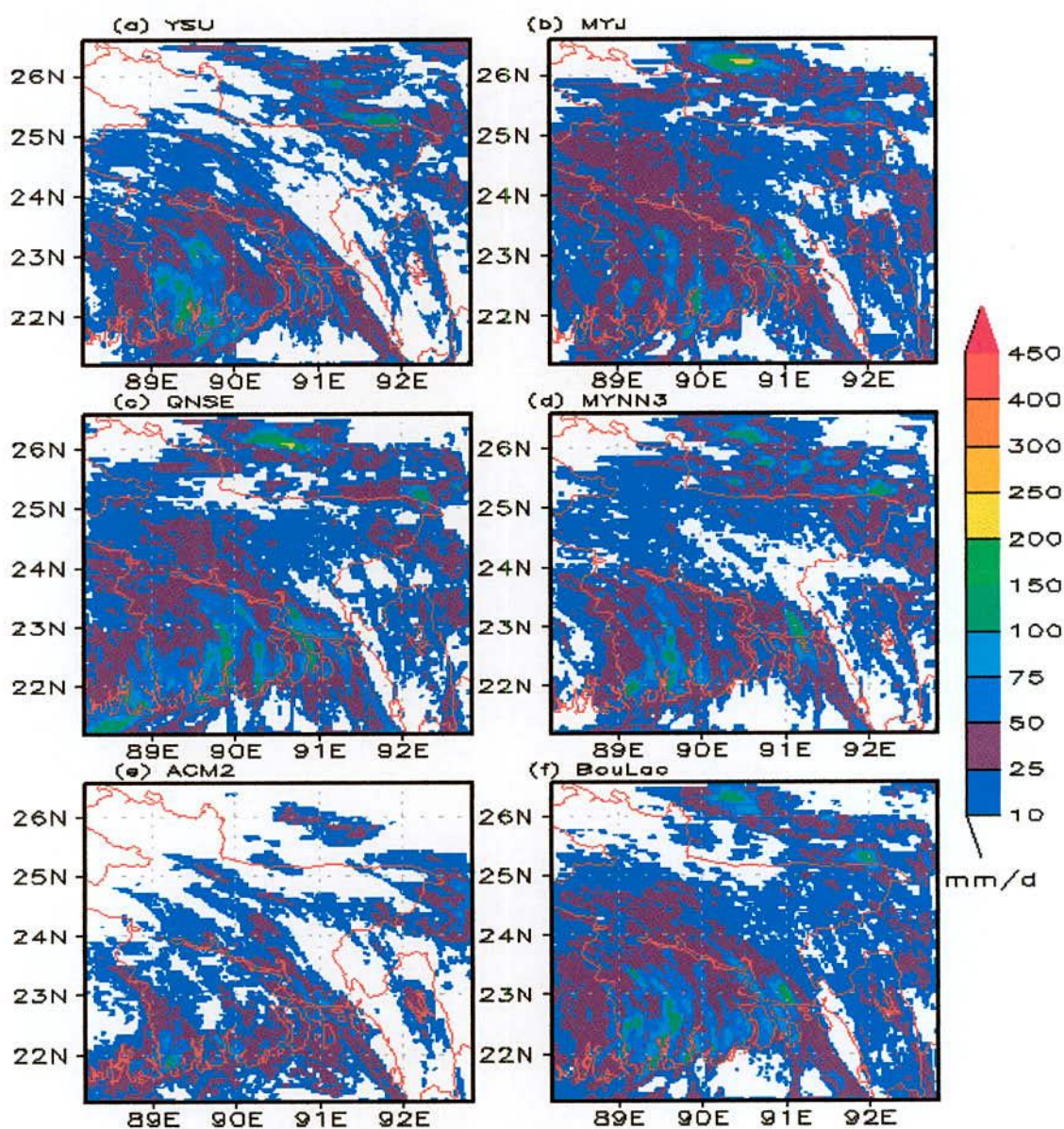


Fig. 69: Spatial distribution of simulated rainfall using a) YSU, b) MYJ, c) QNSE, d) MYNN3, e) ACM2 and f) BouLac schemes on 8 September 2011.

Figure 69(a – f) shows the distribution of WRF model simulated rainfall on 8 September 2011 using different schemes. The YSU (Fig. 69a) and ACM2 (Fig. 69e) schemes have simulated maximum rainfall at the southwestern region and almost no rainfall have been simulated in northwestern region. From Figs. 69(b-d & f) it has also been found that the MYJ, QNSE, MYNN3 and BouLac schemes have simulated maximum rainfall in the south-southwestern region and the minimum rainfall has been simulated in the northwestern. The QNSE, YSU, MYJ, MYNN3 and BouLac schemes have been simulated 100 to 150 mm rain over Hatiya region.

4.4.10 Summary

The QNSE, ACM2 and BouLac schemes have simulated 150 to 200 mm, 100 to 150 mm and 100 to 150 mm rain respectively over Hatiya region but the observed rainfall was 146 mm over Hatiya region on 7 September 2011. The QNSE, YSU and BouLac scheme have simulated 100 to 150 mm rain over Hatiya region on 8 September 2011 whereas the observed rain was 116 mm over Hatiya region. The QNSE and ACM2 schemes have simulated minimum ACHFX in the southeastern region whereas maximum rainfall was observed on 7 and 8 September 2011. The QNSE scheme has simulated maximum ACLHF over Hatiya and Chittagong region where maximum rainfall was observed on 7 and 8 September 2011. The result shows that where the ACLHF is maximum (minimum) the rainfall is also maximum (minimum) in that region. The simulated PBL is minimum at the position where the rainfall is maximum and the MYNN3 scheme simulated minimum PBL over Hatiya and Chittagong region on 7 and 8 September 2011. The YSU scheme has simulated maximum rainfall over Hatiya and Chittagong region where the simulated GLW is minima on 7 and 8 September 2011. The ACM2 and QNSE schemes have simulated minimum OLR over Hatiya and Chittagong region whereas the rainfall is maximum on 7 and 8 September 2011. The maximum reflectivity is simulated in the southern region by QNSE scheme. The maximum wind speed is simulated by all schemes in the southern and southeastern regions at 850 hPa at 1200 UTC on 7 and 8 September 2011 respectively. The relative humidity is simulated by all schemes and is 98 to 100% in the southeastern region on 7 and 8 September 2011.

Chapter V: CONCLUSIONS

In the present study, the Advanced Research WRF (ARW) model of 9 km and 3 km nested domain has been used for the simulation of four heavy rainfall events of 27-29 July 2009, 15-16 August 2009, 26-27 June 2010 and 7-8 September 2011 over Bangladesh using Lin *et al.* scheme in combination of KF scheme with six PBL schemes. The four heavy rainfall events consist of 9 heavy rainfall days. The six different PBL schemes are YSU, MYJ, QNSE, MYNN3, ACM2 and BouLac. To understand the dynamical and thermodynamical characteristics of heavy precipitation systems wind, relative humidity, reflectivity, rainfall, accumulated upward heat flux, accumulated upward latent heat flux, downward long wave flux, outgoing long wave radiation and PBL have been simulated and analyzed.

The BouLac, QNSE and ACM2 schemes have simulated minimum ACHFX in the regions where maximum rainfall has been observed. Minimum ACHFX has been simulated by BouLac scheme over larger area in the southeastern region on 28 and 29 July 2009. The ACM2 scheme has simulated minimum ACHFX in the regions where maximum rainfall is observed during 15-16 August 2009 and 26-27 June 2010. The QNSE and ACM2 schemes have simulated minimum ACHFX in the southeastern region whereas maximum rainfall is observed on 7 and 8 September 2011.

The QNSE and BouLac schemes have simulated maximum ACLHF in the regions where maximum rainfall is observed during 28-29 July 2009 and MYNN3 and QNSE schemes have simulated maximum during 26-27 June 2010. The QNSE scheme has simulated maximum ACLHF over the regions where maximum rainfall is observed during 15-16 August 2009 and 7-8 September 2011. The BouLac and YSU schemes have simulated maximum rainfall in the southeastern region and Sayedpur region where the simulated GLW is minimum on 28 and 29 July 2009. The YSU scheme has simulated maximum rainfall over the regions where the GLW is minimum during 15-16 August 2009, 26-27 June 2010 and 7-8 September 2011.

On 28 and 29 July 2009, the YSU, BouLac and ACM2 schemes have simulated minimum OLR in the eastern and southeastern regions. The minimum OLR has been simulated over the regions where maximum rainfall is observed during 15-16 August 2009 by ACM2 scheme, 26-27 June 2010 by ACM2 and MYJ and 7-8 September 2011 by ACM2 and QNSE schemes.

The MYNN3 scheme has simulated minimum PBL over the regions where the rainfall is maximum during 28-29 July 2009 and 7-8 September 2011. The minimum PBL has also been simulated over the regions where the rainfall is maximum during 15-16 August 2009 by ACM2 and MYNN3 scheme, 26-27 June 2010 by MYJ and MYNN3 schemes. The maximum reflectivity has been simulated in the regions where the rainfall is maximum during 28-29 July 2009 and 15-16 August 2009 by ACM2 and during 7-8 September 2011 by QNSE. The maximum reflectivity has also been simulated by BouLac and ACM2 schemes over M. Court and Sayedpur regions during 26-27 June 2010.

The maximum relative humidity (98 to 100%) is simulated in the regions where maximum rainfall is observed during 28-29 July 2009 by ACM2 and BouLac scheme and 15-16 August 2009 by ACM2 scheme. The maximum relative humidity (98 to 100%) is simulated by all PBL scheme in the regions where maximum rainfall is observed during 26-27 June 2010 and 7-8 September 2011.

The MYJ, ACM2 and BouLac schemes have simulated maximum wind speed at 850 hPa in the southeastern region at 1200 UTC on 28 and 29 July 2009. The ACM2 scheme has simulated maximum wind speed at 850 hPa in the southern region at 1200 UTC on 15 August 2009 and also simulated maximum wind speed in the northwestern region on 16 August 2009. All six schemes have simulated maximum wind speed at 850 hPa in the eastern and southeastern regions on 26 and 27 June 2010. The maximum wind speed has been simulated by all six schemes in the southern and southeastern regions at 850 hPa at 1200 UTC on 7 and 8 September 2011 respectively.

The BMD observed rainfall over Dhaka region is 333 mm on 27 July 2009 but the BouLac, MYJ, MYNN3 and ACM2 schemes have simulated 150-200, 100-150, 75-100 and 75-100 mm respectively. The BouLac, YSU, MYJ, MYNN3, QNSE and ACM2 schemes have simulated 150-200 and 100-150 mm rainfall over Chittagong and Sandwip regions on 28 July 2009 whereas the observed rainfall is 252 mm over Chittagong and 112 mm over Sayedpur. The BouLac, MYJ and ACM2 schemes have also simulated 75-100, 150-200 and 25-50 mm rainfall over Sayedpur region on 28 July 2009. On 29 July 2009, the BouLac, YSU, MYNN3 and QNSE scheme have simulated 150-200 mm rain over Chittagong region and the observed rainfall over Chittagong is 281 mm. The YSU, ACM2 and BouLac schemes have simulated 100-150, 75-100, 25-50 mm and 200-250, 250-300, 150-200 mm rainfall on 15 and 16 August 2009 and the observed rainfall is 138 and 256 mm over Hatiya and Rangpur

respectively. The MYJ, ACM2 and MYNN3 scheme have been simulated rainfall of 150-200 100-150 and 100-150 mm but the observed rainfall is 113 mm over M. Court region on 26 June 2010. The BouLac, MYJ and YSU scheme have simulated 150-200, 150-200 and 100-150 mm rain over Sayedpur and Dinajpur region whereas the observed rainfall is 311 mm over Sayedpur and 174 mm over Dinajpur regions on 27 June 2010. The QNSE, ACM2 and BouLac schemes have simulated rainfall of 150-200, 100-150 and 100-150 mm over Hatiya region but the observed rainfall is 146 mm over Hatiya region on 7 September 2011. The QNSE, YSU and BouLac schemes have simulated 100-150 mm rainfall over Hatiya region on 8 September 2011 whereas the observed rain is 116 mm over Hatiya region.

For the simulation of four heavy rainfall events with four initial conditions the BouLac PBL scheme has given the better result. After BouLac PBL scheme, YSU and ACM2 have given the better result for the simulation of heavy rainfall events.

References:

1. Ahmed R. and S. Karmakar, 1993: Arrival and withdrawal dates of the summer monsoon in Bangladesh, *International Journal of Climatology*, Roy. Met. Soc., 13, 727 – 740.
2. Asnani G. C., 2005: *Tropical Meteorology*, Revised edition Vol.3.
3. Hong S. Y. and H. L. Pan, 1996: Nonlocal boundary layer vertical diffusion in a medium-range forecast model, *Mon. Wea. Rev.*, 124, 2322–2339.
4. Braun S. A., and W. K. Tao, 2000: Sensitivity of high-resolution simulations of hurricane Bob (1991) to planetary boundary layer parameterizations. *Mon. Wea. Rev.* 128, 3941–3961.
5. Li X. and Z. Pu, 2008: Sensitivity of numerical simulation of early rapid intensification of hurricane Emily (2005) to cloud microphysical and planetary boundary layer parameterizations. *Mon. Wea. Rev.*, 136:4819–4838.
6. Steeneveld G. J., T. Mauritsen, E.I.F. DeBruijn, J.V.G. DeArellano, G. Svensson and A.A.M. Holtslag, 2008: Evaluation of limited-area models for the representation of the diurnal cycle and contrasting nights in CASES-99. *J Appl Meteorol Clim* 47:869–887.
7. Holtslag A. A. M. and B. A. Boville, 1993: Local versus nonlocal boundary-layer diffusion in a global climate model. *J Clim* 6: 1825-1842.
8. Holt T. and S. Raman, 1988: A review and comparative evaluation of multilevel boundary layer parameterizations for first order and turbulent kinetic energy closure schemes, *Rev. Geophys.*, 26,761-780.
9. Musson-Genon L., 1995: Comparison of different simple turbulence closures with a one-dimensional boundary layer model. *Mon. Wea. Rev.*, 123:163–180.
10. Sharan M. and S.G. Gopalakrishnan, 1997: Comparative evaluation of eddy exchange coefficients for strong and weak wind stable boundary layer modeling. *J Appl Meteorol* 36:545–559.
11. Cuxart J, A. A. M. Holtslag, R.J. Beare, E. Bazile, A. Beljaars, A. Cheng, L. Conangla, Ek M, F. Freedman, R. Hamdi, A. Kerstein, H. Kitagawa, G. Lenderink, D, Lewellen, J. Mailhot, T. Mauritsen, T. Perov, G, Schayes, G. J. Steeneveld, G.

- Svensson, P. Taylor, W. Weng, S. Wunsch and K. M. Xu, 2006: Single-column model intercomparison for a stably stratified atmospheric boundary layer. *Boundary-Layer Meteorol* 118, 273–303.
12. Svensson G and A. A. M. Holtslag 2006: Single column modeling of the diurnal cycle based on CASES99 data-GABLS second intercomparison project. In: 17th symposium on Boundary layers and turbulence. American Meteorological Society, San Diego, CA, Paper 8.1.
 13. Hu Xiao-Ming, J. W. Nielsen-Gammon and F. Zhang, 2010: Evaluation of three planetary boundary layer schemes in the WRF model. *Journal of Applied Meteorology and Climatology* 49, 1831e1844. doi:10.1175/2010JAMC2432.1.
 14. Hyeyum Hailey Shin and Song-You Hong 2011: Intercomparison of Planetary Boundary-Layer Parametrizations in the WRF Model for a Single Day from CASES-99.
 15. Shamarock W.C., J.B. Klemp, J. Dudhia, D.O. Gill, D.M. Barker, M.G. Duda, X.-Y. Huang, W. Wang and J. G. Powers, 2008: A description of the advanced Research WRF Version 3. NCAR Technical Notes, NCAR/TN-475+STR, Boulder, Colorado, USA.
 16. Deardorff J. W., 1972: Parameterization of the planetary boundary layer for use in general circulation models. *Mon. Wea. Rev.*, 100, 93–106.
 17. Pleim J., 2007b: A combined local and non-local closure model for the atmospheric boundary layer. Part II: Application and evaluation in a mesoscale meteorological model. *J. Applied Meteor. Climatology*, 46, 1396–1409.
 18. Stull R. B., 1988: *An Introduction to Boundary Layer Meteorology*. Kluwer Academic, 666.
 19. Bélair S., J. Mailhot, J. W. Strapp and J. I. MacPherson, 1999: An examination of local versus nonlocal aspects of a TKE-based boundary-layer scheme in clear convective conditions. *J. Appl. Meteor.*, 38, 1499-1518.
 20. Hong S. Y., Y. Noh and J. Dudhia, 2006: A new vertical diffusion package with an explicit treatment of entrainment processes. *Mon. Wea. Rev.*, 134, 2318-2341.
 21. Janjic Z. I., 1990: The step–mountain coordinates: physical package. *Mon. Wea. Rev.*, 118, 1429–1443.

22. Janjic Z. I., 1994: The step- mountain eta coordinate model: further developments of the convection, viscous sublayer and turbulence closure schemes, *Mon. Wea. Rev.*, 122, 927-745.
23. Sukoriansky S, B. Galperin and V Perov, 2005: Application of a new spectral theory of stable stratified turbulence to the atmospheric boundary layer over sea ice. *Boundary-Layer Meteorol* 117:231–257.
24. Janjic Z. I., 2002: Nonsingular Implementation of the Mellor-Yamada Level 2.5 Scheme in the NCEP meso model, NCEP Office Note, No. 437, 61.
25. Zhang D. L. and W. Z. Zheng, 2004: Diurnal cycles of surface winds and temperatures as simulated by five boundary layer parameterizations. *J. Appl. Meteor.*, 43, 157–169.
26. Lin Y. L., R. D. Farley and H. D. Orville, 1983: Bulk parameterization of the snow field in a cloud model. *J. Climate Appl. Meteor.*, 22, 1065-1092.
27. Pleim J. E., 2007a: A combined local and nonlocal closure model for the atmospheric boundary layer. Part I: model description and testing. *J Appl Meteorol Clim* 46, 1383–1395.
28. Bougeault P. and P. Lacarrère, 1989: Parameterization of orography-induced turbulence in amesobeta-scale model. *Mon. Wea. Rev.*, 117, 1872–1890.
29. Troen I. and L. Mahrt, 1986: A simple model of the atmospheric boundary layer: Sensitivity to surface evaporation. *Boundary Layer Meteor.*, 37, 129-148.
30. Kessler E., 1969: on the distribution and continuity of water substance kin atmospheric circulation, *Meteor. Monopgr.*, 32, Amer. Meteor. Soc., 84.
31. Rutledge S. A. and P. V. Hobbs, 1984: The mesoscale and microscale structure and organization of clouds and precipitation in midlatitude cyclones. XII: A diagnostic modeling study of precipitation development in narrow cloud-fronadtal rainbands. *J. Atmos. Sci.*, 20, 2949-2972.
32. Hong S. Y., J. Dudhia and S. H. Chen, 2004: A Revised Approach to Ice Microphysical Processes for the Bulk parameterization of Clouds and Precipitation, *Mon. Wea. Rev.*, 132, 103-120.

33. Hong S. Y. and J. O. J. Lim, 2004: the WRF single- Moment 6-Class Microphysics Scheme (WSM6), *J. Korean Meteor. Soc.*, 42, 129-151.
34. TPB, 2001: Technical Procedures Bulletin (TPB) at <http://www.emc.ncep.noaa.gov/mmb/mmbpII/eta12tpb/> and on the CoMET Page at <http://meted.ucar.edu/nwp/pcu2/etapcp1/.htm>.
35. Dudhia J., S. Y. Hong and K. S. Lim, 2008: A new method for representing mixed-phase particle fall speeds in bulk microphysics parameterizations. *J. Met., Soc. Japan* Vol.86, 33-44.
36. Tao W. K. and J. Simpson, 1993: The Goddard cumulus ensemble model. Part I: Model description. *Terr. Atmos. Oceanic Sci.*, 4, 35-72.
37. Thompson G., R. M. Rasmussen and K. Manning, 2004: Explicit forecasts of winter precipitation using an improved bulk microphysics scheme. Part I: Description and sensitivity analysis. *Mon. Wea. Rev.*, 132, 519-542.
38. Morrison H., G. G. Thompson and V. Tatarskii, 2009: Impact of cloud microphysics on the development of trailing stratiform precipitation in a simulated squall line: Comparison of one-and two-moment schemes. *Mon. Wea. Rev.*, 137, 991-1007.
39. Kain J. S., 2004: The Kain-Fritsch convective parameterization: An update. *J. Appl. Meteor.*, 43, 170-181.
40. Kain J. S. and J. M. Fritsch, 1990: A one-dimensional entraining/detraining plume model and its application in convective parameterization, *J. Atmos. Sci.*, 47, 2784-2802.
41. Kain J. S. and J. M. Fritsch, 1993: Convective parameterization for mesoscale models: The Kain-Fritsch scheme, The representation of cumulus convection in numerical models, K.A. Emanuel and D.J. Raymond, Eds., *Amer. Meteor. Soc.*, 246.
42. Grell G. A. and D. Devenyi, 2002: A generalized approach to parameterizing convection combining ensemble and data assimilation techniques. *Geophys. Res. Lett.* 29(14), Article 1693.
43. Mlawer E.J., S. J. Taubman, P. D. Brown, M.J. Lacono and S.A. Clough, 1997: Radiative transfer for inhomogeneous atmosphere: RRTM, a validated correlated-k model for the long wave. *J. Geophys. Res.*, 102(D14), 16663-16682.
44. Dudhia J., 1989: Numerical study of convection observed during the winter monsoon experiment using a mesoscale two-dimensional model, *J. Atmos. Sci.*, 46, 3077-3107.